Development and Characterization of *in vitro* Microarray Technologies for Cell Biology

Die Entwicklung und Charakterisierung von *in vitro* Mikroarray-Verfahren für die Zellbiologie

In fulfillment of the requirements for the Degree

Dr. rer. nat.

to the faculty „Bio- und Chemieingenieurwesen"
of the „Technischen Universität" Dortmund
Approved Dissertation

Submitted by

MSc Heike Hardelauf

from

Kreuztal/Hilchenbach

Day of oral examination: 24th September 2013
1. Examiner: Prof. Dr. Jörg Tiller
2. Examiner: PD. Dr. Joachim Franzke

Dortmund 2013

Declaration

The research of this thesis was done at the Leibniz-Institut für Analytische Wissenschaften -ISAS-e.V., Department of Miniaturization in Dortmund, Germany. The work presented herein is my own work, unless it is referenced to the contrary in the text.

Dortmund, July 2013

When you have eliminated the impossible, whatever remains, *however improbable*, must be the truth.

The Sign of the Four, ch. 6 (1890)

Sherlock Holmes in *The Sign of the Four* (Doubleday p. 111)

Abstract

Modern cell biology is interested in the use of reproducible, quantitative and high-throughput analytical techniques. The aim of this thesis is the development and characterization of microarray technologies for anti-cancer therapy and neurotoxicity testing applications. The techniques and tools are based on cell micropatterning technologies and are accessible to biologists worldwide.

PDMS (Polydimethylsiloxane) microcontact printing (µCP) was used for the reliable parallel mass production of highly uniform 3D tumour spheroids. The different metabolic gradients make this bio-analytical model a reliable tool for the *in situ* or *ex situ* analysis of potential anti-cancer treatments as well as the physical and biological aspects that affect chemosensitivity.

The micropatterned research is extended to a spatially-ordered analytical display for high-throughput neurotoxicity screening with standardized neurite outgrowth length. This involved the development of a novel bilayer membrane plasma stencilling method. Bilayer plasma stencilling is a simple, rapid, inexpensive, reproducible and effective method to pattern neurons. The network formation assay (NFA) uses interconnectivity as a precise and sensitive analytical end-point to read-out and distinguish between cytotoxicity and neurotoxicity. In addition, the NFA was adapted to the needs of the gold standard primary cortical neurons and neuronal precursor cells using µCP on a cell repellent PLL-*g*-PEG background.

Taken together, this thesis demonstrates the development of microarray technologies for the realization of spatially standardized, highly reproducible and high-throughput cell assays to address modern challenges in cell biology. The assays were developed with the aim to be reliable, inexpensive, easy and adoptable for scientists with a minimum of equipment and expert knowledge.

Zusammenfassung

Die moderne Zellbiologie hat großes Interesse an Hochdurchsatz-Techniken, die reproduzierbare und quantitative Ergebnisse liefern. Ziel dieser Arbeit war die Entwicklung und Charakterisierung von Mikroarray-Technologien für Anwendungen in der Krebs-Therapie und der Neurotoxikologie. Die hier verwendeten Techniken und Werkzeuge basieren auf Mikrodruckverfahren („micropatterning") für Zellen und sind Biologen weltweit zugänglich.

PDMS (Polydimethylsiloxan) „microcontact printing" (µCP) wurde für die parallele Massenproduktion von hochgradig homogenen 3D Tumor Sphäroiden verwendet. Die verschiedenen metabolischen Gradienten ebenso wie die auftretende Chemosensitivität machen dieses bio-analytische Modell zu einem verlässlichen Instrument für die *in situ* oder *ex situ* Analyse von potentiellen Krebsmitteln.

Das Mikrodruckverfahren wurde weiterentwickelt, um ein räumlich angeordnetes analytisches System für neurotoxische Hochdurchsatz-Screenings mit standardisierten neuronalen Auswuchslängen zu entwickeln. Dies beinhaltete die Entwicklung einer neuen Methode, die Doppelmembranschicht Technik, welche mittels Plasma Strukturen in Oberflächen brennt. Die Doppelmembranschicht Technik ist einfach in der Anwendung, schnell, günstig, reproduzierbar und eine sehr effektive Methode um Neuronen strukturiert anzuordnen. Das „Network Formation Assay" (NFA) benutzt Verbindungen zwischen Neuronen als präzisen und sensitiven analytischen Endpunkt, um zwischen Zytotoxizität und Neurotoxizität zu unterscheiden. Zudem wurde das NFA an die Bedürfnisse und Wachstumsbedingungen von kortikalen Primärzellen (Goldstandard) und neuronalen Stammzellen angepasst. Das NFA wurden mittels µCP auf einer zellabweisenden Polyethylenglykol Oberfläche hergestellt.

Diese Doktorarbeit demonstriert die Entwicklung von Mikroarray Technologien für die Umsetzung von räumlich angeordneten und standardisierten, hervorragend reproduzierbaren und für Hochdurchsatzverfahren geeigneten Zellassays, welche Probleme und Fragestellungen in der Zellbiologie angehen. Diese Assays wurden unter den Gesichtspunkten entwickelt, zuverlässig, günstig, einfach in der Handhabung und

mit minimalem Wissen und Equipment durchführbar zu sein, damit möglichst viele Wissenschaftler die Systeme übernehmen und anwenden können.
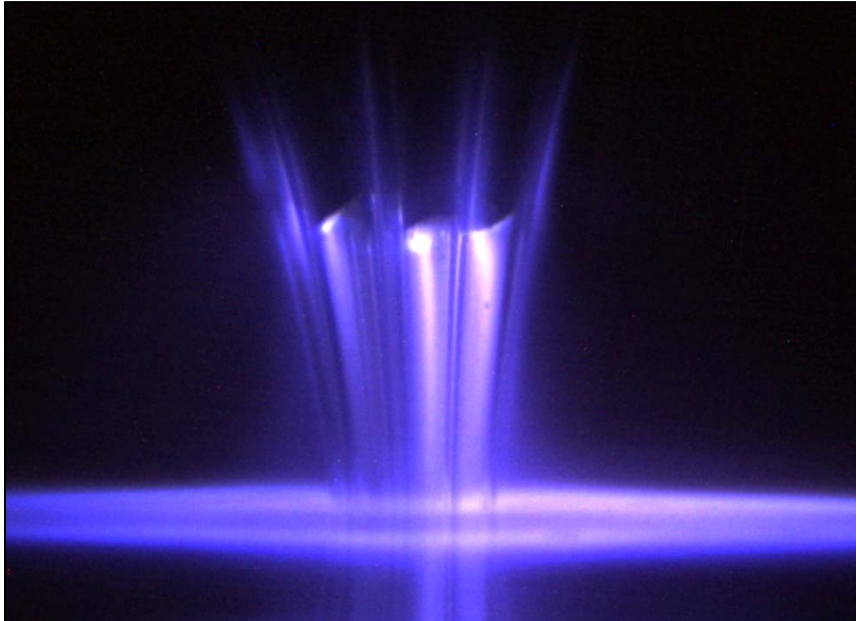
Contents

Contents

Contents

Chapter 1: Introduction

1. Background

The vast majority of cell biology research is done by the *ex vivo* culture of cells or cell lines within flat, hydrophilic plastic containers. Typically, these *in vitro* systems are fabricated from polystyrene materials with a brief plasma treatment used to render the surfaces hydrophilic. Coatings of biomaterials like ECM proteins (laminin, fibronectin or collagen) or peptides (RGDs) can be used for the attachment and adhesion of cell types. Cell seeding is random producing highly heterogeneous tissue-like structures from the cellular distribution. *In vitro* cellular interactions were mainly studied on adhesive cells growing on homogeneous substrates. These systems are a non-optimal analog of the *in vivo* situation. In contrast, mammalian cells within tissues are highly organized over length scales from a few microns to centimeters. The lack of organization does not provide an authentic model for studying cell biology. In addition, the highly disorganized nature of the cell distributions, from isolated single cells, to agglomerates provides different growth conditions. Cells respond to the surface of

adjacent cells (e.g. membrane receptors), the underlying surface (e.g. ECM proteins) and media composition (Folch and Toner, 2000). In traditional cell culture the analytical end-points are typically concerned with the average response of all cells. As such the signal may neither be indicative of either single or multi-cellular states. Uniform *in vitro* cell systems would thus be advantageous. The adaption and incorporation of microfabrication technologies into biology enables the design of surfaces that replicated the spatial organization of cells within tissues. It offers the potential to control cell-surface, cell-cell and cell-medium interaction on a micrometer scale. In addition, spatially ordered *in vitro* assays provide coordinates for high-throughput image analysis to streamline screenings and the evaluation.

In this work techniques were developed and used to spatially pattern cells for defined biological applications. The developed microtechnology methods are easy to adopt by other cell biology labs, without the need of special and expensive equipment or laboratories. All reagents are commercially available, stable, cheap and non-toxic to cells. The assays were developed with the aim of transferring them into standard industrial microtiter plates to make them available for high-throughput analysis.

1.1 New 2D and 3D *in vitro* test models

In research as well as in the pharmaceutical industry *in vitro* models are widely used and aid the discovery and development of new and more effective drugs. The commonly used *in vitro* assay consists of a two-dimensional (2D) cell culture in a dish that offers the possibility to measure or study special biological mechanisms such as drug uptake in a simple, rapid and well controlled way. Compared to *in vivo* models *in vitro* platforms are more cost effective, more rapid, have an easier read-out and with the use of cell lines are not of ethical concern.

Organisms, organs and tissues are three dimensional (3D) arrangements of cells (Yamada and Cukierman, 2007). The ability to understand the formation, function and pathology of tissues have in the past mostly relied on experiments involving 2D cell culture models. Cells growing in a 2D environment often have changed morphologies,

cell-cell and cell-matrix interactions and differ from cells which grow in a more physiological 3D environment (Birgersdotter et al., 2005; Cukierman et al., 2001; Griffith and Swartz, 2006; Nelson and Bissell, 2006). 2D systems are far removed from the *in vivo* state so that the predictive value of the model is questionable. The environment of the 2D cell culture is changing over time. Nutrients in the media get depleted whereas metabolites accumulate, which can cause toxic effects. In an *in vivo* state cells are maintained in a homeostatic environment. They are supplied with fresh nutrients and waste products are removed via the blood circulation system over time.

Animal models are much more complex systems with cells growing in a 3D environment. Unfortunately animal systems do not reflect human beings, so that results gained out of these models must be treated with caution (Seok et al., 2013; Shanks et al., 2009). Animal models do not reproduce adequate features of some drug therapy responses, human tumours, stem cell differentiation or autoimmune disease. A drug compound which is highly effective in rat tests can be completely ineffective or even toxic in humans. The closest *in vitro* models of the *in vivo* state involve the use of ex vivo tissue slices (Fig. 1.1.1a) (Pampaloni et al., 2007; Yamada and Cukierman, 2007). These models preserve the cytoarchitecture and cellular differentiation of the original tissue so that important cell-matrix and cell-cell interactions are maintained. The disadvantages of these systems are the high cost, the viability of the organ/tissue parts *ex vivo* and the availability of human organs. All this make these models unsuitable for standard testing purposes. A good alternative are three-dimensional *in vitro* test systems, which are intermediate models between two-dimensional cell culture and whole animal models (Griffith and Swartz, 2006; Rangarajan et al., 2004). They reflect cell morphology and signaling much better than 2D *in vitro* models. Many 3D *in vitro* assays for different applications have been developed (Figure 1.1.1). The most commonly known one is the multicellular tumour spheroids (MCTS) model for cancer research. It is based on the advantage of many cell types to spontaneously aggregate and cluster together without the external help of scaffolds. Spheroids can be created from a culture of one cell type or co-cultures. Spheroids are conventionally produced by the hanging-drop method (Kelm et al., 2003; Timmins et al., 2005; Timmins and Nielsen, 2007), spinner flasks or rotating – wall vessels (Fig. 1.1.1 b)

(Friedrich et al., 2007a). Spheroids are also broadly applied to biomedical studies (Mueller-Klieser, 1997; Sutherland, 1988; Sutherland et al., 1971) especially in high-throughput screens (Ivascu and Kubbies, 2006; Zhang et al., 2005) and in biotechnology approaches (Kale et al., 2000). The spherical geometry allows the easy study and modeling of dynamic processes like drug up-take, growth and invasiveness of solid tumours (Jiang et al., 2005; Stein et al., 2007).
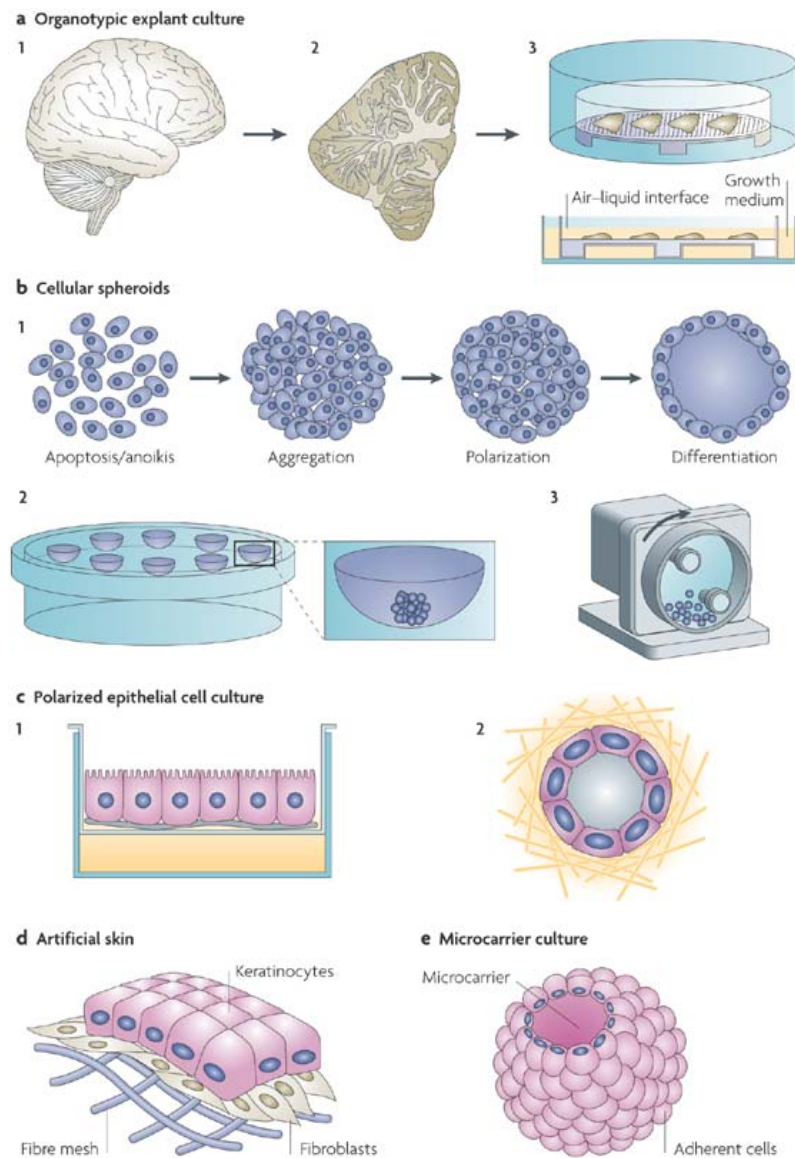
Figure 1.1.1: a) Three-dimensional culture models (Pampaloni et al., 2007). Organ slices (1, 2) cultured on porous substrates at the air–liquid growth medium interface (3). b) Spheroids. Cells aggregate into spheroids to a size of several hundreds of micrometers, their microenvironment express a tissue-like phenotype. Endothelial cells can form a differentiated hollow monolayer

*spheroid (1). Spheroids can be created by different methods like the gold standard 'hanging drop' (2) or in rotating-wall vessels (3). Both methods use gravity for cell clustering. **c)** Polarized epithelial cell cultures. Cells grown at the air–medium interface on porous membranes form polarized monolayers (1). Three-dimensional (3D) clonal growth of Madin–Darby canine kidney (MDCK) cells in hydrated collagen gel yields spherical monolayer cysts (2), which are fully polarized. The baso-lateral surface is in contact with the gel, and the apical side with the fluid-filled internal cavity. **d)** Artificial skin. Biodegradable fiber mesh was used to culture primary fibroblasts. After several weeks in culture, keratinocytes are placed onto the new dermal tissue and form an epidermal layer. **e)** Microscaled materials (microcarriers). Beads consist of dextran, gelatin, glycosaminoglycans and other porous polymers can be used as a 3D support for the culture of anchorage-dependent animal cell lines.*

A different model describes the growth of epithelial cells as polarized monolayers on microporous membranes (Butor and Davoust, 1992) (Figure 1.1.1 c), or as hollow spherical monolayers within an ECM gel (Zegers et al., 2003). These sub-organ structures can be used to develop much more complex epithelial structures like human skin supported by fibre mesh (Fig.1.1.1 d) (Horch et al., 2005).

These 3D models have the potential to become a fundamental research tool in cell biology especially because of their physiological relevance. They provide the advantage of pathophysiological gradients as a disease model for cancer, rapid experimental manipulations and a better real-time and/or fixed imaging system than animal models. 3D models enable the collection of data from different fields like genomics, proteomics and molecular cell biology. Those powerful tools are of value in drug discovery and clinical research by generating physiologically relevant screening assays.

The recently started "registration, evaluation and authorization of chemicals" program of the EU (REACH) is a large-scale toxicity screening endeavor and will require millions of laboratory animals. Recent estimations published in *Nature* says that approximately 54 million test animals will be needed for REACH (Hartung and Rovida, 2009). As an alternative, organotypic 3D models can be established to minimize the amount of test animals. This is more ethical and less costly. A big challenge for the

future of the life sciences will be to further explore 3D culture models and to establish them as standard models.

Compared to 3D *in vitro* systems 2D *in vitro* assays can also be adequate systems to replace animal models for REACH. Simplified *in vitro* cell culture experiments for high-throughput screenings can be a valuable alternative in the current chemical safety assessment procedure. An important field of the substance evaluation is neurotoxicity. Unfortunately, the data from *in vitro* experiments and the ones from the gold standard, acute oral *in vivo* toxicity tests did not correlate, making the development and validation of new cell based *in vitro* assays necessary to provide better predictive data and to avoid animal tests. New platforms should produce equivalent results to existing methods to act as a reference standard and to get accepted by neurotoxicologists. Neurite outgrowth assays are valuable 2D models to determine development, inhibition and degeneration of neurite outgrowth. Interconnection and networking between neurons are also critical cellular events which should be mimicked in new *in vitro* assays as they are hallmark neurodevelopment endpoint indicators. The commonly used neurite outgrowth assay determine sparsely seeded neurons and their outgrowth which is extremely time consuming and manually intense. Automated image capture systems can help analyzing the chaotic neurite outgrowth, but for this the neurons need to be fixed and antibody stained (Radio et al., 2008; Ramm et al., 2003) which terminates the experiment and the dynamic networking progress. Simple methods to quantify the neurotoxic effects of the test substances are still needed; this thesis will demonstrate the value of microtechnologies to develop relevant biological models and effective analytical tools.

With the aid of microtechnology microfluidic systems have been developed to determine axon guidance (Dinh et al., 2013; Francisco et al., 2007) and neuronal regenerative processes (Taylor et al., 2005; Taylor et al., 2003). Simple cell patterning methods (Folch et al., 2000; Kane et al., 1999; Mrksich et al., 1997; Whitesides et al., 2001) have been used to spatially control neuron cells and to couple them with electrodes for potential propagation measurements (Mourzina et al., 2006; Romanova et al., 2004). A huge step forward was the development of the microcontact printing

method for patterning adhesion molecules and thus pattern cells (Ruiz et al., 2008; Singhvi et al., 1994). These established microtechnologies aid to advance spatial organized 2D cell platforms to answer certain neurobiology questions and challenges in the life sciences.

1.2 Photolithography and soft lithography

Photolithography is a process that uses light to transfer a geometric structure to a photosensitive chemical; it is commonly used in the semiconductor industry to microfabricate integrated circuits (Qin et al.; Xia and Whitesides, 1998b). Today photolithography has been adopted by a wide variety of other fields, and is increasingly being used to impact biological research and medicine. Photolithography can be described as a process where a pattern will be transferred from a mask onto a thin film of photoresist (photosensitive polymer) that is supported on the surface of a substrate. The first step when using photolithography is the creation of a pattern via industry standard computer-aided design programs like AutoCAD or Coventor, or freeware such as L-edit or DraftSite. The patterns are typically transferred with an electron-beam writer to a thin layer of chrome onto an optically transparent (250-2400 nm) quartz substrate. Alternatively, high resolution ink-jet printing (32-128,000 dpi) onto acetate films can be used for lower-resolution applications where good UV transmission is not critical for the photoresist chemistry (Palmer and Decker, 1973). A silicon or glass wafer spin coated with a thin film (typically, sub-micron) of photoresist is placed behind the mask and a source of ultraviolet light. The mask and wafer are in close contact while the UV exposure transfers the pattern to the photoresist supported on the wafer. UV exposure goes through regions of the mask which are without a chrome layer and activate the photoresist, whereas chrome shield areas stay inactivated. Two different kinds of photoresist types can be used: With positive photoresist (e.g. AR-U4040) the UV treated regions are soluble and can subsequently be removed with an organic solvent (e.g. acetone), whereas the untreated areas are insoluble creating an inverted pattern of the mask. With a negative photoresist (e.g. SU-8) the pattern of the chrome mask gets replicated. The UV treated regions are

insoluble whereas untreated areas are dissolved by a solvent to create a pattern consisting of areas with and areas without photoresist. The features of the produced pattern can be as small as 100 nm, with a vertical dimension between 100 nm and hundreds of microns. For example, different grades of SU-8, a negative photoresist, can be used for the realization of structures in the range from a micron to 100 microns. Multi-layer processing can be used to achieve millimeter scale patterns (Michel et al., 2001).

The first demonstrations of the use of photolithography for cell patterning were in the 1990's. Healy *et al* coated a glass slide with photoresist and patterned it with UV treatment (Healy et al., 1994; Healy et al., 1996). An alkylsilane was covalently bound to the substrate areas that were exposed (i.e. where the photoresist had been photolithographically removed), after removing the remaining photoresist the newly exposed substrate was modified by an aminosilane creating a chemically-defined surface pattern. Cells attached in a regioselective manner to only the positively charge aminosilane areas, whereas the uncharged alkylsilane areas prevented cell attachment.

Photolithography is one of the most powerful patterning tools in microfabrication. Nevertheless, it has drawbacks and it is not suitable for all applications: Photolithography is an expensive technology with the need of a cleanroom for the production of the masters, which restricts the technologies to laboratories which have access to microfabrication labs. A major disadvantage is that it is not suitable for patterning non-planar surfaces. The chemistry of the surface is not very variable in generating patterns of specific chemical functionalities. Especially cells need adhesion proteins or specific binding motifs, but it is problematic or impossible to modify a photoresist surface with these substances as the solvents and conditions required for processing denature and damage biological molecules (Douvas et al., 2002; Sorribas et al., 2002).

To overcome these problems an additional step has been developed by George Whitesides and collaborators (Weibel et al., 2007; Xia and Whitesides, 1998b). The photolithographic wafers were used as masters themself to cast an elastomeric polymer of the pattern. The fabrication of the master can be commercially outsourced

or be produced by a microfabrication collaborator, so that the biologists only have to do the replication bit in their labs. These stamps or moulds replicated from the masters were made of 'soft material' like gels, polymers and organic monolayers instead of glass or silicon, with the name 'soft lithography' coined for this new technology. A central compound in soft lithography is poly(dimethylsiloxane) (PDMS) which is used as a soft material to create stamps. Before casting PDMS on the wafer pattern, the wafer has to be treated with a surface coating such as hexamethyldisiloxane (HMDS) to prevent the PDMS strongly adhering to the microstructured wafer surface. Without this step, delamination of the PDMS mould can, by mechanical action, remove the microstructures, such as SU-8 structures. The degassed liquid polymer is poured on the master restricted and then thermally cured (at ~ 70°C) for 30 min (Figure 1.2.1). The peeled off PDMS mould can be removed by hand and contains an inverted pattern of the features on the surface of the master and can easily be done by biologists in their own lab.
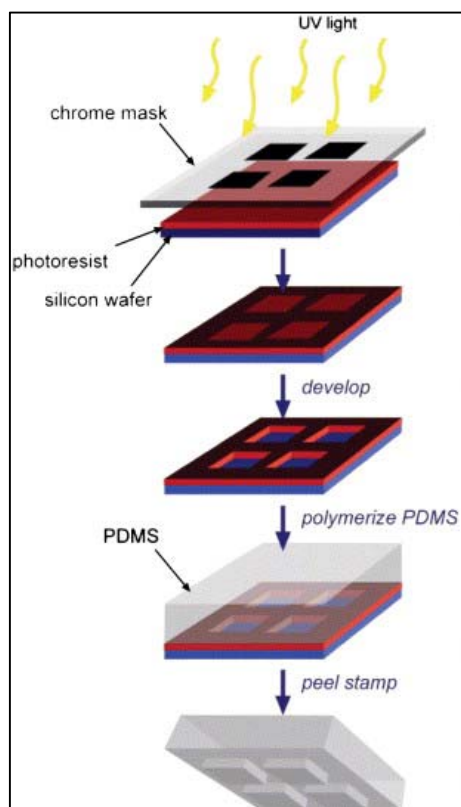

Figure 1.2.1: Soft lithography (Goubko and Cao, 2009). Photoresist is spin coated on a silicon wafer. The mask is placed between the photoresist and the UV light. d) UV light exposure through the mask hard bakes the photoresist. An organic solvent removes the not cross-linked

photoresist. A master with the critical dimension in bas-relief is shown. e) A PDMS mould is produced on the master. f) The PDMS stamp has structures embossed in its surface.

A major advantage of soft lithography is that the same master can be repeatedly used for replication: Moulding a structure from a master can be repeated more than ten times without damaging the structures of the wafer. And a stamp itself can be easily reused 30-40 times without any influence of the structure quality. The second major advantage is that moulding and stamping processes can be achieved with good results in normal laboratory conditions (i.e. outside the cleanroom), such as within a laminar flow hood. Therefore, photolithography can be outsourced to microfabrication facilities such as MST, TU Dortmund and GeSIM. Today this is inexpensive and within the reach of typical biological research budgets. The photolithographically-patterned 3D microstructured substrates can then be used for PDMS replication within the users own laboratory.

These topographically patterned layers of PDMS can themself be used as masters to transfer the structure into other materials or it can be plasma activated and sealed against flat surfaces to form microchannels to enable microfluidics (Siegel et al., 2006; Whitesides, 2006). The PDMS can form microchambers to isolate or culture cells and more important for this work, the PDMS mould can be used as a stamp for microcontact printing (μCP); the transfer of (bio) material patterns to a substrate of choice.

1.2.1 Microcontact printing (μCP)

Microcontact printing (μCP) was invented in the 1990s and was first used to pattern electronically conductive structures onto gold substrates (Kumar and Whitesides, 1993). The transfer of this method to cell biology applications happened a year later. Singhvi *et al.* (1994) patterned a self-assembled monolayer of alkanethiols for the spatially defined adsorption of proteins to guide patterned cell attachment (Kumar and Whitesides, 1993; Singhvi et al., 1994). The direct printing of adhesion proteins on cell culture substrates was first done by Bernard *et al*. in 1998 (Bernard et

al., 1998; Bernard et al., 2000). Since then a lot of different materials and surfaces have been tested for different kind of applications. Several excellent reviews have been published summarizing these achievements and techniques (Falconnet et al., 2006; Ruiz and Chen, 2007; Xia and Whitesides, 1998a; Xia and Whitesides, 1998b).

The basis of µCP is the use of an elastomeric PDMS stamp with 3D structures produced by moulding from a thick photoresist (e.g. SU-8) on a master. The process can be described as follows: The material to be transferred as a pattern is termed the "ink". Oxygen or air plasma is used to activate the stamp surface by increasing the surface free energy for higher and more reproducible molecule absorption (Figure 1.2.2). The molecular ink such as proteins are solved in buffers and are distributed on the microstructures of the stamp surface or the stamp is inverted in the buffer solution. Once the molecules have adhered on the stamp surface (typically in minutes), excess solution and unbound molecules are removed by rinsing in water or PBS. The stamps are then dried and placed into direct contact with a substrate. The PDMS stamp is elastomeric, such that by only gently pressing the stamp it conformally contacts the surface for molecular transfer and adsorption to the substrate to produce homogeneous and high quality patterns. The molecular pattern is transferred within a matter of seconds. Using the µCP method several kinds of proteins, peptides or adhesion molecules can be printed on different substrates. Commonly used proteins are from the extracellular matrix (ECM), which promote cell attachment on surfaces such as laminin (Lauer et al., 2001), collagen (Chen et al., 1997) or fibronectin (Klein et al., 1999; Lehnert et al., 2004). The peptide poly-*L*-lysine (James et al., 1998) acts as an electrostatic 'glue' to attach negatively charged cell surfaces to the negatively charged hydrophilic substrate surfaces (e.g. polystyrene and glass). More specific methods involve the use of synthetic peptides containing the amino acid sequence Arg-Gly-Asp (RGD) (Schaffner and Dard, 2003), which can directly bind to ECM-binding integrin molecules present on cell surfaces. After printing the adhesive pattern the intervening areas are passivated by molecules which resist cell adhesion like serum albumin. It is also possible to microcontact print cell resistant molecules like poly(ethylene glycol) (PEG) (Chen et al., 1998; Mrksich et al., 1997; Singhvi et al., 1994) and backfill with proteins or peptides to adhere cells. Another example is to stamp

octadecyltrichlorosilane (OTS) as a cell repellent material onto silicon wafers and backfill with N1[3-(trimethoxysilyl)propyl]diethylenetriamine (DETA) to adhere the cells (Kam et al., 1999; St John et al., 1997). The most commonly used approach is to print adhesion molecules onto inert surfaces.

Casting method

Cast a silicone replica from the silicon master.

Cover the stamp with protein solution.

Dry the stamp.

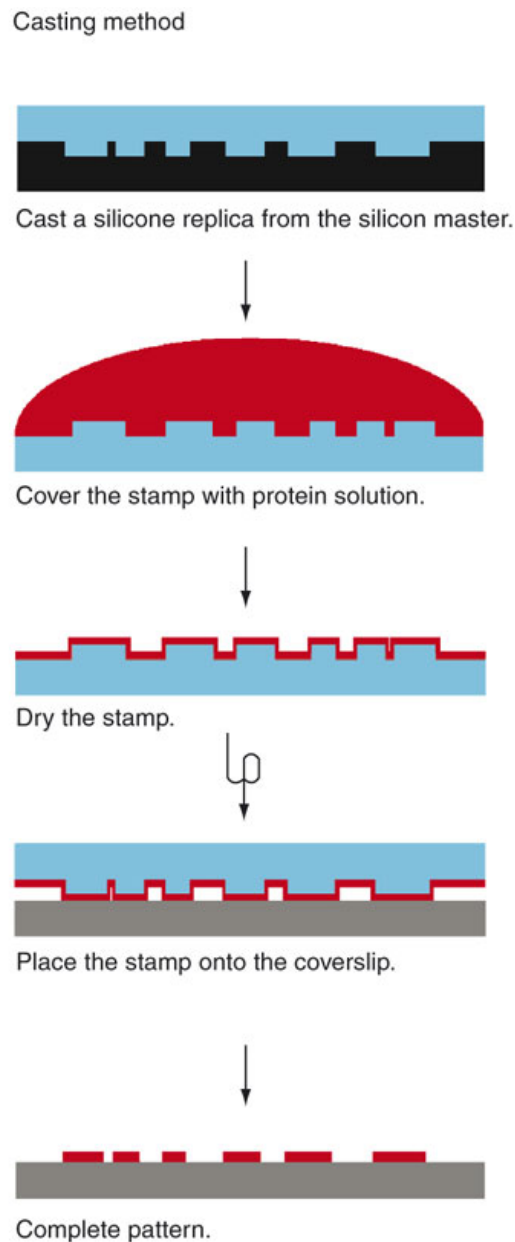Place the stamp onto the coverslip.

Complete pattern.

Figure 1.2.2: Microcontact printing. The PDMS stamp with recessed features gets incubated with a solution containing adhesion molecules. After drying the stamp gets inverted to contact print on a cell culture substrate and creates a negative pattern of the stamp (von Philipsborn et al., 2006).

Printed proteins have to remain functional to enable cell binding. Graber *et al.* showed that the most printed antibodies and molecules retain their functionality after µCP (Graber et al., 2003). A second important issue is the way of how printed molecules bind onto the surface. In the simplest case the molecules are only physisorbed on the surface (Falconnet et al., 2006); this is problematic in longer-term cell-culture studies, because cell media (especially when it contains serum) can interfere with molecule adsorption (Nelson et al., 2003). The strongest binding of molecular pattern to the underlying substrate is mediated by a covalent linkage. The formation of covalently linked patterns can be done by silanization of glass or silicon oxide surfaces (Cornish et al., 2002; Scholl et al., 2000; Wheeler et al., 1999) or the chemical activation of polymeric surfaces (Hyun et al., 2001; Lahann et al., 2002).

Like every technique µCP has also its drawbacks. The printing quality is very much dependent on the mechanical properties of the stamp. The stamp must be soft to guarantee good conformal contact, but it must be also rigid enough for the precise geometric definition of the pattern. This also limits the dimension of the possible pattern; normal PDMS stamps can have structures as small as 1 µm, for the production of smaller structures down to ~ 100 nm special stamp material is needed (Csucs et al., 2003a; Lehnert et al., 2004). It is difficult to produce homogeneous prints especially over large areas (> 2 x 2 cm²), that limits the reproducibility across chip, from chip to chip and between batch to batch (Fink et al., 2007). In addition, small features spaced by large distances are difficult to fabricate as a result of 'sagging'. Those features can deform under pressure by printing and cause pattern deformation. However, µCP is a rapid, simple and cheap technique for patterning cells. It can be used outside the clean room and can easily be adopted by scientists without any training.

1.3 Cell patterning

Microfabrication techniques can help to understand cellular behavior by controlling the adhesion and the growth area of cells. Patterned cells align themselves to the shape of the underlying substrate, which induces changes in the cytoskeletal features. Théry *et al.* developed arrays to spatially control cell adhesion. They showed

that the adhesion (micro-) environment controls the cell division axis, (Théry et al., 2005) the cytoskeletal architecture (Théry et al., 2006a), as well as the internal organization and orientation of polarity (Théry et al., 2006b). The geometrically defined shape of an adhesive footprint and its size has influence on the cell shape and various cell fate decisions. The size of the pattern can change the phenotypes of cells. Cells grown on a restricted area can induce apoptotic cascades (Chen et al., 1997) or hepatocyte cells decrease their albumin secretion as the adhesive area is limited (Singhvi et al., 1994).

Another interesting observation has been made with stem cell differentiation. Mesenchymal stem cells (MSC) were patterned on fibronectin islands of various sizes. Cells on large pattern areas adhered and flattened, whereas cells on small pattern stayed in a spherical morphology. The spread cells differentiate into an osteoblastic phenotype, the spherical cells differentiated into an adipocytic type (Gregoire et al., 1998; McBeath et al., 2004; Sikavitsas et al., 2001). A crucial parameter in cell patterning is the shape of the footprint. It could change the cells shape itself, which has a direct influence on the nucleus. Nuclear distortion by a shape change of the cell is systematically connected with reduced cell growth (Khatau et al., 2009; Roca-Cusachs et al., 2008; Thakar et al., 2009). The organelles and the DNA distribution in cells will be disturbed leading to changes in cell function (Alvarez et al., 1997; Maniotis et al., 1997). Effects like this could not be observed in typical cell culture dishes, where cells can grow and spread without spatial restriction.

Micropatterning approaches can mimic the structure, the composition and mechanical properties of tissues and organs and places individual cells or multi-cellular arrangements in physiological relevant conditions. The cell morphology depends on the pattern geometry, affects gene expression, proliferation, differentiation, apoptosis and with thus cell fate (Chen et al., 1997; Chen et al., 1998). The manipulation and fine-tuning possibilities of the cell culture microenvironment made by micropatterning gives fundamental insights into cell biology.

1.4 Replacement, Refinement and Reduction (The 3Rs)

Animal testing is a central part in many areas of research like genetics, behavioral studies, developmental biology, toxicology and drug tests as well as biomedical research. Many achievements especially in pharmaceutical and biomedical areas have been made because of the use of animals. The results of using animals for human purposes has tremendous benefits for mankind, and most would argue that it is preferable to testing humans. Animal tests aid the development of many valuable materials and methods: e.g. new drugs, cosmetics, new surgery and organ transplantation methods and many more. In science animal tests are well established and have been accepted as a reliable tool for gaining new biological information. With such a methodological tradition it is difficult to faithfully evaluate these and alternatives. In many cases animal tests are not mandatory or necessary. And most importantly the animal model does not recapitulate the human biological system (Seok et al., 2013; Shanks et al., 2009). Animal tests could be replaced by different methods or if that is not possible at least the amount of animals could be reduced by a better planning of the experiments. For over 50 years there has been an on-going discussion on how to deal with animal testing and the associated ethics. In 1959 Professor William Russell and Rex Burch first introduced in their book "The principles of humane experimental technique" the principles of the 3Rs: Replacement, Refinement and Reduction of animal testing. Specifically it states (Russell, 1995):

1. Replacement: Methods should be used, which avoid or replace the use of animals in an area where they otherwise would have been used to achieve the same scientific aim.

2. Refinement: Improvements to the scientific methods that minimize potential pain, suffering, distress and enhance the animal welfare where the use of animals is unavoidable.

3. Reduction: Methods that minimize the amount of used animals and enable researchers to obtain comparable levels of information from fewer animals or

to get more information from the same amount of animals, thereby reducing future use of animals.

Computer modeling, *in vitro* methods like tissue engineering or human volunteers are absolute replacement technologies, which do not need animals at any point of the experiment (http://www.nc3rs.org.uk). Alternatively there are relative replacements that avoid or reduce the use of "protected" (living vertebrates) animals. Animal cell lines could be established; material can be obtained from an abattoir, or the protected animals could be replaced by other non-protected animals like invertebrates, such as worms or larvae.

This thesis was also done with the focus to develop new *in vitro* test assays to avoid or minimize animal testing. In the following chapter a microchip will be introduced for the massive production of uniform tumour spheroids. These tumours can be used to screen databases for potential drug compounds or eliminating the molecules which does not show any effects. The number of animals tested can therefore be decreased. The second microarray method is based on the idea of developing a neuronal network on a chip. This chip will be applicable for testing chemicals for their neurotoxic and neurodevelopmental effects. Unfortunately the gold standard dictates the use of primary mouse cells, so that this assay has, in the short term, to be based on the use of animal cells too as a necessary step towards validation. Nevertheless, the design of the network formation assay allows obtaining much more information from a single mouse so that the amount of test animals can be massively reduced (each NFA chip saves one mouse). Normally 21 mice are needed for a concentration range experiment of one chemical in triplicate. Compared to this, taking the cells of one mouse is enough to cover 100 NFA chips to test 3-4 chemicals in triplicate. Additional, every negative tested chemical saves around 80 mice in the field of neurotoxicity and even more animals for neurodevelopmental toxicity (~ 140 dams and ~ 1000 pups). The developed microarray systems should not only fulfill the criteria of reduced animal waste, but they should also be reliable, simple and easy to handle, so that scientists can directly adopt this technique in their different laboratories.

1.5 Content of this Thesis

The research in this study was undertaken with the goal of developing methods for cell patterning to answer biological questions. The methods are characteristically inexpensive, rapid, and easy to adopt techniques suitable for cell biology labs. Another important issue was the development of test systems with the potential to reduce the use of test animals.

In chapter two the development of a microarray for the culturing of tumour spheroids using thin film PDMS µCP is presented. Spheroids of human cells can be used as intermediate models between simple cell cultures and complex animal models. The use of tumour spheroids for the selective screening of drug compounds reduces the amount of substances, which ultimately have to be tested in animals. A deeper characterization of the tumour spheroids growing on microarrays follows in chapter three. Spheroids grown on chip develop pathophysiological gradients, equivalent to those occurring in the *in vivo* state. These influence the uptake of potential drug compounds. The spheroids are chemosensitive depending of their size and viability. In an early state the spheroids are healthy and reflect normal human tumours connected to the blood circulation system. Older and larger spheroids develop a necrotic core and mimic avascularised tumours, which have different kind of drug targets than proliferating spheroids. The assay can be used to screen for drug compounds affecting tumours in different developmental states.

In chapter four the establishment of the network formation assay as a read-out system for neurotoxicity is described (Frimat et al., 2009). The array has fixed assay coordinates, defined neurite outgrowth length to easily measure neurite connectivity. The assay allows the rapid analysis of test substances for their neurotoxic effects on standard cell lines. To meet the demands of primary and stem cells the patterning technique requires tracks to enable neurite outgrowths to be extended unhindered by the local adhesive environment. To achieve this I have developed a novel bilayer plasma stencilling method. Chapter 5 describes the development of NFA microchip methods and chemistries suitable for primary and neuronal precursor cells. In addition,

the research was extended to investigate methods to improve the long-term stability of the micropatterns for distributed testing.

Taken together, this thesis demonstrates the development and characterization of techniques and assays for spatially defined biological applications. The techniques are simple, reproducible, inexpensive, and can straightforwardly be adopted by other scientists. The presented thesis is truly multidisciplinary, combining surface modification, material patterning, cell culture and characterization for the development of *in vitro* microarray techniques for neurotoxicity testing and anti-tumour therapy screening applications.

Chapter 2: Microarrays for Culturing Tumour Spheroids
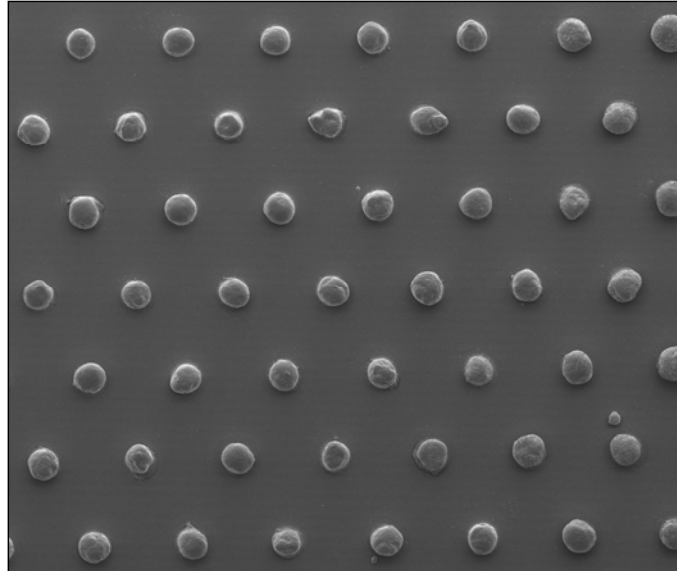
The work in this chapter was published in part as:

"Multicellular tumour spheroids: an underestimated tool is catching up again."

Hirschhaeuser F, **Menne H**, Dittfeld C, West J, Mueller-Klieser W, Kunz-Schughart LA. Journal of Biotechnology. 2010, 148(1):3-15. *

* This review was one of the TOP-5 referenced articles of J. Biotechnology in the years 2009-2011.

Part of this work in this chapter won Best Poster Award at Nano-Bio-Tech 2009:

"Micropatterning Approach for the Massively Parallel Production of uniform Tumour Spheroids."

Menne H, Frimat JP, Cadenas C, Franzke J and West J. The 13th Annual European Conference on Micro and Nanoscale Technologies for the Biosciences, Montreux; Schwitzerland, November 2009.

2.1 Introduction

The development of new drugs swallows up billions of dollars till bringing it onto the market. New systems have been integrated into the drug development process to make this procedure more effective. One very promising approach is the use of multicellular tumour spheroids (MCTS) in e.g. the field of anti-cancer therapy platform. Normally, effects of potential drug compounds get tested on a monolayer cell culture. The drug compounds are in direct contact with the cells; this does not reflect the tissue architecture, cell-cell and cell-matrix interaction and mass transfer barriers of *in vivo* tumour tissues. Unlike classical monolayer culture, tumour spheroids strikingly mirror the 3-dimensional (3D) cellular context, metabolic and pathophysiological gradients of *in vivo* tumours. The main potential of spheroids is the elimination of poor drug candidates, which shows less efficiency or is slightly toxic, at the pre- animal and pre- clinical state. Drugs lose efficacy caused by the penetration barrier and the metabolism in 3D pathophysiological environment, which can be used as a negative selection process to reduce animal testing. But some potential targets and signalling pathways especially or even exclusively play a role in 3D environment (Dardousis et al., 2007; Frankel et al., 2000; Howes et al., 2007; Poland et al., 2002). MCTS can be used to identify promising drugs candidates which failed in the classical 2D cell assays. The major goal is the replacement of the very simple monolayer culture system against tumour spheroids. It is a good way to improve the pre-animal and pre-clinical selection of the most promising drug candidates and develop novel, future-orientated treatment modalities (Abbott, 2003; Friedrich et al., 2007a; Friedrich et al., 2009; Kunz-Schughart et al., 2004; Mueller-Klieser, 1997; Mueller-Klieser, 2000).

Drugs tested in a complex system like the MCTS have to deal with or get influenced by different factors like penetration barriers, altered expression profiles, signalling pathways of particular targets, modulation of DNA damage and repair mechanism, and *in vivo* like distribution of biological response modifiers and survival signals as well as cell cycle distribution (Hirschhaeuser et al.). Pathophysiological gradients (oxygen, nutrients, catabolists) are developed in MCTS at diameters between 200-1000 μm. Cells located in the outer rim of the spheroids reflect the *in vivo*

situation of tumour cells adjacent to capillaries while inner cells stop proliferating and eventually die via apoptosis or necrosis. This reflects very well the *in vivo* situation of avascularised tumours, micrometastases and tumour nodules (Friedrich et al., 2007a; Kunz-Schughart et al., 2004; Mueller-Klieser, 1987; Mueller-Klieser, 1997; Mueller-Klieser, 2000; Sutherland, 1988) and it is a classical approach which maintain the functional phenotype of human tumour cells.

MCTS systems containing not only the culture of one cell type, there is also the possibility to co-culture spheroids with a second or even more cell types like immune cells or endothelial cells. Which kind of system is fitting is very much dependent on the application. Great care is required to take the right model for each therapeutic investigation: For example monocultures of spheroids from human tumour cell lines have been proven to be a good tool to study the microenvironmental regulation of tumour cell physiology and therapeutic problems associated with metabolic and proliferative gradients in a 3D cell context (Rodriguez-Enriquez et al., 2008).

To fulfil the requirements of getting integrated into a standard drug test routine the used system has to be well characterized containing spheroid uniformity, 3D cytoarchitecture, pathophysiological gradients, tumour cell response of the *in vivo* tumour state and the production of thousand spheroids in parallel to fit the high-throughput manner. Various technologies have been developed to fit these demands. Many technologies work with resisting cell-surface interaction to promote cell-cell coupling and aggregation of dense cellular clusters, like the continuous agitation of cell suspensions in spinner flasks, roller tubes, rotating wall vessels or gyratory shakers (Friedrich et al., 2007a; Ingram et al., 1997). The drawback of these technologies is the inhomogeneous form of the spheroids and the long culture time, nevertheless it is possible to produce large numbers of spheroids in parallel. Methods for the formation of homogeneously-sized spheroids are basing on the gravity forced aggregation of individual cells. Aggregation into a spheroid can be achieved by letting tumour cell suspensions sediment onto concave and cell repellent surfaces, such as microtitre plates coated with poly-hydroxyethyl methacrylate (poly-HEMA) (Ivascu and Kubbies, 2006) or a droplet air-liquid interface like the hanging drop method (Kelm and Fussenegger, 2004; Sutherland, 1988; Timmins and Nielsen, 2007). These methods are

more suitable for small scale production because of being manual intense, tedious and with limited scope for mass production. The gold standard method is microtitre plates coated with agarose (Friedrich et al., 2009). It is combining the advantage of producing relatively homogenous tumour spheroids in high numbers without being too manual intense. In combination with an automated pipetting system it can be used for high-throughput screenings. Nevertheless, to drive widespread acceptation of the spheroid model in cancer therapy process new automated and simple methods for the scalable production of uniform tumour spheroids are needed (Hardelauf et al.).

Microtechnologies can help aiding these problems, especially tissue engineering approaches like encapsulating the aggregation process within scaffold pockets formed by monodisperse microparticles (Lee et al., 2009; Zhang et al., 2005) or a two-phase microfluidic reactor for droplet preparation (Sakai et al., 2009) tackle it. Microfluidic systems also have the advantage to provide continuous perfusion to spheroids in the assembly process. Fluidic devices are produced with the cell repellent material poly(dimethylsiloxane) (PDMS) (Frimat et al., 2009; Frimat et al., 2009). The aggregation process of spheroids is a quiet sensitive procedure. A bilayer system with a semi-porous membrane can be used without interrupting the aggregation too interface the culture chamber with neighbouring perfusion channels (Hsiao et al., 2009; Kamei et al., 2009; Powers et al., 2002; Torisawa et al., 2007; Torisawa et al., 2009) or a central chamber can be separated by micropillars from neighbouring perfusion channel (Ong et al., 2008; Toh et al., 2007). Another method with similar effects is hydrodynamic trapping to culture cellular aggregates during continuous perfusion (Wu et al., 2008). Non fluidic process, like microwell arrays, can be used to cage cells and let them aggregate during sustained culture. The cells get seeded in suspension on the wells in equivalent distribution for the automated mass production of uniform tumour spheroids. Microwell arrays have been fabricated in poly(methyl methacrylate) (PMMA) by UV-LIGA (Akinari Iwasaki, 2009), or in PDMS using anisotropically etched silicon(Ungrin et al., 2008) or microstructured SU-8 moulds (Gallego-Perez et al.; Nakazawa et al., 2006; Park et al., 2007). Another method to avoid cell adhesion is the passivation of surfaces with poly(ethylene glycol). There are several techniques how to make microwell arrays, like embossing a PEG layer (Karp et

al., 2007) or by the self-assembly of thiolated PEG onto platinum-coated PMMA microwells (Sakai and Nakazawa, 2007). Alternatively, adhesion proteins like collagen (Fukuda et al., 2006; Mori et al., 2008) or Arg-Gly-Asp peptides (Inaba et al., 2009) can be microcontact printed (µCP) as adhesion islands for spheroids into the microwells to centre spheroid growth. Fundamentally, µCP of adhesion islands is enough to enable direct cell assembly and spheroid growth in parallel. Here, the 3D physical environment gets replaced by a cell repellent background like PEG brushes or hydrogels (Kojima et al., 2009; Otsuka et al., 2004; Tamura et al., 2008; Wang et al., 2009; Yoshimoto et al., 2009). This 2D aggregation form enables unstrained growth basing on a better supply with nutrients and waste removal.

In this study we used thin film PDMS micropatterning for the scalable mass production of uniform and metabolically-relevant tumour spheroids and demonstrate the value of this approach for drug discovery applications and cancer research.

Unlike µCP of proteins, where adhesion proteins are printed, PDMS prints regret cell attachment, but providing areas next to the PDMS prints which are suitable for cell adhesion. PDMS µCP can be undertaken of tissue culture substrates like glass or polystyrene. The method works similar like protein µCP, but instead of proteins liquid PDMS is transferred from a stamp onto a surface and get cured out on a hotplate to create a stable print. Compared to protein µCP, where reproducibility of pattern with uniform quality remains challenging, PDMS prints are reproducible and can easily be proven under a conventional microscope. PDMS has been used before to generate hydrophobic-hydrophilic contrasting surfaces for patterning cells (De Silva et al., 2004; De Silva et al., 2006; Patrito et al., 2007; Rhee et al., 2005). Here, PDMS gets microcontact printed onto standard cellular surfaces to produce micropattern for cell adhesion. The hydrophobic areas containing PDMS are cell repellent, whereas areas which stay PDMS free are hydrophilic and thus cell adhesive. In theory, adhesion proteins in the cell media denaturize on the hydrophobic PDMS surface and lose their function, whereas proteins on hydrophilic surfaces keep their functionality and mediate cell adhesion.

Thin film PDMS µCP can be used to generate single cell arrays, offering geometrically control of cells as well as precise pattern over large areas with absolute freedom of design (Figure 2.1.1).
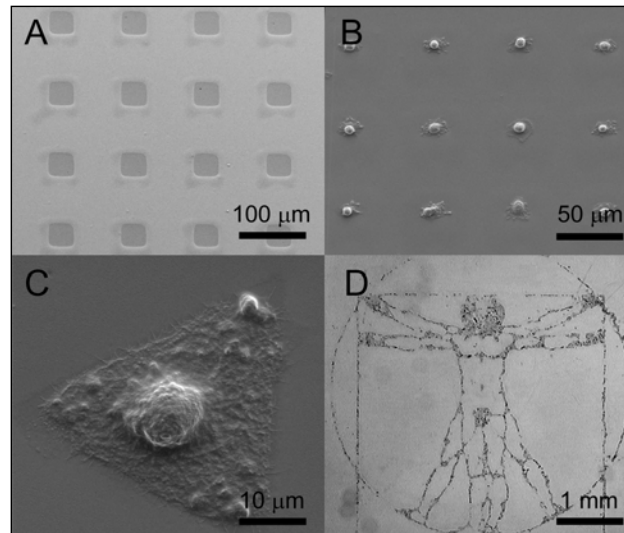

Figure 2.1.1: Thin film PDMS microcontact printing (A), single cell array (B), geometric control (C) and the Vetruvian man of Leonardo DaVinci showing the precision control over large areas. This work was done and kindly provided by Dr. Jean-Philippe Frimat (Frimat et al., 2009).

PDMS µCP is a very simple and highly effective method to produce reproducible pattern from chip to chip and batch to batch for cell adhesion. The lack of complex instrumentations and missing further surface modification makes PDMS µCP suitable for the easy adoption in the biology community. It can be used as a highly reproducible tool providing lots of uniform tissue for statistically relevant data output and help to develop new test platforms for cell biology. Here, we show the capabilities of such a tool in form of the scalable production of uniform tumour spheroids for anti-cancer research. Another platform basing on PDMS µCP, called the network formation assay, will be described in another chapter.

2.2 Material & Methods

2.2.1 PDMS microcontact printing

In this study a hexagonal design of cell adhesion islands with a diameter of 150 µm were used to pattern liquid PDMS on a glass surface across an area of 20 x 20 mm (Figure 2.2.1).
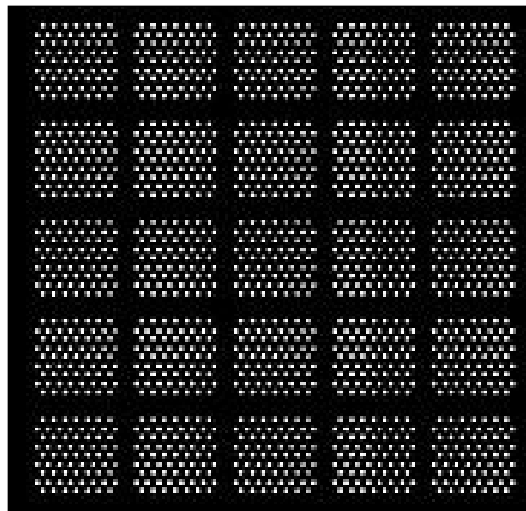

Figure 2.2.1: AutoCAD file showing the arrays with 1675 x 150 µm adhesion islands for the production of large numbers of spheroids.

Spatially differentiated designs consisting of arrays with different pitch diameters and different numbers of adhesion islands were used in this study: 400 µm (x 2411), 450 µm (25 sub-arrays totalling 1675), 700 µm (x 739), 1000 µm (x 409), 1250 µm (x 263), 1500 µm (x 149), 2000 µm (x 104). PDMS stencils were prepared by moulding SU-8 masters fabricated by standard photolithography methods. A PDMS prepolymer (Sylgard® 184, Dow Corning) was mixed with curing agent at a ratio of 10:1 (w/w). The mixture was degassed for 30 min by using a vacuum chamber. The stencils were created by pouring PDMS onto the SU-8 master bordered by a frame and cured at 70°C for 20 min. The SU-8 mould incorporated protruding circular structures causing in PDMS stamps with recessed features. The PDMS stamps were inked by conformal contact for ~ 10 s with a liquid PDMS and curing agent mixture (5:1, w/w) prepared by spin coating a 500 µL volume of PDMS in chloroform (1:10, w/w) on a glass slide for

30s at 6000 rpm. The inked stamp was used to make a preprint (to be discarded) on a polystyrene surface to remove excessive PDMS. The second print has higher feature resolution than the first print and was done on a glass culture slide. The microcontact printing process is illustrated in Figure 2.2.2.
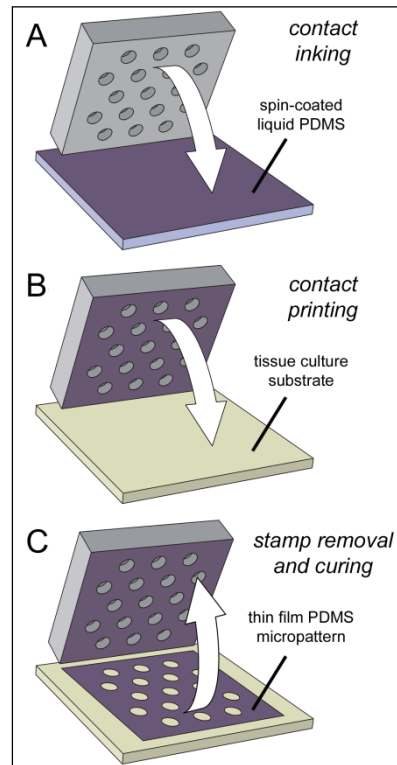

Figure 2.2.2: Schematic of the µCP process. A PDMS stamp with recessed features gets inverted and covered with liquid PDMS ink by contact (A), the liquid PDMS ink is transferred to a cell culture substrate by contact printing (B); and by removing the stamp and thermal curing the print remains on the substrate (C)(Frimat et al., 2009).

Thermal curing on a hot plate at 70°C for 10 min is enough to produce a stable thin film PDMS pattern on glass. The glass surface bordering the print was passivated with PDMS to restrict seeded cells to the adhesion spots alone.

2.2.2 Cell culture

Human colon carcinoma cells HT29, NCI-H1792 lung carcinoma cells and BT474 breast carcinoma cell lines were purchased from DSMZ (Germany) and ATCC (USA).

Cell culture media and consumables were ordered from Sarstedt AG& Co. (Germany). The Dulbecco´s modified eagle media (DMEM) was modified with 10% (v/v) foetal bovine serum (or 10% (v/v) foetal bovine serum gold (PAA, Germany) for the HT29 cell line), 1% (v/v) Glutamax and 1% (v/v) penicillin and streptomycin. The cells were cultured at 37 °C in a humidified 6% CO_2 atmosphere. Cells were harvested using 1 mL trypsin/EDTA for a 25 cm^2 culture flask once ~ 80% confluence was attained.

The PDMS surface was not further modified. Cells were seeded on the array within 1 mL media suspension containing 2 x 10^5 cells. Media exchange of 6 mL volume took place periodic every 2-3 days. For analysing the spheroids off-chip they were harvested by pipetting.

2.2.3 Physical spheroid characterization

The spheroids were documented using an inverted microscope (IX71, Olympus). Images were recorded using a colour digital camera (XC30, Olympus) and were analyzed by Cell A (Olympus). Higher resolution images of prints and spheroid arrays were made by scanning electron microscopy (SEM; Quantam200F, FEI) operating at 90 Pa. SEM imaging with cell compounds required fixation. The arrays of spheroids were incubated twice in 1x PBS for 5 minutes and then fixed for 24 hours in SAV neutral buffered 4% formaldehyde (Liquid Production, Germany). Finally the array was washed in 1x PBS for 5 minutes and air dried for a further 24 hours. For electron imaging the samples were coated with gold.

Spheroid morphology was determined by embedding them in agarose to provide a hydrated environment to prevent collapse by dehydration. The spheroids were inserting into molten 2% (w/v) agarose, following a cooling phase for gelation. Small cubes (1mm³) of agarose containing one spheroid were cut from the agarose block using a razor blade and analyzed by inverted microscopy from all three axis. The circularity measurements were done using ImageJ (NIH).

The spherical shape of the spheroids enables the tissue density to be estimated from the sedimentation velocity (assuming steady-state sedimentation). Spheroid sedimentation velocity within a 25 mL serological pipette filled with 1x PBS was

recorded (1 mL of the volume scale corresponds to 7.75 mm). The Stokes equation was used for calculating the spheroid density:

$$\upsilon_s = \frac{2r^2 g(p_s - p_f)}{9\eta} \qquad \text{Stokes equation}$$

Converting to density gives:

$$p_s - p_f = \frac{9\eta \upsilon_s}{2r^2 g}$$

v_s = sedimentation velocity (m/s)

r = radius (m)

ρ_s = density spheroid (kg/m³)

ρ_f = fluid density (kg/m³)

η = fluid viscosity (1.002 x 10^{-3} kg m^{-1}s^{-1})

g = gravity (9.81 m/s²)

The number of cells per spheroid was determined by pooling 30 spheroids together in triplicate. The supernatant was removed and the spheroids were washed twice with 1x PBS, following a trypsin treatment for 30 minutes at 37°C with vortexing every 5 minutes. An aliquot of 100 µL of this single cell suspension was diluted in 10 mL Casyton for cell counting with a Casy® instrument (Innovatis AG, Germany).

An accurately model of the volumetric growth of avascularised spherical tissues is the Gompertz equation (Brunton and Wheldon, 1980; Chignola et al., 2000; Kunz-Schughart et al., 1996). The spheroid volume at a given time, $V_{(t)}$, is given by:

$$V_{(t)} = V_{(0)} \times \exp^{\alpha/\beta(1-\exp^{\beta_t})}$$

Where $V_{(0)}$ is the initial spheroid volume, α is the growth regression rate and β is a growth retardation constant. The growth behaviour of spheroids on microarrays with

pitches ranging from 400 to 2000 μm was evaluated with the Gompertz equation. The spheroid volume V_s was calculated from the diameter using a capped spherical model:

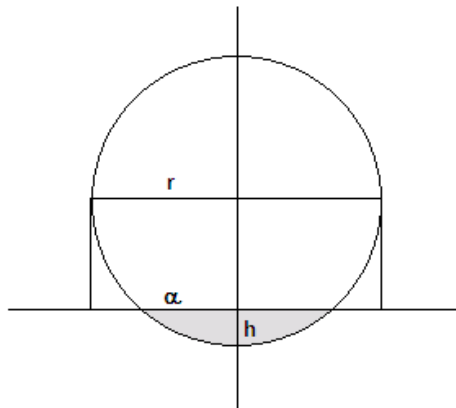$$V_s = (4/3\pi r^3) - (\pi h(3a^2 + h^2)/6)$$

Figure 2.2.3: Geometric spheroid model

 r = radius of the spheroid

α = radius of the cap (adhesion spot)

h = height of the cap

2.3 Results & Discussion

2.3.1 The Spheroid Microarray

The principle of thin film PDMS microcontact printing (µCP) on cell culture substrates is to provide areas where cells can bind, next to areas which resist cell adhesion. A stamp with recessed features and the following print on glass are shown Figure 2.3.1. The PDMS covers the glass with the exception of areas where the recessed features had been. Proteins and with this cells can adhere on the glass spots, whereas on the surrounding PDMS cell binding is not possible.
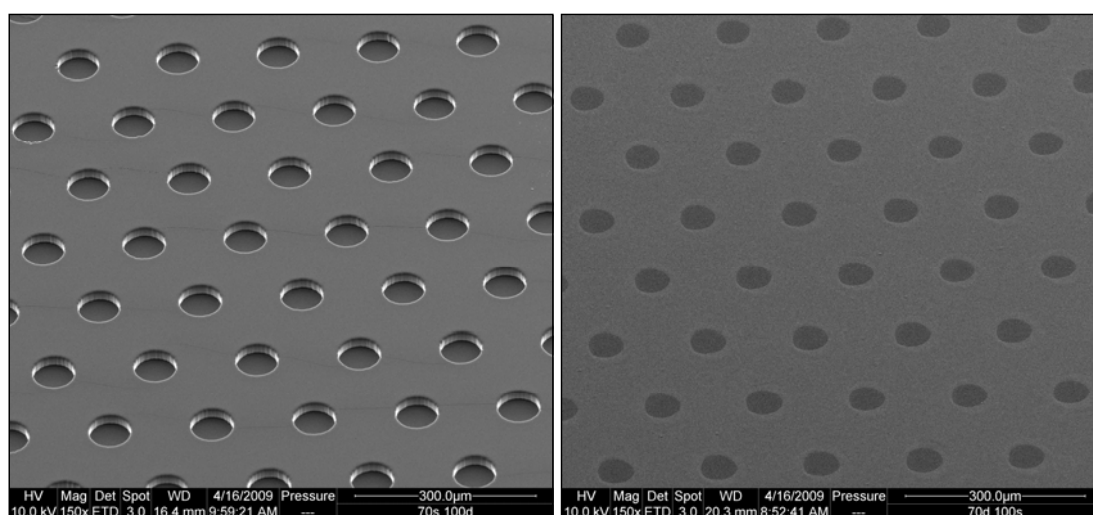

Figure 2.3.1: SEM images of a PDMS stamp with recessed features (left) and the complimentary thin film PDMS print with spots exposing the glass substrate where cells can adhere (right).

In our experiments the PDMS is characteristically hydrophobic with a contact angle of 107.4 ± 1.5°. Adhesion proteins which are needed by cells to adhere on cell culture substrates, denaturise on the hydrophobic surface causing in a loss of their functionality. The conformation change of the proteins also changes the position of the binding motifs for the surface receptors of the cells, so that cells cannot bind on the denaturised proteins. White light interferometry (WLI) has been used to characterize the second prints normally used as the adhesion platform for cells. The thickness of the printed structure had a height of ~ 40 nm (Figure 2.3.2). Topographical analysis showed "sand bag" features on the border between PDMS and substrate with a

maximum of about 120 nm. The source of this extra PDMS is likely from PDMS adsorption and capillary flow onto the vertical surface of the stamp features during printing process (Suh et al., 2001). Nevertheless, the overall thickness of the thin film PDMS remains much lower than the size of an adherent cell (~2 µm), so that the prints can be consider being essentially 2D in nature.
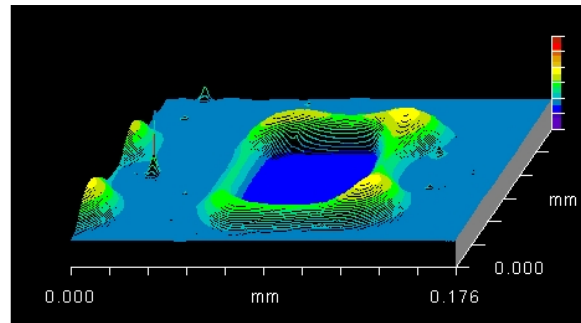

Figure 2.3.2: White light interferometry analysis of a thin film PDMS print. The square provides "sand bags" on the border of a maximum height of 120 nm (yellow peaks) surrounded by the thin film print of an average height of 40 nm.

A hexagonal design was used throughout this study to provide equally spacing between spheroids and with thus uniform diffusion gradients surrounding them. Different sizes of adhesion island diameter were tested to find optimal growth conditions for spheroids (70 µm, 150 µm and 250 µm spot diameters). Spheroid growth on 70 µm was too long to produce large spheroids, whereas on 250 µm spot arrays the cells formed a carpet instead of tumour spheroids. A spot diameter of 150 µm provided good growth kinetics and was chosen for the culture of large and homogeneous sized tumour spheroids.

Traditionally used production methods for spheroids involves the clustering of cells within a droplet or wells with a concave surface over a period of 3-4 days (Figure 2.3.3). The spheroids aggregate by gravity force, whereas the droplet curvature forms the spheroids.
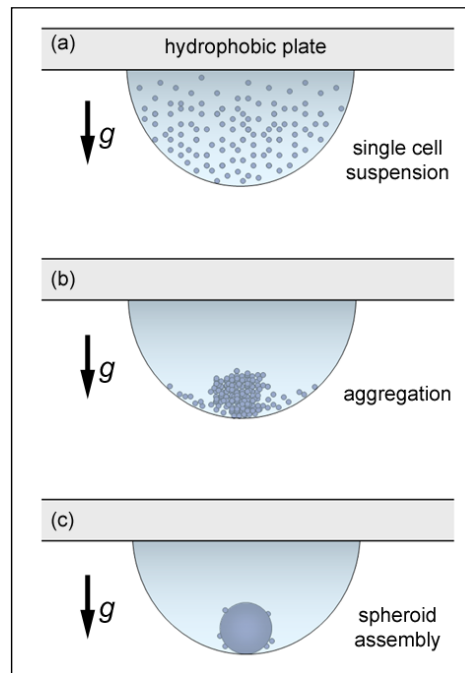
Figure 2.3.3: The gold standard hanging drop method. A droplet of single cell suspension gets manually pipetted on a petri dish lid and turned around (A). The cells sediment by gravity force (B). The concave surface of the droplet forces the cells in a spherical form (C).

The array method provides the cells only a 2D flat surface for adhering. Nevertheless, the cells grow on this flat surface to a nearly perfect spheroid. A small subpopulation of proliferating cells within each adhesion island lead to the growth into a compact cellular structure. This expansion from a small subpopulation into a spheroid may more accurately reflect the lineage expansion during *in vivo* tumour development (Clarke et al., 2006).

For the production of tumour spheroids 2×10^5 HT29 human colon carcinoma cells were seeded per array. After a sedimentation and assembly period of 3 days, not adhering cells were removed and fresh media was exchanged every other day. Spheroid development on array can be divided in three different growth phases. Within 24 h the cells adhere to the adhesion islands supporting 40-50 cells (Figure 2.3.4 A). In the following 24 h the cells assemble together into a smooth monolayer (B). In the first 48 h the cells cover the complete available surface area; proliferating cells have now only the possibility to grow into top direction leading to the formation of a 3D tissue, producing a hemisphere by day 4 (C). The spheroids are fully developed after a period of 10 days with a spheroid diameter of 235 µm (SD ± 12 µm) (D).
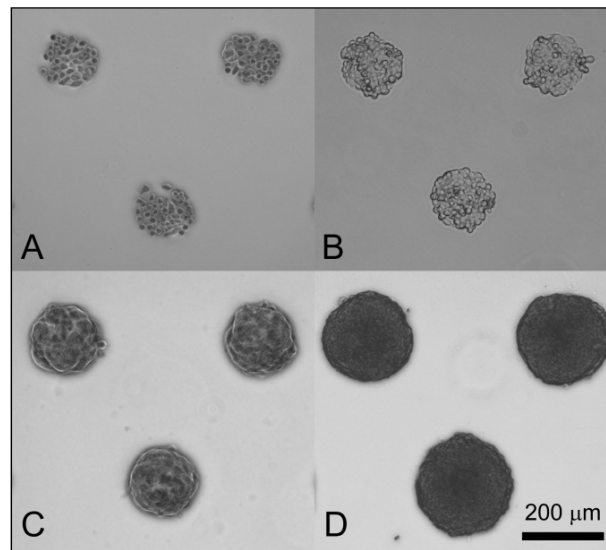
Figure 2.3.4: Spheroid development. Cells assembly after 24 h (a) and grow into a monolayer (b), hemisphere forming after 96 h (c) and a fully developed spheroid after 10 days (d).

The formation of spheroids on a 2D platform is possible, because the cells show strong cell-cell and cell-matrix interactions. During array-based culture the gene expression of E-cadherin is significantly up-regulated ($p < 0.001$), whereas the expression of $\alpha5\beta1$ integrin remains unaltered (Figure 2.3.5). These results promote the formation of tightly packed 3D cellular bodies.
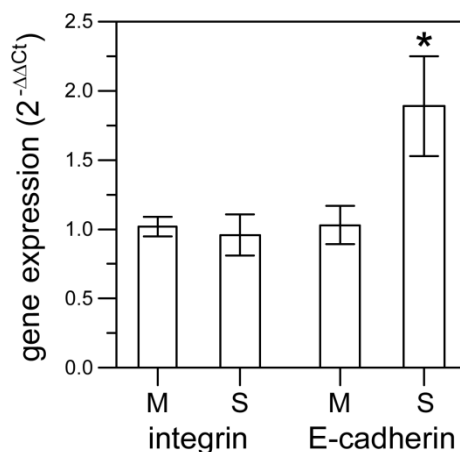

Figure 2.3.5: Gene expression analysis. The expression of integrin stayed the same for monolayer culture and spheroids, whereas the production of E-cadherin was significant up-regulated ($p < 0.001$).*

The aim of array-based spheroid growth was the mass production of uniformly sized- tumours with a spherical morphology larger than 200 µm. Spheroids developed on the original used 450 µm pitch system started with a diameter of 140 µm (SD ± 7) on day one and ended with a diameter of 254 µm (SD ± 21) on day 12 (figure 2.3.6). Spheroid growth follows a sigmoid trend (Marusic et al., 1994) with standard deviation less than 10% throughout growth. For research purposes it is necessary to standardize the size of spheroids to guarantee similar experimental conditions.
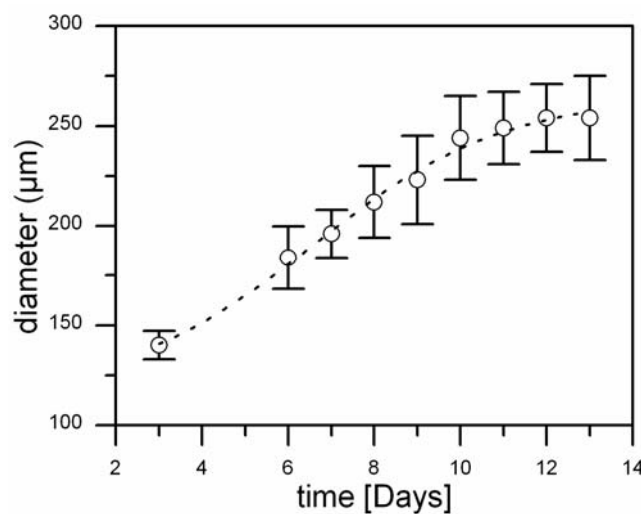

Figure 2.3.6: Spheroid growth monitored over a period of 13 days on a 450 µm pitch array with 150 µm adhesion islands.

The microarray technology allowed the development of spheroids larger than 200 µm; another very important issue is the spherical morphology of the tumours. Only the spherical shape of tumours guarantees the symmetrical diffusion of oxygen, nutrients, metabolites and finally drugs. For the determination of the sphericity of the produced tumours, the spheroids were harvested of the array and embedded into an agarose hydrogel for 3-axis imaging (Figure 2.3.7 C). The spheroids were individually injected into warm molten agarose, which was rapidly cooled down to position the spheroids within the polysaccharide. The agarose was cut into cubes containing a single spheroid and analyzed from all three sides of the cube by bright field microscopy giving a 3D impression of the spheroid.
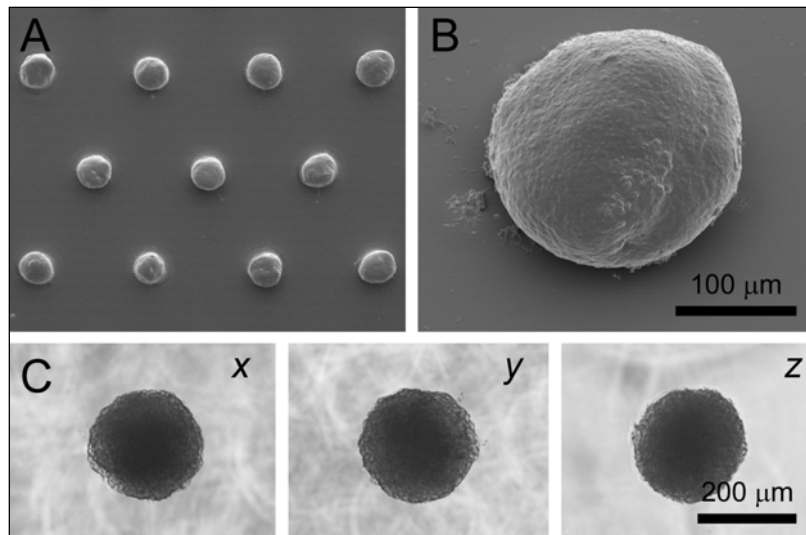
Figure 2.3.7: Spheroids grown on the array showed high uniformity and spherical morphology. SEM imaging of a formaldehyde-fixed array showing homogeneous sized spheroids (A) and a single adhering spheroid on an island (B). Agarose embedding was used for 3-axis imaging (C), the circularity measurement of the shown spheroid (x = 91%; y = 93%, z = 94%) was done with ImageJ.

The circularity of all three axis of the spheroids were analyzed with ImageJ determined to be x = 91%; y = 92%, z = 93% (n = 6). As shown on Figure 2.3.7 the spheroid has a truly spherical geometry making them a good mimic of an avascularised *in vivo* tumour. The sphericity enables the determination of the tissue density by sedimentation rate analysis.

The density is an important indicator of life-like tumour spheroids, which are compact and characteristically organotypic dense packed. Spheroids which are loose packed and have a low density can disaggregate during testing periods. Spheroids grown on a microarray had typically a density of 1040 kg/m³, which is equivalent to the density of *in vivo* tissues. Because of this high compact quality the spheroids can easily be harvested by pipetting without damage for off-chip investigations.

To determine the density of the spheroids, sedimentation rate analysis was done. Individual spheroids were pipetted into a capillary with graduated length. As the spheroids reached their terminal velocity the time was measured, which the spheroids needed to sediment for a defined length (1.55 cm). The Stoke`s equation was used to calculate the density of the spheroids (Chapter 2.2.3).

2.3.2 Mass production of uniform tumour spheroids

The microarray technology fulfilled many important requirements of spheroid production, like uniformity and spherical morphology of cultured spheroids as well as dense spheroids. Also spheroids on our microarrays grow into a spherical form, starting from just a couple of cells, reflecting an *in vivo* avascularised tumour much better than a spheroid formed by aggregation. It would also be possible to create microarrays to grow spheroids starting from single cells, which aids identifying progenitor tumour cells. Another very important issue is the mass production of tumour spheroids to match the demands of high-throughput screenings.

Our arrays can be used as mother dishes for the highly parallel production of uniform tumour spheroids. Only a single pipetting step with a cell suspension is needed for the automated mass production, whereas the formation of spheroids by the hanging drop or agarose overlayer method requires individual pipetting steps per spheroid. The array method is not only a much faster technique it also eliminates pipetting errors and makes media exchange tremendously easier without the risk to lose spheroids. Media exchange e.g. cannot be done by spheroids growing in a hanging drop.
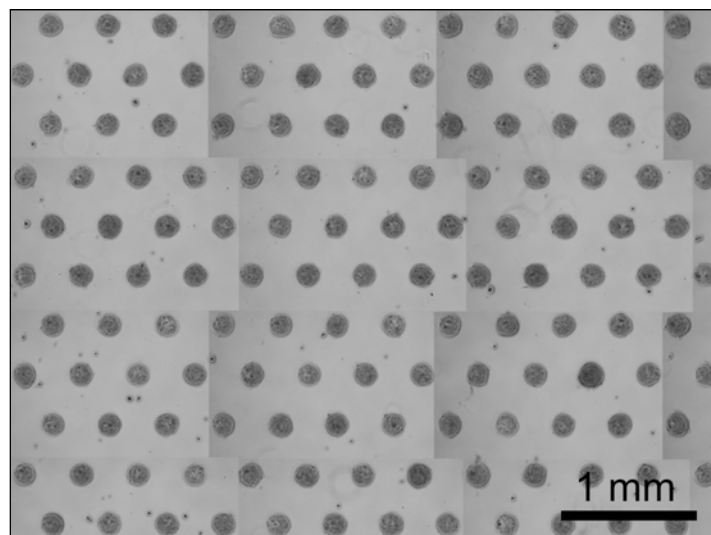

Figure 2.3.8: Mass production of tumour spheroids on an array with a pitch of 450 μm. Image compilation of a 0.55 cm² region of an array containing 137 uniformly sized spheroids following culture for 5 days.

The microarray provides an area of 20 x 20 mm with 1675 adhesion islands for the parallel production of tumour spheroids. The occupancy level across chip, chip to chip and batch to batch was > 95%, showing the high efficiency of the microarray technology (Figure 2.3.8).

To demonstrate the mass production capabilities, six arrays were placed into a standard 6-well plate (altogether 10,050 adhesion islands) for spheroid culture shown in Figure 2.3.9.
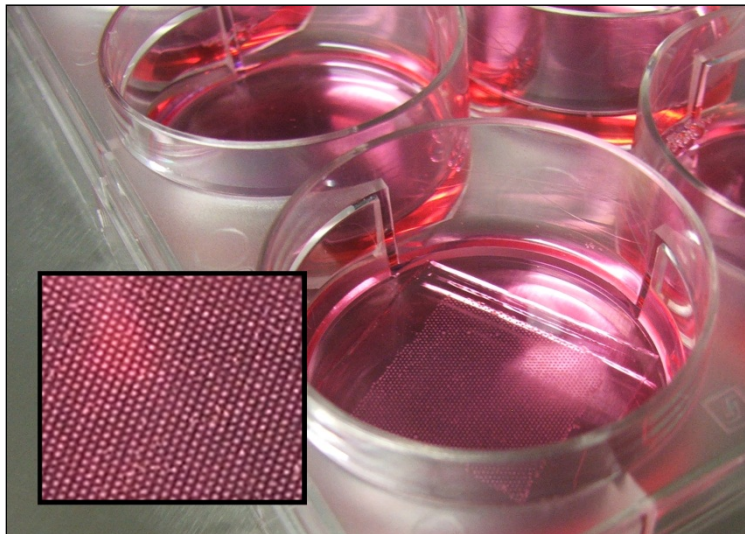
Figure 2.3.9: Standard 6-well plate containing the microarrays. The inset picture shows a detailed view on a chip, showing hundreds of homogenous sized tumour spheroids growing in parallel.

The occupancy level was 97.3% (9779 spheroids in total) and the harvesting efficiency was 99.0%. Altogether 9678 (96.3 %) uniformly sized spheroids were produced, showing the high efficiency of the preferential cell resistant PDMS pattern. These levels of production fit easily the requirements of high-throughput screenings. Microarrays can like the hanging drop method be used as a mother dish for spheroid mass production, but with the advantage of being manually simple and fast. Instead of pipetting 10.000 single droplets the microarrays reduce the pipetting steps to 1 mL cell suspension per well in a 6 well plate.

2.3.3 Growth kinetics can be manipulated by pitch tuning

Spheroids cultured on our original microarray design (450 μm pitch, 1675 adhesion islands) had a maximum size of 254 μm (SD ± 21, Day 13). Is there a possibility to generate larger spheroids on microarrays and what requirements are needed for that? To answer these questions, a different approach was designed: The pitch which is separating the adhesion islands was changed. Experiments using arrays with pitches from 400 to 2000 μm were undertaken.
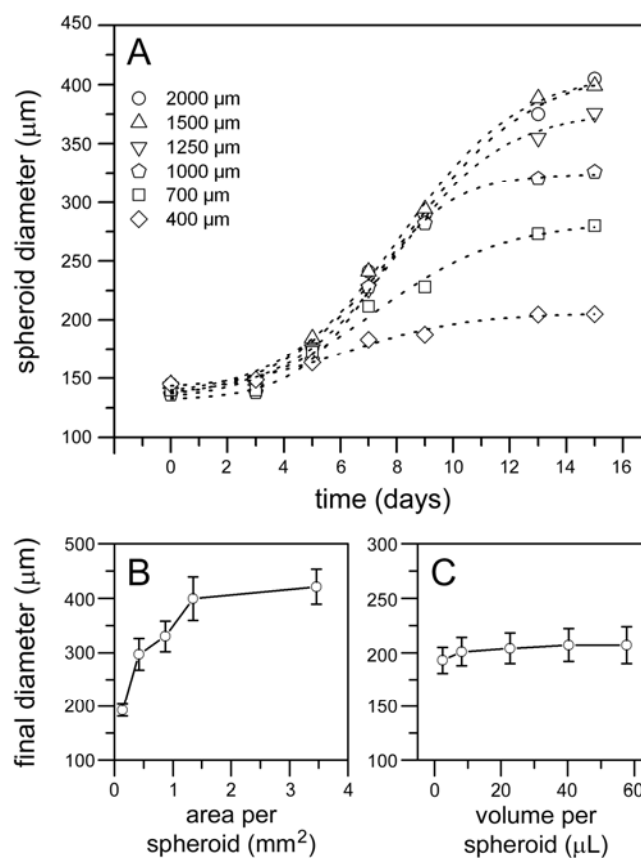
Figure 2.3.10: Spheroids growth curve for 400 to 2000 μm pitches (A). A Boltzmann function was used to fit the sigmoid curves. The spheroid diameters were highly uniform (SD ≤ 10%, data not shown). Array pitch variation impacts the final spheroid diameter (104 adhesion islands per array) (B). Adhesion island number variation by fixed pitch distance of 400 μm had minimal effect on the final spheroid diameter (C). Measurements were done in triplicate, with each involving 15-30x spheroid diameter measurements.

Spheroids grown on the smallest pitch distance of 400 μm produced spheroids with maximal diameters of 200 μm (SD ± 11) (smaller spheroids than the one grown on a 450 μm pitch system) by day 16. Even larger HT29 spheroids were produced on 700 μm pitch arrays with maximal diameters of 276 μm (SD ± 25) by day 17. This is equivalent to HepG2 spheroids cultured on 600 μm pitch arrays (Tamura et al., 2008) the largest previously reported array-cultured spheroids. Compared to spheroids grown on our 2000 μm pitch arrays (548 μm (SD ± 45 by day 27) the HepG2 spheroids are small. The different growth curves are documented in figure 2.3.10. The sigmoid growth characteristics indicate that over time nutrient availability and waste removal becomes limited during sustained culture.

On the microarrays it is now possible to culture very large spheroids, but to distinguish if spheroid density (different diffusion gradients) or available volume per spheroid or a combination of both is the important factor another experiment has to be done.

There are two different parameters, which can be varying: The pitch and the total amount of adhesion islands on the chip. In the following designs, one parameter was always fixed, whereas the other one was changed. The first array set had a fixed number of adhesion islands (104 per chip) with varying pitches (400, 700, 1000, 1250 and 2000 μm, Fig. 2.3.10 (B)) to prove the effect of available volume per spheroid. The second set had a fixed pitch of 400 μm with different numbers of adhesion islands (104, 351, 739, 1306 and 2411, Fig. 2.3.10 (C)) for proving spheroid density. The arrays with variation number of adhesion islands had minimal effect on spheroid growth, so that spheroid density is not the critical factor. The approach with the different pitches providing more volume per spheroid in a sustained culture, which dramatically affect spheroid growth (cell division rate), growth duration and consequently the final spheroid size. The less array density the more diffusive exchange of media and waste removal gets limiting. This effect can be observed from pitches of 400 μm to 1250 μm leading to enhanced growth. Arrays with pitches larger than 1250 μm (1.35 mm² per spheroid) does not show enhanced growing, no diffusive competition of media anymore of neighboring spheroids. At this dimension the total volume of media gets limiting. A spheroid on 2000 μm pitch array has a volume available of 60 μL, compared

to 200 μL per spheroid in the liquid overlay method. The final size of spheroids in the liquid overlay method is larger, but in return not as large as spheroids made by spinner flask. The final size of a spheroid is very much dependent on the total available volume of media and the production method. The original working condition of the microarray system was 6 mL media in a small petri dish with media exchange every other day. To enhance spheroid growth the total volume of media can be raised and use more frequently media exchange (e.g. daily or every 12h) or media perfusion. Without these modification large pitch arrays (≤ 1250 μm) still produce spheroids with large dimensions (≥ 500 μm) which mimic the pathophysiological state of avascularised tumours and *in vivo* like mass transfer gradients.

The Gompertz equation (chapter 2.2.3) is an established method to describe volumetric spheroid growth (Kunz-Schughart et al., 1996) and was used to evaluate the growth kinetics by curve fitting (Figure 2.3.11). The spheroid volume was calculated using a capped spherical model, subtracting the part lost by the adhesion island.
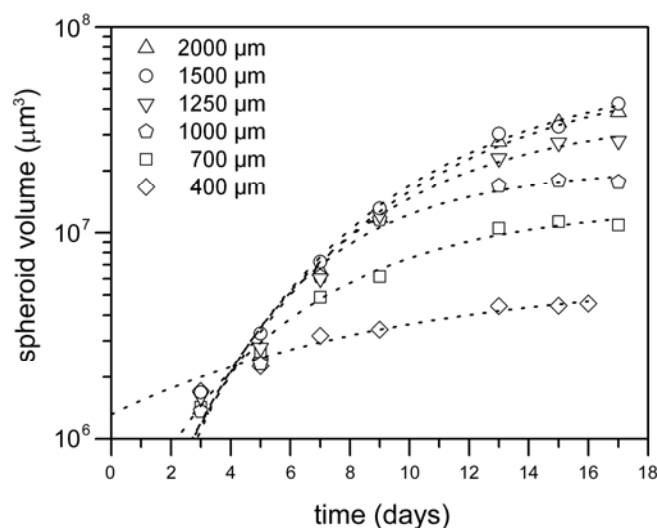

Fig. 2.3.11: Volumetric growth plotted with Gompertz function for spheroids cultured on pitches ranging from 400 to 2000 μm. Curve fitting correlated well with the data (r² ≤ 97%). The correlation is greatly increased (r² ≤ 99%) for spheroids cultured on arrays with pitches ≤ 1000 μm.

The excellent correlation values ($r^2 \leq 99\%$ for pitches ≤ 1000 µm and $r^2 \leq 97\%$ for pitches of 400-700 µm (capped spheroids)) indicates that the microarray technology impart the same growth kinetics as other traditional spheroid culture methods.

The spheroids cultured on the different pitch arrays were harvested at the plateau phase and characterized in terms of diameter, cell number, density and sphericity (Table 2.3.1). The cell number was proportional to the spheroid diameter indicating homogeneous densities.

Table 2.3.1: Physical characterization of tumour spheroids on arrays with different pitches. Spheroid diameter measurements were average of 30 values, the cell number obtained by triplicate pooling 30 spheroids and the density value has been calculated from 5 sedimentation rate measurements. Tumour sphericity was measured by 3-axis imaging 5 spheroids following by a circularity analysis using ImageJ. The lowest measured value was set as x-axis and the highest as z-axis value. A value of 100% on all three axes would indicate perfect sphericity.

Array pitch µm	Harvest day	Diameter µm	Cell number	Density kg/m³	Sphericity x-axis (%)	y-axis (%)	z-axis (%)
400	16	200 ± 11	2009 ± 153	1044 ± 7	87 ± 5	91 ± 3	94 ± 2
700	17	276 ± 25	5984 ± 297	1047 ± 6	89 ± 3	91 ± 3	94 ± 3
1000	17	324 ± 30	9438 ± 955	1048 ± 5	90 ± 2	91 ± 2	94 ± 2
1250	17	379 ± 38	15676 ± 709	1037 ± 5	89 ± 3	92 ± 2	94 ± 3
1500	27	531 ± 54	-	1033 ± 5	89 ± 2	91 ± 2	92 ± 2
2000	27	548 ± 45	35000	1035 ± 3	89 ± 2	90 ± 1	92 ± 3

The typically density was 1040 kg/m³ in average which is comparable with the density of organs. Fat tissue has a density of 970 kg/m³, brain 1020 kg/m³ and skeletal muscles 1040 kg/m³ (Dietrich). A dense and robust spheroid enables an easy harvesting process without damaging the spheroids for off-chip investigations. The spheroids grown on the different pitch approaches were also characterized in terms of cell number. The input number per microarray was 2×10^5 HT29 cells, in average 25 cells / adhesion island adhered in the spots after 24 h. Unspecific binding cells were

washed away. The final cell number of a spheroid was measured using the Casy® instrument. The increase of cell number is proportional to the size of the spheroid. The circularity of all three axes was ~ 90% showing highly spherical tissue assembly. Sphericity is an important fact for equivalent distribution gradients in tumours and mandatory for an effective spheroid model, alike densely organized cellular structure. In addition the microarrays produce uniform spheroids in large numbers with sizes ranging from 200-550 μm in a highly reproducible way with minimal effort required for preparation. All these qualities make the microarray method a good competitor to other available spheroid production methods.

2.4 Outlook and Conclusion

PDMS microcontact printing is a reliable tool for the production of microarrays for tumour spheroid culture. These microarrays can be used for the automated and scalable production of tumour spheroids with diameters of 200 μm to 550 μm. The spheroids grow in sustained culture with optimal growth kinetics on arrays with pitch of ≤ 1250 μm. The microarray technology allows the mass production of highly uniform tumour spheroids with different scales and different magnitude gradients for the analysis of potential drug candidates.

In the present study we worked with human colon carcinoma cells (HT29) for the massive production of tumour spheroids. To demonstrate the wider application of the microarray, BT474 breast carcinoma and NIC-H1792 lung carcinoma cell lines were used for culturing tumour spheroids (figure 2.4.1).
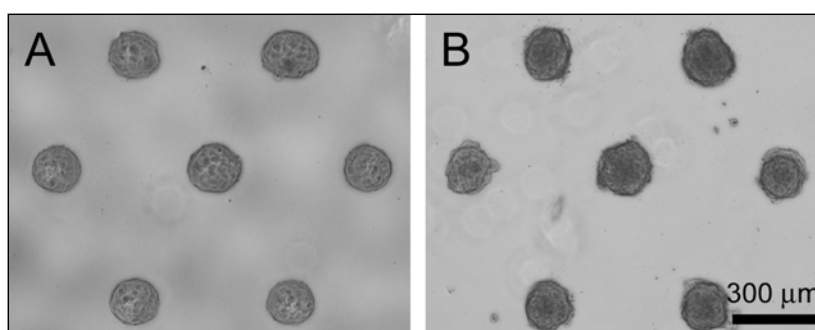

Figure 2.4.1: Spheroid production on a thin film PDMS microarray. Spheroids cultured of BT474 cells at day 3 (A) and NCI-H1792 cells at day 7 (B).

Other spheroid forming cell lines including members of the NIH-DTP 60 cell line are likely suitable for array-based culture (Friedrich et al., 2007a; Friedrich et al., 2009).

A more direct application of our microarray system is the potential to monitor specific growth inhibition experiments *in situ* with coming back to the same spheroid every day. For the better detection of inhibitory effects, large pitch arrays will be required to support optimal growth and the spheroids do not inhibit the growth of their neighbor spheroids. Because of the fixed coordinates of each spheroid this method can be combined with automated imaging for a high content screening approach to therapy testing. The *in situ* anti-cancer therapy screening method can be further improved by packaging the microarray platform within the industry standard microtitre plate format for lower volume drug testing. The PDMS material used for the spheroid arrays could also be used for plasma bonding (Chaudhury and Whitesides, 1992). In each well of a 96-well plate (Ø = 6.5 mm) 14 spheroids separated by a pitch of 1500 µm are fitting to provide more replicates for enhanced statistical confidence, for higher throughput screening 3 spheroids can be placed in each well of a 384-well plate (Ø = 3.0 mm), but with lower confidence. Arrays with 400 µm pitch can be used to produce large numbers of small spheroids. 480 fit within each well of a 96-well plate and 100 in a 384-well plate. With these simple modifications the potential of the spheroid array format can be greatly enhanced for spheroid research in both academic and industrial trails.

In this chapter is shown that spheroids can be cultured on microarrays growing from a 2 dimensional starting point of a few cells to a fully developed spherical tumour within 2-3 weeks. The spheroid end-size can be manipulated by pitch tuning with a maximum spheroid size of 550 µm. The mass production on the microarrays allows high-throughput analysis of potential drug candidates.

To fully validate the microarray spheroids and to determine their suitability as models for testing anti-cancer treatments, the next chapter involves biological characterization, gene expression and protein distribution analysis. Finally the spheroids were evaluated as tissue models for a dose response experiment with the anti-cancer agent irinotecan.

Chapter 3: Chemosensitive Tumour Spheroids
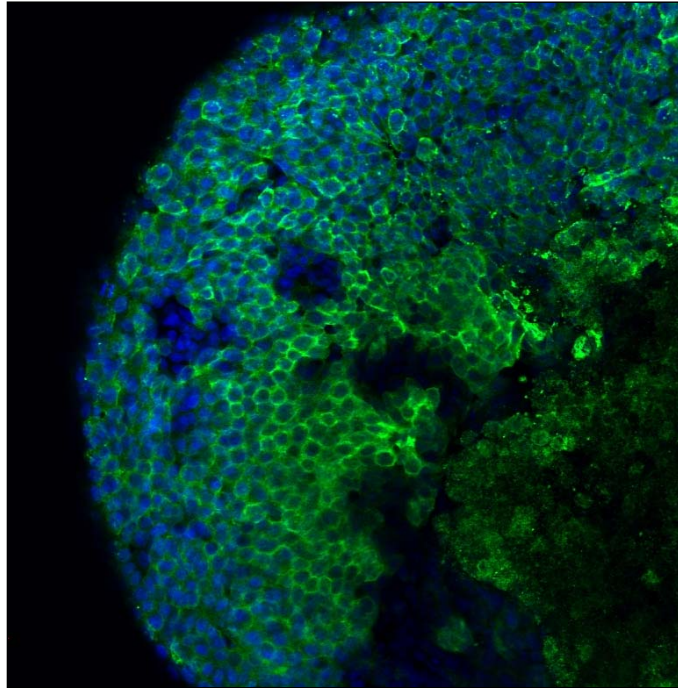
<u>The work in this chapter was published in part as:</u>

"Microarrays for the scalable production of metabolically-relevant tumour spheroids: A tool for modulating chemosensitivity traits".

Hardelauf H, Frimat JP, Stewart JD, Schormann W, Chiang YY, Lampen P, Franzke J, Hengstler JG, Cadenas C, Kunz-Schughart LA and West J; *Lab on a chip.* 2011, 11(3):419-28.

3.1 Introduction

On-chip spheroid research has almost exclusively focused on the physical characterization of spheroids like size, shape and total cell number (Otsuka et al., 2004; Sakai et al., 2009; Sakai and Nakazawa, 2007; Tamura et al., 2008). The biological aspects of spheroid production are a very important part of providing a useful tool for anti-cancer research. The pathophysiological gradients (Fig. 3.1.1) of a spheroid play a crucial role in the intake and the metabolism process of potential drug candidates.
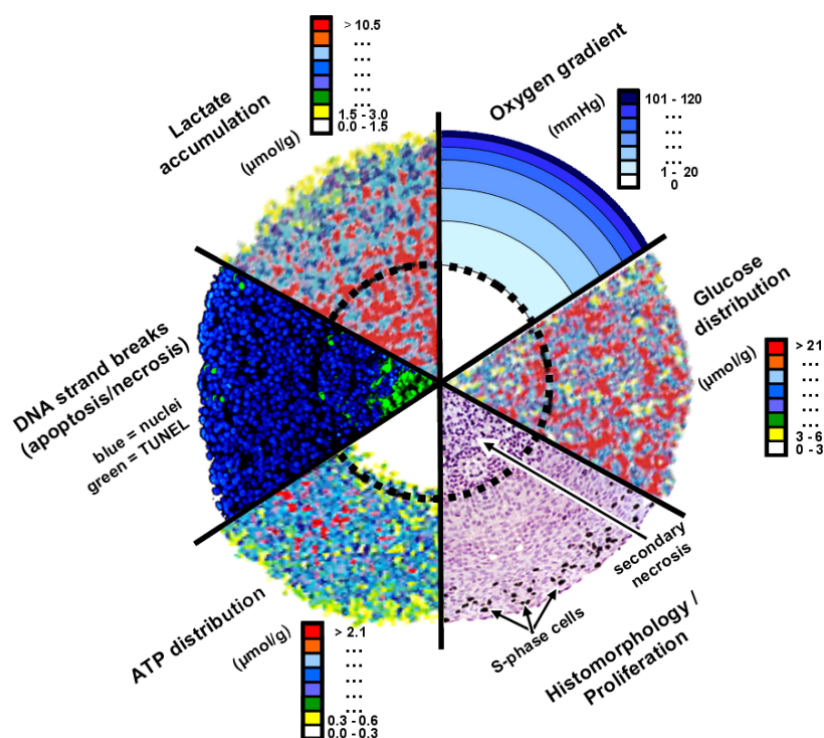
Figure 3.1.1: Shematic median section through a tumour spheroid (Hirschhaeuser et al.).

Tumour spheroids develop chemical gradients (catabolites, nutrient and oxygen) whereas the outer rim of cells reflects the *in vivo* situation of actively cycling tumour cells connected to blood vessels. Cells at the rim are in direct contact to the cell media and get fully supplied with oxygen. These cells keep on proliferating and are the first one, which get into contact with a potential drug candidate. Instead of this, the inner once get quiescent because of the lack of access to oxygen and nutritions. The metabolism stops working and the cells might die via necrosis or apoptosis. These

pathophysiological gradients mainly established within raising spheroid size are comparable with the situation of avascular tumours.

Depending of the size and age of the spheroids they have different pathophysiological gradients, which affect the mode of functioning of drug targets. A new technology for evaluate drug candidates on spheroids has to be sufficiently well characterized to resemble the tumour like 3D cytoarchitecture, the pathophysiological micromilieu and simulate the tumour cell responses on the *in vivo* tumour state (Hirschhaeuser et al.). Many technology produce so called spheroids or spheres which are not more than lose aggregates that easily detach and disaggregate. These spheroids lack cell-cell and cell-matrix interactions and often the true spherical geometry. But without these compact cell scaffold the pathophysiological gradients developed in genuine tumour spheroids is not established. The uniform geometry and the clear defined 3D structure are mandatory requirements prior to the possibility to produce thousands of identical tumour spheroids for implementation of the assay into primary drug testing routines.

The pathophysiological gradients cause intracellular homeostasis of central cells created by the stress of the diffusion gradients (Hirschhaeuser et al.). This affects in combination with the complex 3D network of cell-cell and cell-matrix interactions the expression of RNA and proteins and the penetration, binding and effect of drug candidates. Dependent on the size of the spheroids the microenvironment and with this the chemosensitivity to a drug can vary. This provides the possibility to test drugs in a different state of spheroid growth and viability.

In this study we go beyond the physical characteristics and provide a fully comprehensive characterization of the biological nature in terms of gene and protein expressions to complete the physical data from the previous chapter. The resulting physical-biochemical framework was used to design a dose response assay to compare chemosensitivity of spheroids in different regimes.

3.2 Material & Methods

3.2.1 Spheroid Gene Expression

Gene expression analysis: RNA isolation from spheroid and monolayer cultures was undertaken using the QIAzol Lysis Reagent Kit (Qiagen) following the manufacture´s protocol. The RNA concentration was determined with ND1000 software (Nanodrop). Reverse transcription polymerase chain reaction (RT-PCR) was used to reverse transcribed 2 µg gotten RNA with random primers and the high capacity cDNA Reverse Transcription Kit (Applied Biosystems).

The master mix of a total volume of 10 µl per sample was prepared on ice containing:

10x RT Buffer	2.0 µL
25x dNTPs	0.8 µL
10x RT Random Primers	2.0 µL
Reverse transcriptase	1.0 µL
H_2O	4.2 µL

For the reverse transcription process following thermocycle profile was used:

Temperature °C	Time (min)
25	10
37	120
85	5
4	∞

After completion cDNA was diluted to a final concentration of 10 ng/µL.

Real-time PCR (qPCR) was undertaken with an ABI Prism 7700 (Applied Biosystems) and the Quanti-Tect SYBR Green PCR Kit (Qiagen).

The mix of a total volume of 25 µl per sample was prepared out of:

2x QuantiFast SYBR Green RT-PCR master mix	12.5 µL
10x QuantiTect Primer Assay	2.5 µL
cDNA	5 µL
H$_2$O	5 µL

QuantiTect primer assays (Qiagen) were used for the amplification of all gene expression targets: actin (QT01680476); a5b1-integrin (QT00068124); E-cadherin (QT00080143); PCNA (QT00024633); cyclin D (QT004925285); p21 (QT00062090); and VEGF-A (QT01682072).

The following RT-qPCR program was used for the transcription:

	Temperature °C	Time
Hot start	95	15 min
Denaturation	94	15 s
Annealing	60	30 s
Extension	72	35 s

Denaturation, annealing and extension were run for 40 cycles before finishing with generating a melting curve from 55 °C to 95 °C. Data were analyzed using the 2$^{-\Delta\Delta Ct}$ method (Livak and Schmittgen, 2001), where actin was used as the housekeeping gene and the untreated monolayer cultures used as the calibrator. Each condition was undertaken in triplicate, with each sample measured in triplicate.

3.2.2 Spheroid sectioning

Spheroids sections were made using a microtome (Microm HM450). The spheroids were embedded in 1% agarose, fixed in 4% buffered formaldehyde overnight at 4 °C and then embedded in paraffin for cutting the spheroid in 4 µm thick sections. The paraffin was removed immediately before staining by rinsing in Rotihistol (4 x 5 minutes), followed by a dehydration series using ethanol (100%, 90%, 70%, 50%

and 30% for 5 minutes each) with finally rinsing in water. The spheroid staining was made with Mayer´s haematoxylin (Merck) for 5 minutes and 1% eosin for 3 minutes both steps followed by a water rinse. Sections were dehydrated in isopropanol and fixed with Enstellen® (Merck) for microscope imaging.

For the identification of proliferating cells, spheroids were incubated in 10 µM 5-bromo-deoxy-uridine BrdU for 6 hours, followed by a formaldehyde fixation. For BrdU and HIF-1α immunostaining, antigens were made accessible by placing the slides in a citrate buffer (0.01M, pH 6.0) and heated in a microwave for 2 x 7 minutes. After the section of the spheroids cooled down they were treated for 10 minutes with 2 N HCl. The slides were rinsed twice in 1x PBS and put into a humidity chamber. Non-specific binding was blocked with 3% BSA/PBS/0.1% Tween 20 for 1 hour followed by the addition of the primary antibodies which were directed against BrdU (rat anti-BrdU, Serotec, 1 : 25 in 0.3% BSA/1x PBS/0.1% Tween 20) or HIF-1a (mouse anti-HIF-1a, Novus Biologicals, 1 : 25 in 0.3% BSA/1x PBS/0.1% Tween 20) and incubation for 1 hour, followed by 1x PBS washing (3 x 5 minutes). Cy2-conjugated rat or mouse secondary antibodies (Dianova, Hamburg, 1:100 in 0.3% BSA/1x PBS/0.1% Tween 20) were used for slide incubation for 1 hour and washed with 1x PBS (3 x 5 minutes). The nuclei were stained for 5 minutes with 4`,6 -diamidino-2-phenylindole (DAPI, Invitrogen) at room temperature. Slides were stored in Mowiol solution and a laser confocal scanning microscope (Fluoview 1000, Olympus) was used for fluorescent imaging.

3.2.3 Drug dose response to Irinotecan

To identify the altered chemosensitivity stated of tumour spheroids, a dose response experiment using the anti-cancer drug irinotecan was undertaken. Spheroids were cultured on arrays with pitches of 400 and 1500 µm with irinotecan exposure for 3 days at concentration ranging from 3.16 µM to 1000 µM. Two approaches were run in parallel: Irinotecan was added at different time points, during pre-hypoxic and in the other approach in the hypoxic phase of spheroid culture. Monolayer cultures were used as experimental controls. Microtitre plate well (96 well plate) were each seeded

with 6×10^2 cells and cultured for 4 days at 37 °C in a 6% CO_2 atmosphere. Irinotecan was exposed at concentrations ranging from 1 µM to 3.16 mM for a further three days. To measure the inhibitory effects of irinotecan on cell viability (Friedrich et al., 2007b; Yang et al., 1996) the acid phosphatase assay was used. After the exposure with irinotecan the spheroids were washed twice with 1 x PBS, and then harvested by pipetting for transfer into a 96-well plate. Both the monolayer cultures and the spheroids in the microtiter plate were immersed in a 200 µL volume of a 1:1 mixture of 1 x PBS and 0.1 M sodium acetate buffer containing 0.1% Triton X-100 and 400 µg *p*-nitrophenyl phosphate (Pierce Biotech Inc.) and incubated for 90 minutes at 37 °C in a 6% CO_2 atmosphere. The phosphatase activity was quenched by the addition of 10 µL of 1 N NaOH to each well and within 10 minutes the absorbance at 405 nm was measured using a plate reader (Multiskan® FC, Thermo Fisher). The experiment was undertaken in triplicate with each replicate involving the measurement of 8 spheroids.

3.3 Results & Discussion

3.3.1 Determination of plateau phase spheroids in terms of necrosis, proliferation and hypoxia

The spheroids cultured on the microarrays have already been physical characterized, the inner part of the spheroids and their biological profile are analyzed in the following chapter. Spheroids were harvested in the plateau phase and determined in terms of proliferation, expression of hypoxia markers and necrosis. The spheroids were median sectioned and stained with hematoxylin and eosin (HE staining). For all three chosen plateau phase spheroids central secondary necrosis has been found (Figure 3.3.1, spheroid diameter 220 µm (400 µm pitch, harvest day 16) (A), spheroid diameter 390 µm (1250 µm pitch, harvest day 17) (B) and spheroid diameter 550 µm (2000 µm pitch, harvest day 27) (C)).

The largest spheroids of the 2000 µm pitch array (500-600 µm spheroids in necrotic phase) were further characterized: Bromodeoxyuridine (BrdU) was used to incorporate into proliferating cells. A narrow rim of 25 µm at the spheroid periphery was identified

as the only area with proliferating cells (Figure 3.3.1 (D) green rim). The hypoxia inducible factor 1α (HIF-1α) was used for immunostaining. Widespread expression of HIF-1α was identified surrounding the necrotic core of the spheroid (Figure 3.3.1 (E)).
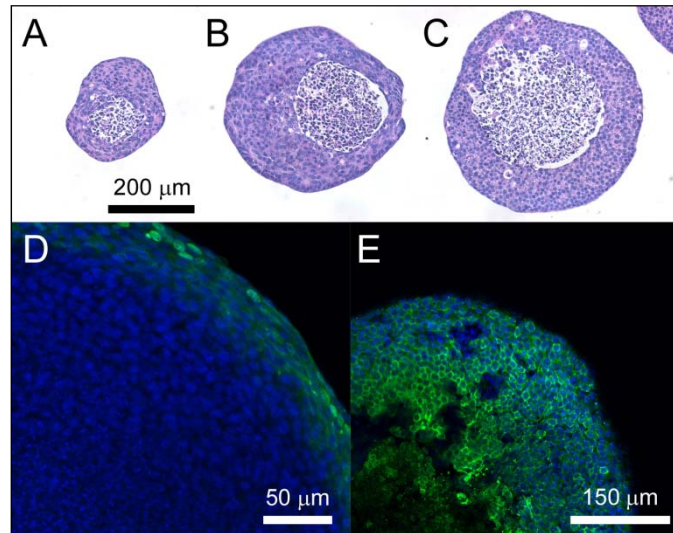

Fig. 3.3.1: HE staining of a 200 µm diameter spheroid (400 µm pitch, harvested day 16 (A)), a 390 µm diameter spheroid (1250 µm pitch, harvested day 17 (B)) and a 550 µm diameter spheroid (2000 µm pitch, harvested day 27 (C)). BrdU incorporation (green) (D) showing a small proliferating rim and HIF-1α (green) (E) distribution mapping by immunostaining of median sections from a largest spheroid. Cell nuclei were stained with DAPI (blue).

Combined, the spheroid is subdivided into three sections: a necrotic core, surrounded by hypoxic cells and an outer rim of proliferating cells. Sustained culture on arrays is producing spheroids with different layers caused by the surrounding diffusion gradients, which indicates threshold levels resulting from the gradients. These spheroids can be used as models reflecting the pathophysiological state of avascularised tumours and microtumours *in vivo*.

Further investigations were done by determining the expression of markers for proliferation, cell cycle arrest and hypoxia by plateau phase HT29 spheroids. The gene expression level of four different markers was analyzed: proliferating cell nuclear antigen (PCNA), cyclin D, p21 and vascularising endothelial growth factor (VEGF). The expression levels of small (~ 200 µm diameter) and large (~ 500 µm diameter) spheroids were compared to a monolayer culture grown under hypoxic condition (1%

oxygen) used as a control for depleted oxygen state. The positive control was a monolayer culture grown under normoxia conditions (20% oxygen). Results are shown in Figure 3.3.2.
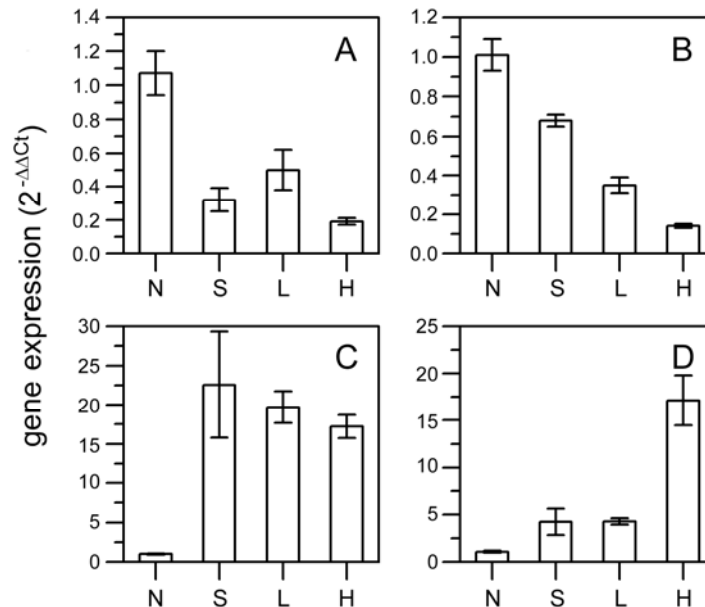

Figure 3.3.2: PCNA (A), cyclin D (B), p21 (C) and VEGF (D) gene expression level of small (S) and large (L) spheroids, as well as monolayer samples cultured under oxygen depletion (1% oxygen, (H)) and normal condition (20% oxygen, (N)). Values are normalized to normoxia monolayer culture. The experiment was done in triplicate, data points are mean values.

PCNA and cyclin D (Fig. 3.3.2 (A, B)) expression are down-regulated in small, large spheroids and in the hypoxia sample compared to the normoxia monolayer culture. The expression for p21 (Fig.3.3.2 (C)) is significant up-regulated compared to the normoxia sample. Together with the decreased expression of PCNA and cyclin D this indicates a cell cycle arrest in small, large spheroids and in the hypoxia monolayer sample. VEGF gene expression, a classic marker for hypoxic stress (promote blood vessel formation) was equally up-regulated in small (4.23-fold, SD ± 1.40) and large (4.28-fold, SD ± 0.33) spheroids. It was completely over expressed in the hypoxic monolayer (17.14-fold, SD ± 2.67).

The expression levels are indicating that both small and large spheroids are developing hypoxia over time. Different metabolic gradients and pathophysiological

states will also result during sustained culture causing in the temporary lack of oxygen. Smaller spheroids will have steeper gradients than larger tumour spheroids.

The question now is, when the spheroids are starting getting hypoxic and from which time-point on are they developing a necrotic core. Do only spheroids in the plateau phase have a necrotic core? To determine this; spheroids from a 400 µm pitch and a 1500 µm pitch array were harvested at several time points. The median sections of the spheroids were stained with HE to identify secondary necrosis (Figure 3.3.3). Spheroids from a 400 µm pitch array (202 µm diameter SD ± 13) developing secondary necrosis on day 14 when they are already in the plateau phase. The necrosis has a portion of <5% of the total volume of the spheroid. On the 1500 µm pitch arrays secondary necrosis also became evident (<5% by volume) by day 14 in spheroids with diameter of 389 µm (SD ± 26). This conflicts with observations that onset of necrosis is size depending occurring within 100 to 200 µm diameter spheroids (Glicklis et al., 2004; Tamura et al., 2008; Yoshimoto et al., 2009). But these kinds of spheroids were grown in microporous or microarray systems with pitch far beneath 1250 µm, which is the required distance for optimal oxygen supply and spheroid growth (Fig. 3.3.3 (B)).
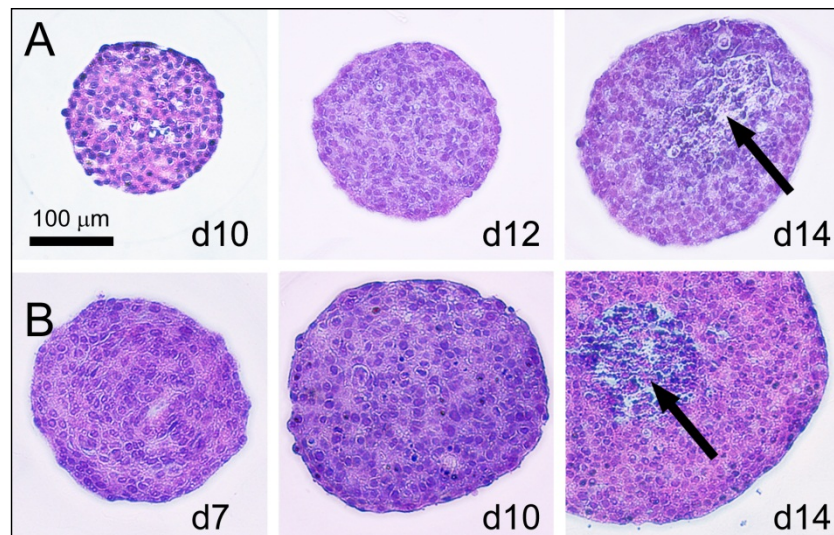

Figure 3.3.3: Hematoxylin and eosin staining of median sections of spheroids grown on a 400-µm (A) and 1500-µm pitch array (B). The spheroids were harvested on different days (d7 (day 7) -> d14 (day 14)). Secondary necrosis occurs in the spheroids both on day 14 marked with arrows.

These results show that not only scale is an important factor for spheroid development, but also the culture history for the development of metabolic and secondary necrosis. To grow large and viable spheroids in a sustained culture system it is necessary to have low microwell and microarray densities.

Secondary necrosis is a cause of oxygen and nutrient deprivation; cells do not have access anymore to essential compounds and so they first get into a hypoxic state before they die. To determine the first onset of hypoxic stress within spheroids VEGF gene expression was used a diagnostic marker. Spheroids which have not any access to blood vessels, try in situation of oxygen absence to promote other cells (endothelial) to form vessels (up-regulation of VEGF) to get access to blood and with this oxygen. Again from both systems 400-μm and 1500-μm pitch arrays a growth curve combined with the determination of the VEGF gene expression was analyzed and plotted in figure 3.3.4. The VEGF expression level is connected with spheroid size depending on the different pitches of the arrays. The expression level from spheroids cultured on the densely packed 400-μm pitch arrays were significantly ($p < 0.001$) up-regulated by day 7 with diameters of 179 (SD ± 14). On the larger and less dense packed 1500-μm pitch array VEGF expression was up-regulated ($p < 0.001$) from day 10 on with diameters of 320 μm (SD ± 29).

This later response in a larger spheroid shows, that oxygen supply can be modulated and controlled over the spheroid density per array. Importantly, these results demonstrate that the modulation of the array density can be used to produce well-defined spatio-temporal models of developing pathophysiology. This can be used to define operation windows of pre-hypoxic, hypoxic (but pre-necrotic) and necrosis culture phases, in which the effect of metabolic status can be elucidated or the responsiveness of spheroids to anti-cancer treatments.
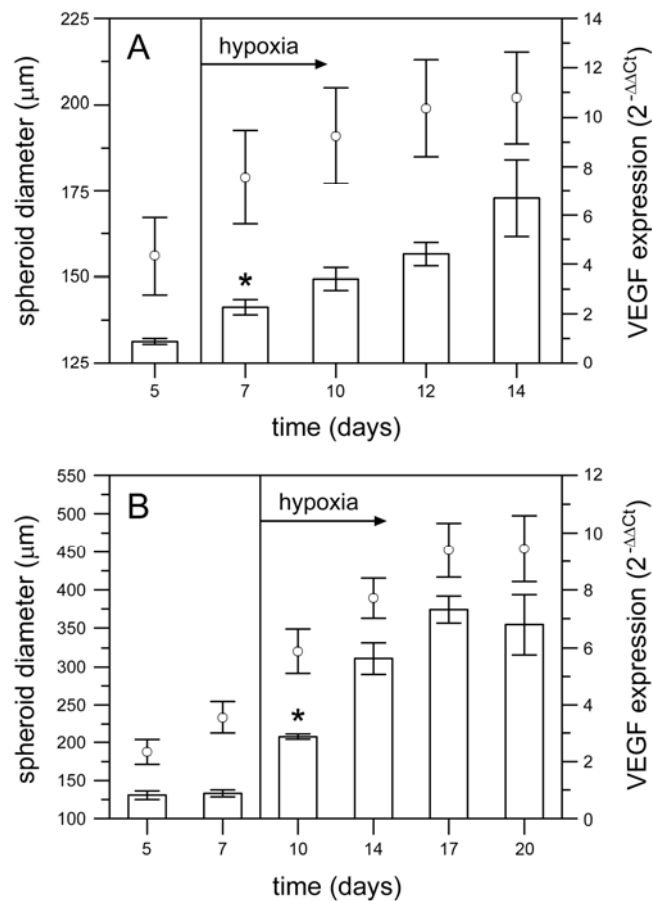
Figure 3.3.4: VEGF gene expression (bars) of spheroids grown on a 400-µm pitch (A) array and 1500-µm pitch (B) array was determined under the aspect of spheroid diameter (circles) and time (up to 20 days). Mean diameter values ± standard deviations are from 30 measurements. Expression levels are normalized relative to levels from monolayer cultures. Data points are mean expression values ± standard deviation from triplicate conditions, with triplicate measurements from each sample (*p < 0.001).

For applications fully viable spheroids are required, the 400-µm microarray system can be used as a mother dish, like the hanging drop method. It is then possible to create thousands of healthy spheroids, harvest them early before they develop hypoxia and transfer them for another 24 h into a petri dish with media. Because of the strongly aggregation of spheroids grown on the microarray, it is no problem to harvest them in an early stage of development (day 7). The 24 h in a non-adhering culture flask helps correcting the capped spheroid morphology for natural shape remodeling (N.C. Rivron et al., 2012) into a highly spherical tissue (x = 91%; y =95%; z = 96%).

3.3.2 Spheroid chemosensitvity

We have seen in the chapters before that the spheroids on chip develop pathophysiological gradients, which now should be analyzed in terms of chemosensitivity. The arrays are used as a mother dish for drug testing of potential new compounds. The anti-cancer agent irinotecan was used in an *in situ* dose response experiment. Irinotecan stops the DNA-replication process in the S1-phase of cells by inhibiting the DNA-Topoisomerase I (Hsiang et al., 1989; Jaxel et al., 1989). Again arrays with pitches of 400 µm and 1500 µm were chosen to compare the response of rapid and slow growing spheroids. Irinotecan was added at two different pathophysiological states: pre-hypoxic and hypoxic state (but pre-necrotic) to compare the different phases of culture. The spheroids were exposure for 3 days with irinotecan on chip, following a measurement of the acid phosphatase activity in a 96 well plate, a reliable indicator of viable cell count of HT29 spheroids with diameters up to 650 µm (Friedrich et al., 2007a; Friedrich et al., 2007b). Originally spheroid diameter should have been used as indicator for drug efficiency, but the spheroids did not response to drugs in a measureable way. Dead cells do not disappear and spheroid growth was not compatible with the drug concentration, so that size measurements were unaffected.

The results of the irinotecan treatment on spheroids were compared to the gold standard method, testing new drug compound on monolayer cultures. The irinotecan dose-response experiment on monolayer cultures gave a 50% inhibition concentration (IC_{50}) value of 32 µM (95% CI 22-49), significantly ($p < 0.001$) lower than the IC_{50} values of spheroid cultures: Pre-hypoxic phase spheroids cultured on the 400-µm pitch arrays (Exposure days: 4-7) had an IC_{50} of 102 µM (95% CI 49-239) which was significantly ($p < 0.001$) increased to 307 µm (95% CI 144-634) during the hypoxic culture phase (Exposure days: 11-14) (see fig. 3.3.5 (A)) regarding to the changed metabolism. The pre-hypoxic spheroids cultured on the 1500-µm pitch array (Exposure days: 4-7) had an IC_{50} of 62 µM (95% CI 23-96) which was also significant ($p < 0.001$) increased to 224 µM (95% CI 123-408) in the hypoxic culture phase (Exposure days: 10-

13) (Fig. 3.3.5 (B)) depending on the hypoxic metabolism and the increase in spheroid size.
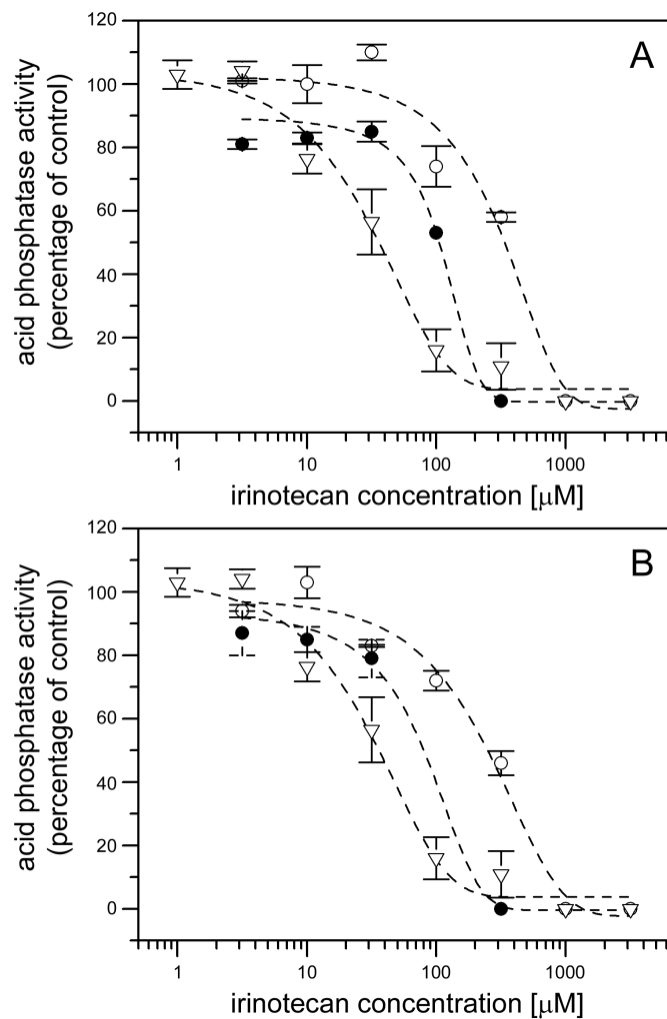
Figure 3.3.5: Irinotecan dose response curve with 400-µm pitch array (A) and 1500-µm array (B) spheroids in pre-hypoxic (filled circle) and hypoxic (white circle) phase. The irinotecan concentration is plotted against the acid phosphatase activity (relative to untreated controls) for monolayer cultures (triangle). Curves were fitted using a Hill function with variable slope. Mean values ± standard deviation is from triplicate experiments, with each replicate involving the measurement of 8 individual spheroids.

A table with the treatment periods, culture conditions, spheroid diameter, volumetric growth and the IC_{50} values can be found in the appendix 1, Table 1. In summary the spheroids show a very much reduced sensitivity towards irinotecan than simple monolayer culture.

In simple monolayer cultures irinotecan has direct contact to the cells. The drug does not need to penetrate through layers of cells to affect them; the only barrier is the cell membrane. In spheroids the 3D character, scale, cell proliferation rate and hypoxia state plays an important role which can lead to reduced drug efficacy. Irinotecan inhibits DNA synthesis; this explains the reduced drug efficacy in slowly proliferating spheroids cultured on 400-µm pitch arrays. As described in Table 1, Appendix the cell proliferation rate tends to zero in the hypoxic phase of culture (spheroid diameter and volumetric growth data) producing spheroids which are only 17 µm larger than the one cultured in the pre-hypoxic phase. This still standing of proliferation (cell cycle arrest) results in a reduced irinotecan efficacy (IC_{50} = 307 µM). The spheroids cultured on the 1500-µm pitch array have a higher proliferating rate throughout the experimental time-scale (240 µm diameter spheroid pre-hypoxic phase, 363 µm diameter hypoxic phases). Here the reduced chemosensitivity can be caused by the penetration barrier irinotecan has to cross to get into this large tissue. However, in the hypoxic phase of culture it is unclear, if the increased scale and/or the metabolic gradients causally relate to the reduced drug efficacy (IC_{50} = 224 µM). To determine this, more experiments using microarray format are required to figure out which factors are responsible for the reduced chemosensitivity.

3.4 Outlook and Conclusion

In this study we used our microarray technology for the production of fully developed HT29 spheroids with diameters up to 550 µm. On the microarrays tumour cells do not just aggregate together, but grow starting from a monolayer causing in mass transfer gradients surrounding and within the spheroids mimic very well avascularised tumours *in vivo*. The array dimensions dictate the spheroid model type to determine the development of metabolic and pathophysiological gradients. The microarray technique allows the production of tumour spheroids with different scales and different magnitude gradients for the *in situ* or *ex situ* analysis of potential anti-cancer treatments. The influence of cell proliferation rate, impact of scale and

metabolic status on drugs can be determined. All together these benefits show the large potential of the array format supporting the widespread adoption of the tumour spheroid model in anti-cancer treatment investigation, especially under the aspect of delivering high content information in response to pathophysiological gradients. The import of our PDMS microcontact printing technology into standard microtitre plates offers the potential to use the spheroid platform for high-throughput screenings. The compound databases could be screened under different aspects of drug chemosensitivity depending on the development and growth stage of the tumour spheroids.
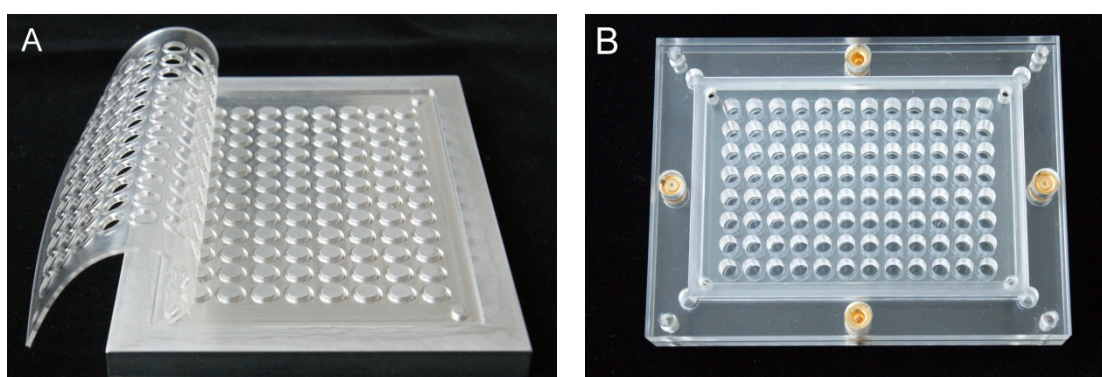

Figure 3.3.6: A moulded 1-mm-thick PDMS gasket array (A) can be used to seal printed glass slides via magnetic coupling to the frame of an industry standard 96-well plate (B).

The present study has been focused on the physical and biological aspects of the cultured HT29 spheroids that affect chemosensitivity. Other applications are imaginable like radiotherapy of the spheroids on chip followed by hyperthermia and chemotherapy, gene therapy or cell-and antibody-based immunotherapy (Desoize et al., 1998; Desoize and Jardillier, 2000; Dubessy et al., 2000; Mueller-Klieser, 1997; Olive and Durand, 1994; Santini et al., 1999). Too mimic the heterogeneity of tumour tissues, the chip can be used for the production of co-culture spheroids like a mixture of different breast cancer cell types (Karacali et al., 2007) or the mix of cancer cells with fibroblasts (Friedrich et al., 2007a; Krueger et al., 2005). The investigation field for spheroid research is huge especially under the aspect to find so called tumour- or cancer-initiating cells (TIC/CIC) (Ricci-Vitiani et al., 2007; Singh et al., 2004). In theory one single cell could be responsible for tumour growth. Internal of a cell line

population cells could show heterogeneity. Microarray technology could help addressing this question.

Still spheroid culture methods provide tumours with necrotic cores simulating avascularised tumours or metastasis. Already there are investigations to mix tumour spheroids with endothelial cells to grow vessels within the spheroid to mimic the cancer microenvironment *in vivo* (Hsiao et al., 2009). The challenge is not to produce vessels, but to initiate a micro-flow through them to supply the spheroids continuously with nutrients. These models are also used for the identification of pro- and anti-angiogenic potential of drugs (Ghosh et al., 2007; Kern et al., 2009; Kunz-Schughart et al., 2006; Wenger et al., 2005).

Chapter 4: Microtrack patterning improving the Network Formation Assay
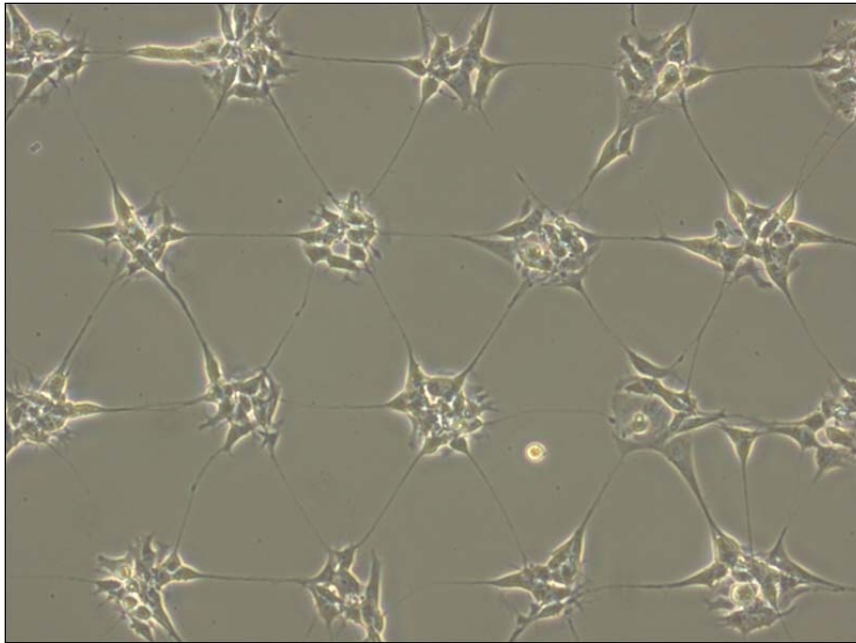
The work in this chapter was published in part as:

"The network formation assay: a spatially standardized neurite outgrowth analytical display for neurotoxicity screening".

Frimat JP, Sisnaiske J, Subbiah S, **Menne H**, Godoy P, Lampen P, Leist M, Franzke J, Hengstler JG, van Thriel C and West J; *Lab on a chip*. 2010, Volume 10:701-706*

"High fidelity neuronal networks formed by plasma masking with a bilayer membrane: analysis of neurodegenerative and neuroprotective processes."

Hardelauf H, Sisnaiske J, Taghipour-Anvari AA, Jacob P, Drabiniok E, Marggraf U, Frimat JP, Hengstler JG, Neyer A, van Thriel C and West J; *Lab on a chip*. 2011, Volume 11:2763-2771*

"Plasma stencilling methods for cell patterning"

Frimat JP, **Menne H**, Michels A, Kittel S, Kettler R, Borgmann S, Franzke J and West J: Analytical and Bioanalytical Chemistry, 2009, 395, 3, 601-609 **

"Cell patterning for spatially standardized cell biology"

Thesis: Frimat JP

* The work presented was highlighted in the media, including the RSC´s Chemical Technology, the New York Times, the MIT Technology Review, Sat.1, WDR and Deutschlandfunk.

** Winner of the "ABC Best Paper 2009" award.

A German and an international patent were successfully filed as:

"Verfahren zur Messung des Neuritenwachstums" („A Standardized Neurite Outgrowth Assay"); West J, Frimat JP, Sisnaiske J, Hengstler JG and van Thriel C.

DE 10 2009 021 876.9, EP 09 012 960.2 and PCT/EP2010/002811. May, 2010

Part of this work in this chapter won Best Poster Award at "Marktplatz bio.Dortmund 2011":

"High fidelity neuronal networks formed using bilayer plasma stencilling."

Hardelauf H and West J. The 1st Annual NRW Conference on Biotechnologies, Dortmund; Germany, September 2011.

4.1 Introduction

In the last chapter the successful establishment of the PDMS µCP method has been demonstrated for the mass production of uniformly-sized tumour spheroids. In this chapter a second application, the "network formation assay", will be described. Instead of tumour spheroids, neuron cells will be patterned for the screening of neurotoxic substances. Further improvements of the system lead away from PDMS µCP to another surface modification to deal with the demands of primary cells.

The nervous system is a very sensitive organ. Chemicals can affect the nervous system at different end points, like the cytoarchitecture structure of the neurons or interfere with the neuro-chemical processes, which are responsible for the information exchange. A lot of daily used substances have never been tested on their neurotoxic potential. The Europe´s Reach legislation (Registration, Evaluation and Authorization of Chemicals) and the United States Environmental Protection Agency directives have now defined that 30.000 chemicals out of 100.000 substances available on the market must be tested for their toxicity including neurotoxicology. These chemicals have not been adequately tested nor appropriately evaluated over the last decades.

The basis of valuation is the use of *in vivo* rodent models, making the screening of large numbers of chemicals impractical, expensive, time consuming and unethical. To avoid many animal experiments there is a tendency to use simplified *in vitro* cell culture experiments for high-throughput screenings of chemicals (Coecke et al., 2007; Lein et al., 2005; Leist et al., 2008; Radio and Mundy, 2008). These systems can be used to identify substances without neurotoxic effects, so that these substances do not have to be tested in a rodent model. This saves around 80 test animals per negative tested substance in the field of neurotoxicity and even more animals for developmental neurotoxicity (~ 140 dams and ~1000 pups).

One promising *in vitro* approach is the "neurite outgrowth assay" for the measurement of axonal and dentritic outgrowth (collectively termed neurites in neurotoxicology). Neurite outgrowth is a sensitive end point for the determination of neuronal interconnectivity and neuronal network formation and can be used as a marker for neuronal development. In combination with physiological-basing

pharmacokinetic models the results of the neurite outgrowth assays correlate well with *in vivo* observations and can be used to determine the neurotoxic potential of substances (Forsby and Blaauboer, 2007). In these assays neurons get seeded in a low concentration to get isolated neurons and easy detectable neurites. In the easiest form the assay measures neurites per neuron or the percentage of neurons with neurite outgrowth (Radio and Mundy, 2008). Importantly, neurite only counts as an outgrowth when it is longer than the neuron itself (Adlerz et al., 2003; Morooka and Nishida, 1998), that makes the measurement procedure time-consuming and to a very complicated process. Each individual cell must be manually identified, imaged and the length of the non-linear outgrowth has to be measured. To avoid this, automated systems for high-throughput screenings have been developed to analyze the neurite outgrowth (Liu et al., 2007). Unfortunately, these systems require fixation and antibody staining of the cells (Radio et al., 2008; Ramm et al., 2003), so that dynamic processes cannot be used as a potential readout marker. The development of neurite outgrowth over time with or without drug treatment cannot be monitored. Also these automated systems are very expensive (up to 200.000 €) and so limiting the availability for many labs. This hampers the inter-lab validation of the tested substances, which is an important aspect of the REACH guidelines. There is a need for a standardized *in vitro* platform using neurite outgrowth as marker which is rapid, simple, reproducible and records neurite development to test and identify neurotoxic substances.

Microtechnologies can be used to meet many demands for fundamental research. Especially micropatterning techniques can be applied to different fields like industrial applications in tissue engineering (Nelson and Tien, 2006), drug discovery (Castel et al., 2006; Hardelauf et al.; Hirschhaeuser et al.; Khetani and Bhatia, 2008) and toxicology screenings (Frimat et al., 2009c; J. West, DE 10 2009 021 876.9 and PCT/EP2010/002811; Khetani and Bhatia, 2008). The cell structure and thus the behavior get preserved on these arrays by ordering the cultures within tissue dimensions, geometries and diffusion gradients. Ordered array systems have also the advantage to provide a display for rapid and high content analysis (Frimat et al., 2009; Schauer et al.; Wissner-Gross et al.). This ordered form-function relation of the nervous system has resulted in the replication of engineered analogs in the form of

spatially defined neuronal networks. The first work on patterning neurons on chip involved photolithographic silane patterning (Corey et al., 1996; Healy et al., 1994; Kleinfeld et al., 1988), later the focus changed to microcontact printing of cell adhesion materials (Nam et al., 2006; Ruiz et al., 2008; Shi et al., 2007). The first generation of our novel neuronal microarray, termed network formation assay (NFA) (Frimat et al., 2009) was produced by thin film PDMS microcontact printing. It is a simple neurite interconnection display and was used for the rapid and sensitive analysis of the dose-dependent inhibition measurement of acrylamide neurotoxicity (Fig. 4.1.1).
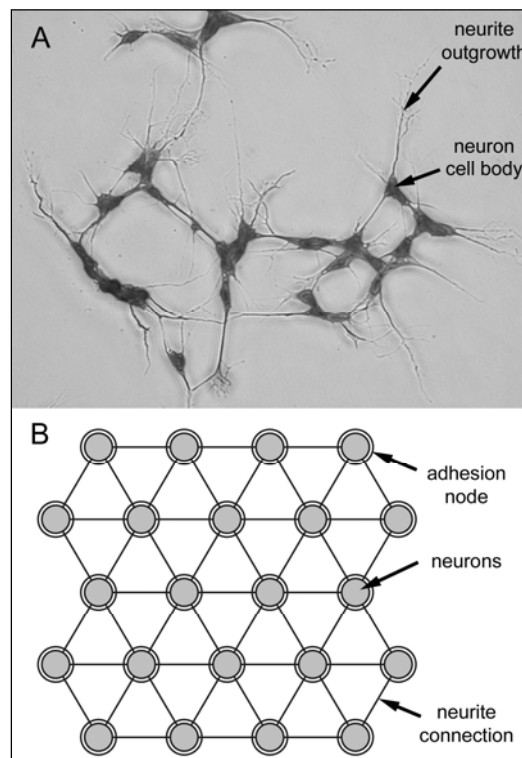

Figure 4.1.1: Differentiated SH-SY5Y neurons cultured in a standard tissue flask are irregular distributed and have irregular neurite outgrowths (A). The network formation assay (NFA) provides an ordered hexagonal system with equidistant spots that ensure the same length of all neurite interconnections and, importantly, these exceeded the length of a neuron (Frimat et al., 2009).

Thin film PDMS microcontact printing provides simply hydrophilic-hydrophobic surface contrasts. Other routes like UV photochemical patterning (Corey et al., 1996; Ravenscroft et al., 1998; Welle et al., 2005), photoresist masking (Corey et al., 1996;

Detrait et al., 1998) or with stencils (Frimat et al., 2009; Rhee et al., 2005) during plasma-based oxidative patterning of hydrophobic background have been used to contrast surfaces, too. These surface patterns can be used for patterning standard cell lines. Our previous work was based on thin film PDMS printing to pattern cell adhesion. This approach was suitable to array neuron-like cell lines for undertaking the NFA.(Frimat et al., 2009) The human neuroblastoma cell line SH-SY5Y was used as a model system to recapitulate aspects of the human *in vivo* state with neurodevelopmental end points. The cells are differentiated with retinoic acid which induces neurite outgrowth and the formation of functional synapses.(Adem et al., 1987; Pahlman et al., 1990) Differentiated SH-SY5Y cells have low levels of proliferation and the affinity for cell adhesion,(Pahlman et al., 1984) which helps patterning the cells.

It has been reported before that neuron cells do not adhere on hydrophobic PDMS (De Silva et al., 2004; De Silva et al., 2006; Frimat et al., 2009; Millet et al., 2007; Reyes et al., 2004) underlining the ability to pattern the cells with PDMS μCP. No further surface modification steps were needed to pattern SH-SY5Y cells. The cell media contain adhesion proteins, which can only assemble correctly in a bio-active state on the hydrophilic regions promoting cell adhesion and cell patterning. The hydrophobic PDMS pattern was stable for at least 2 weeks.

The NFA consists of glass slides (25 x 25 mm) which contain 25 arrays each with 367 adhesion nodes separated by 100 μm, which fulfills the neurite classification criteria that an outgrowth has to be equal to or longer than the cell body diameter (cell diameters are typically 10 to 25 μm (Adlerz et al., 2003; Morooka and Nishida, 1998)). The assay provides a total of 9175 adhesion nodes with 70 μm diameters, each accommodating 7 cells on average. Differentiated SH-SY5Y cells occupied the pattern across the array with >70% of the nodes occupied. The occupancy levels were reproducible on all arrays from the same batch as well as from different batches (Fig. 4.1.2), making the NFA to a reliable tool with excellent reproducibility. Higher pattern occupancies were not observed in this assay format. This could be explained by the natural behavior of these neuron cells which tend to cluster together in already

occupied nodes, instead of migrating to nearby empty nodes, necessitating transport across the PDMS material that prohibits cell adhesion.
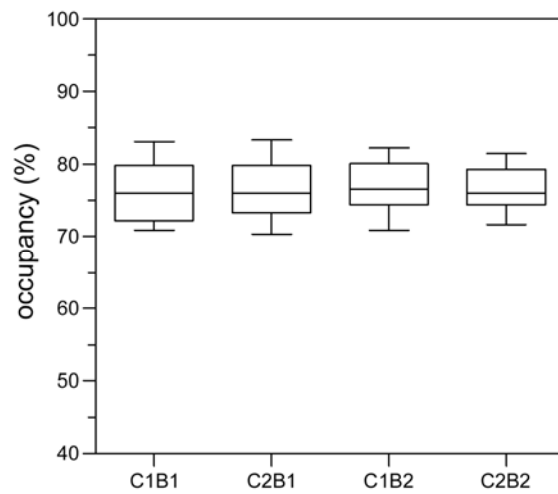

Figure 4.1.2: Box and whiskers plot showing the reproducibility of pattern occupancy across the 25 arrays for pairs of chips (C1 and C2) and two different batches (B1 und B2) (Frimat et al., 2009).

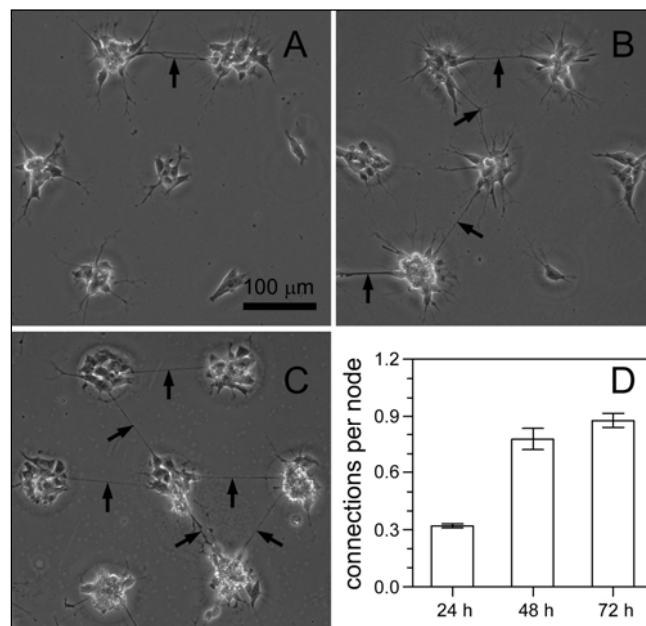*Figure 4.1.3: Development of neuronal networks at 24 h (A), 48 h (B) and 72 h (C). Black arrows highlight the interconnections. During the 3 days of culture, the mean number of connections per node increased from 0.32 to 0.88 (D) (Frimat et al., 2009).*

The development of an on-chip neuronal network in the hexagonal orientated arrays is shown in figure 4.1.3 (A - C). 24 h after seeding the SH-SY5Y cells start forming

interconnections which are indicated by the arrows in figure 4.1.3 (A). Cell division and proliferation still occurs on chip. A time lapse video showing that neurons are able to move to vacant nodes by inch along neurite outgrowths is available online: (http://www.ifado.de/en/research_applications/research_groups/neurotox/network-plasticity/index.html). Array-based neuronal migration events have been reported before by Ruiz (Ruiz et al., 2008). Nevertheless, PDMS acts as a strong cell repellent material, the neurite outgrowth are able to cross the PDMS barrier and interconnect with neighboring nodes. It is suggested that chemical gradients direct the growth cones of neurites to find other neurons guide network formation. Another observation on live networks suggests that once connections are formed, they are not fixed to the PDMS surface, but are instead suspended. This is evidenced by the fact that agitation of the culture medium causes the interconnections to vibrate.

The NFA is a simple and rapid analytical read-out. The dose response analysis of 7707 nodes (367 nodes, with 7 different concentrations in triplicate) takes around 3 h. In contrast, the manual assessment of neurite length using the traditional neurite outgrowth assay is labor intensive and takes about 10 h for the analysis of only 200 cells (Radio and Mundy, 2008). The defined coordinates of the nodes and the interconnections also enable this system to be highly desirable for automated image capture and processing. For the read-out the system does not need to be fixed or stained, so that the analytical endpoints are not terminal. This allows the collection of information of the network in its dynamic state by capturing periodically or continuously the connection formation.

A dose-response experiment using the neurotoxin acrylamide was undertaken with differentiated SH-SY5Y cells (Frimat et al., 2009). After an acrylamide uptake of 24 h the dose dependency was compared with data from the CellTiter-Blue® Cell Viability Assay (Figure 4.1.4 left). The sigmoidal dose-response curve produced over two orders of magnitude was almost 10-fold more sensitive than the cytotoxicity test, revealing specific neurotoxicity effects whereas the viability assay only captures gross cytotoxic effects. The CellTiterBlue® assay gave a 50% inhibition concentration (IC_{50}) of 5.1 mM (95% CI 4.2–6.1) whereas the concentration that caused a 20% reduction in network formation (NI_{20}) relative to controls was 0.26 mM (95% CI 0.12–0.46). These values are

equivalent to the 20% SH-SY5Y neurite degeneration (ND_{20}) acrylamide concentrations (0.25 and 0.21 mM) reported by Nordin-Andersson and colleagues (Nordin-Andersson et al., 1998; Nordin-Andersson et al., 2003). A following NFA experiment gave an NI_{20} value of 0.28 mM (95% CI 0.17–0.38, Fig. 4.1.4 right) showing the excellent reproducibility of the assay with a narrow 95% confidence demonstrate the robust character.
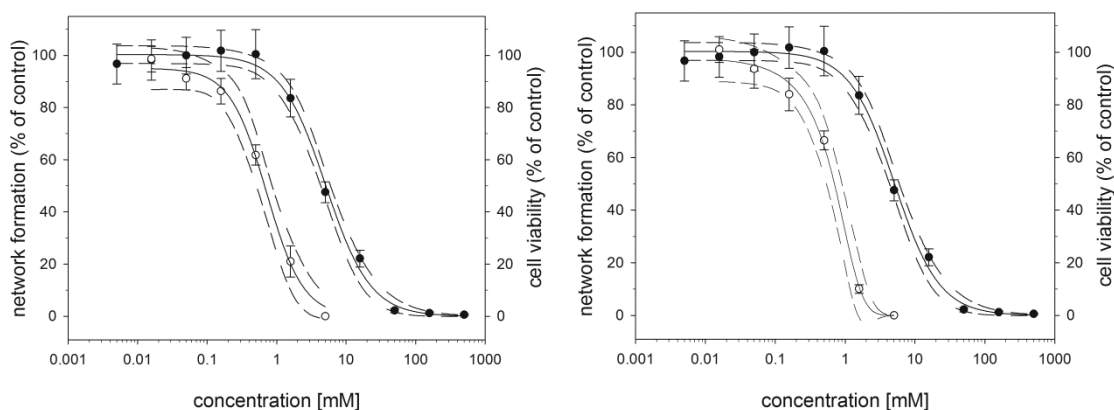

Figure 4.1.4: Sigmoidal acrylamide dose–response curves from the NFA (open circles) and the CellTiter-Blue® Cell Viability Assay (black circles). Data were measured 24 h after the exposure to acrylamide. Data points with standard deviation are plotted along with non-linear regression curves for the mean (continuous line) and the 95% confidence intervals (dashed lines) (Frimat et al., 2009). The excellent reproducibility of the experiment is shown in the right figure.

The network was kept on monitored daily over a period of 3 days following the exposure of acrylamide. Networks with acrylamide concentration < 0.5 mM recovered to control levels on day 3, demonstrating that sensitive neurotoxicity testing requires early stage analysis. Higher acrylamide concentrations of 1.58 mM and 5 mM were cytotoxic observed by occupancy depletion from day 2 on. Pattern occupancy can therefore be used as a surrogate cytotoxicity measure. In this way the NFA showed very clear distinction between neurotoxic from cytotoxic effects using the same cells. A dose-dependent reduction in network formation at non-cytotoxic concentrations was also shown by the inhibition of the mitogen-activated protein kinase (MAPK) ERK1/2 and phosphoinositide-3-kinase (PI-3K) signaling pathways done by *Frimat* et al.

The first generation of the network formation assay was designed for the human SH-SY5Y cell line. In future the NFA should be used to test substances on their potential neurotoxicity on gold standard primary mouse neurons. However, primary and stem cell cultures need special adhesion proteins mainly constituents of the extracellular matrix like collagen, laminin or ornithin. These proteins mimic the *in vivo* adhesion microenvironment of cells. Problematic, photoresist processing is not sufficiently biocompatible for most proteins (Douvas et al., 2002; Sorribas et al., 2002), so that instead soft lithography in form of microcontact printing is used to pattern directly biologically active adhesion proteins on a surface (André Bernard, 1998; Kane et al., 1999). The proteins get transferred by a PDMS stamp, in which the elastomeric character allows conformal contact to surfaces for micron-scale patterning outside the cleanroom. Protein µCP is a simple, rapid and inexpensive replication technology for biologists, (Whitesides et al., 2001; Xia and Whitesides, 1998a) which has been widely used to pattern neurons (Vogt et al., 2005).

Patterns for the development of neuronal networks of primary and progenitor neurons need micron-scale protein tracks which allows neurite outgrowth, but are narrow enough to prevent cell adhesion. The printing technique needs to be reproducible across chip, chip to chip and batch to batch to undertake experiments with confidence. Protein µCP has its limitations under the aspect of producing homogeneous prints especially at the prints edges (Falconnet et al., 2004; Fink et al., 2007). PDMS microcontact printing with interconnected pattern has been done on PLL-coated substrates to establish a primary neuronal network (Fig 4.3.2). However the reproducibility and stability of the micron-scale tracks were not sufficient enough for the formation of neuronal networks. On the other hand thin film PDMS printing is also not suitable with the recommendation of printing micron-scale tracks over large areas. Because of its liquid state in the printing process excessive PDMS spreads into the micron tracks before it can be thermally cured. This prevents the reproducible fabrication of thin film PDMS prints for neuronal networks with micro-scale tracks. The partial or complete loss of the track prevents guided neurite outgrowth from primary and progenitor neurons. Neither µCP of proteins nor thin film PDMS µCP seems to be

suitable for this application so that a different kind of surface modification has to be found to pattern neuronal networks.

Poly(ethylene glycol) (PEG) is a well-known material that resists protein adsorption and thus cell adhesion (Malmsten et al., 1998; Zhang et al., 1998). The grafted copolymer of poly-L-lysine coupled with PEG (PLL-*g*-PEG) can be contact printed on culture surfaces, whereas proteins can assemble on uncoated areas and support cell adhesion (Csucs et al., 2003b). Again the across pattern reproducibility is not efficient enough and instead photoresist-based processing of the PEG layers can be used (Falconnet et al., 2004; Shah et al., 2009; Thomas et al., 1999). As an alternative deep UV (185 nm) photolithography can be used to pattern by photodegradation (Alang Ahmad et al.; Azioune et al., 2009). Importantly, for micron-scale patterning contact masking is required which reduces the lifetime of the expansive quartz masks necessary for UV transmission. Whereas μCP technologies can be used in every lab photolithography methods demand clean room conditions, which limits the access to most end-users, the biologists (Azioune et al., 2009; Fink et al., 2007; Whitesides et al., 2001).

In this chapter we show the establishment of the NFA for neuron-like cells by interconnected pattern arrays to meet the demands of primary neuron cells. For this we developed a bilayer membrane comprising multiple through-holes interfaced with microchannels and used it to pattern a PEG layer by plasma stencilling.

4.2 Material & Methods

4.2.1 PDMS microcontact printing

The PDMS microcontact printing process has been described before in chapter 2.2.1. For the network formation assay minor changes in design and printing process have been made: The entire 20 x 20 mm pattern consists of a 5 x 5 matrix of individual arrays with each containing 367 (altogether 9175) adhesion nodes. Each node had a diameter of 70 μm and was separated from neighbouring nodes by 100 μm. For the network formation assay for primary cells narrow tracks are needed. To create these tracks, excessive PDMS has to be removed in the printing process. For this the second print was not used to pattern cells, but the third and fourth ones. These prints have a higher resolution than the first and second print and were done on glass microscopy slides.

4.2.2 Cell culture

The human neuroblastoma cell line SH-SY5Y (DSMZ, Germany) was used in this study as a standard neuron cell line. The cells were cultured in Dulbecco´s modified Eagle medium (DMEM) supplemented with 10% (v/v) foetal bovine serum (FBS), and 1% (v/v) penicillin and streptomycin. SH-SY5Y cells were differentiated by adding 10 μM *trans* retinoic acid (Sigma-Aldrich) for 4 days. Clustering behaviour gets reduced, which increases the level of array occupancy than a 3 day treatment. Cells were harvested using 0.25% (w/v) trypsin and seeded on the array in a 1 mL suspension containing 2.0 x 10^5 cells and were incubated overnight at 37°C in a 5% CO_2 atmosphere. The arrays were washed with 1x PBS to remove non-adherent cells. Culture medium was replaced with fresh media also containing retinoic acid. A phase contrast inverted microscope (IX71, Olympus) was used to image the cell patterns and FITC-labelled protein patterns.

Lund human mesencephalic (LUHMES) cells were kindly provided from the Leist Lab (University of Konstanz, Germany) and cultured in advanced DMEM/F12 media.

Culture flasks were coated with 1 μg/mL Fibronectin and 50 μg/ml poly-L-Ornithine (PLO). The proliferation media was modified with 2 mM L-Glutamin (Sigma-Aldrich), 1% (v/v) N2 (Invitrogen) and 40 ng/mL FGF (fibroblast growth factor; R&D systems). The additives for the differentiation media were 2 mM L-Glutamin, 1% (v/v) N2, 1 mM cyclic AMP, 100 ng/mL Tetracyclin (both Sigma-Aldrich) and 20 pg/mL GDNF (glial cell lined-derived neurotrophic factor; R&D systems). The cells were cultured at 37 °C in a humidified 5% CO_2 atmosphere and harvested using 1.25 mg/mL trypsin/EDTA for a 25 cm^2 culture flask once ~ 80% confluence was attained.

Cells were seeded on the array within 1 mL media suspension containing 3.5 x 10^5 cells. The adhesion areas were modified with several substances, like PDL, Fibronection, Laminin or PLO. Media exchange of 6 mL volume took place periodic every 2-3 days.

4.2.3 CellTiter-Blue® Assay

Cytotoxicity was measured using the CellTiter-Blue® Viability Assay (Promega) using the following instructions: 100 μL medium containing 5 x 10^4 pre-differentiated SH-SY5Y cells were added per well of a 96 well plate. The cells were cultured with acrylamide at concentrations ranging from 0-500 mM for 24 h. After the exposure time 20 μL of CellTiter-Blue resazurin reagent was added to the culture media and incubated for 4h at 37°C: Viable cells convert the reagent into the fluorescent compound resorufin. Fluorimetry involved excitation at 540 nm and emission detection at 595 nm using a plate reader (Make, country).

4.2.4 Surface PEGylation

Glass substrates were ethanol and plasma cleaned and incubated for 1h at room temperature with the cationic copolymer of poly-L-lysine grafted with poly(ethylene glycol) by submersion in a 10mM HEPES (4-(2-hydroxyethyl)-1-piperazine ethanesulfonic acid, pH 7.4; AppliChem, Germany) buffer containing 100 μg/mL of PLL(20)-g-[3.5]-PEG(2) (Surface Solutions, Switzerland). Substrates were rinsed with a

sequence of 1 x phosphate buffered saline (PBS), MilliQ water and dried with in a N_2 stream.

4.2.5 Membrane fabrication and plasma masking

A SU-8 master was fabricated to prepare the PDMS membranes. The first layer of SU-8 2 (Shipley) was spin coated to a depth of ~1.0 μm and patterned using standard lithography for the interconnecting tracks. The second layer of SU-8 50 (Shipley) was spin coated to a depth of ~ 60 μm for the nodes, which were aligned to the nodes of the first layer. The arrays contain hexagonal patterns with 70-μm-diameter pillars connected via microchannels with a length of 100 μm and a width ranging between 1.0 to 4.0 μm. The arrays containing either 367 or 202 nodes divided in 16 or 36 square across a 24 x 24 mm area. For moulding, PDMS prepolymer and curing agent was mixed (10:1 (wt/wt), Elastosil® RT 601, Wacker) and first degassed before it was diluted in silicone fluid (1:4 (wt/wt), AK35, Wacker). 2 ml volume of the mixture was spin coated at 1600 rpm for 50 s followed by thermal curing at room temperature over night to produce ~ 55 μm thick membranes. The membranes were peeled from the wafer and oxygen plasma bonded (Femto, Diener Electronic) to a PDMS frame for easier handling. The bilayer membrane was imaged using a SEM (Quanta 200 F, FEI) shown in Fig. 4.3.4.
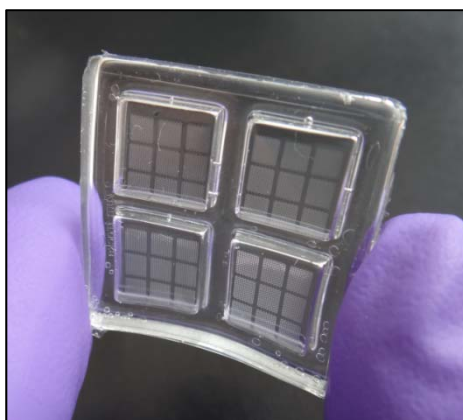

Figure 4.2.1: Bilayer membrane divided in four squares with 9 arrays each containing 202 adhesion nodes. The membrane is stabilized with a 2 mm thick PDMS frame. The picture was kindly provided by Sarah Waide.

For plasma masking, the PDMS bilayer membranes were conformally contacted to the PEGylated substrate surfaces, a virtue of the elastomeric nature of PDMS. The substrates with PDMS mask in place were plasma treated (70W, 40 kHz (Femto, Diener Electronic)) in a 0.2 mbar oxygen atmosphere for 60s.

4.2.6 Surface analysis

The physicochemical properties of the PEGylated surface were analyzed by contact angle measurements using 1 μL sessile water droplet. The zeta potential response of bovine serum albumin (Sigma Aldrich, Germany) in a 1 x PBS (pH 7.0) buffer at a concentration range of 6 nM to 18 μM were measured using SurPASS instrument (Anton Paar, Austria). PLL-*g*-PEG adlayers with and without plasma treatment were compared to plasma treated glass surface for their ability to resist protein adsorption using a sequential dosing experiment. X-ray photoelectron spectroscopy (XPS, AXIS-HS-spectrometer Kratos, Manchester, UK) was used to determine the chemical stoichiometry of PLL-*g*-PEG before and after plasma treatment. Glass was replaced with silicon substrates with the native oxide providing a glass-like substitute. For excitation a non-monochromatic Mg-Kα radiation source was used, with detection using a hemispherical analyzer with fixed analyzer transmission. Scan surveys were first undertaken using a 80 eV pass energy with 1 eV steps, followed by scans of the O1s, C1s, N1s and Si2p regions using a 20 eV pass energy with 0.1 eV steps. Relative quantification factors were obtained by calibration using poly(ethylene glycol) and poly(sodium 4-styrenesulfonate) standards.

4.2.7 Network analysis

The first generation of the NFA and preliminary experiments used a 24 x 24 mm substrates patterned with 16 arrays, each containing 367 nodes. This has been further developed to a design of 36 arrays each containing 202 nodes. The readout of the assay was defined as node occupancy, connection per node and track occupancy. Node occupancy is defined as the percentage of adhesion nodes occupied by one or more

cells. Connection per node is defined as the number of neurite interconnections relative to the number of occupied nodes across the entire 202-node array. Track occupancy is the percentage of tracks which are occupied by one or more neurons and is therefore blocked to form neurite interconnections. Reproducibility analysis involved measuring the patterning efficiency E_{patt}. (Frimat et al., 2009). It is defined as the number of cells adhering to plasma treated area N_p relative to the number of cells adhering to an equivalent sized non-activated area N_u and was calculated as a percentage according to:

$$E_{patt} = 2 \times (\frac{N_p}{N_p + N_u} - \frac{1}{2}) \times 100$$

4.2.8 Acrylamide degeneration assay

The degenerative effects of acrylamide along with the protective effects of co-treatment with calpeptin or brain derived neurotrophic factor (BDNF) were investigated. SH-SY5Y cells were differentiated for 4 days as explained in Chapter 4.2.3. The cells were then cultured for two further days on chip to establish a highly connected neuronal network. The media was replaced after the network establishment with serum-free media containing B27® (Invitrogen, Germany), retinoic acid. The networks were treated with 0.5 mM and 1 mM concentrations of the neurotoxin acrylamide (ACR, Sigma-Aldrich, Germany). A quarter of the arrays were daily co-treated with 1 µM calpeptin (CP, Merck, Germany), or once with 100 ng/mL BDNF (PAN-Biotech, Germany). The other quarters were samples only treated with acylamide and the untreated controls. The development of the neuronal networks was measured by counting the neurite connections daily for 3 days. Treatments were done in triplicate. Results were analyzed using a 2-factorial 4 x 7 ANOVA using the repeated measurements factor *time* (4-ary: 0, 24, 48 and 72 h after treatment) and the between subject factor *treatment* (7-ary: control, 0.5 mM ACR, 1 mM ACR, 0.5 mM ACR + 1 µM CP, 1 mM ACR + 1 µM CP, 0.5 mM ACR + 100 ng/mL BDNF, 1 mM ACR + 100 ng/mL BDNF). The network quality was measured in terms of `connections per node` (cpn)

and used as the dependent variable. Dunnett t-tests were used to compare the mean values at the 4 experimental intervals. For simplification the results of cpn values were normalized to the respective control conditions. All statistical analyzes used the raw data.

4.3 Results & Discussion

In the introduction the NFA has been introduced as an alternative read out system for neurotoxicity. The spatially standardized display allows high throughput screenings of potential neurotoxic substances. Traditional neurotoxicity tools rely on neurite outgrowth measurements as end-point indicators whereas the NFA measures the number of connection between neurons (the basis of memory and learning) which is a streamlined and therefore faster method than undertaking multiple (neurite and cell) length measurements. In addition, connectivity is a better functional indicator than outgrowth alone. The assay has been used to monitor inhibitory effects of acrylamide. The results were nearly identical with the data from the gold standard neurite outgrowth assay. All this indicates that the network formation assay has the potential to be a reliable tool to help testing 60.000 chemicals in a quicker and simpler way. The essential step is the transfer of this technology to the adhesion requirements of primary cells which are the gold standard cell material. The SH-SY5Y cells used for prior investigations required only a glass surface for adherence and growth. Compared to this primary cells need molecules, typically polyamines, such as poly-*L*-lysine (PLL) or poly-*D*-lysine (PDL). In a preliminary experiment it was possible to µCP a thin-film, patterned PDMS coating onto a PLL surface. The primary cells were not able to connect over the PDMS surface like the SH-SY5Y cells did. From this we concluded that the cells need connection tracks from one node to the neighboring nodes to allow guided outgrowth of neurites for the formation of a network. The development of the network formation assay for the demands of primary cells will be outlined in the following chapters.

4.3.1 Network formation assay with tracks

Microcontact printing of PDMS worked well as platform for the network formation assay (Frimat et al., 2009). To fulfill the demands of primary cells a stamp was designed, which had nodes, connected by tide tracks. Each stamp could be used for several prints in a row. The first print was discarded because of the excessive PDMS. Further prints showed that even a bit of excessive PDMS can block the tracks (Figure 4.3.1 left). Only the fourth print of the same stamp worked well with all tracks open. An example of a print is shown in figure 4.3.1 (right) with a channel width of 3.73 μm ± 0.35 μm. Unfortunately the PDMS height of ~ 4 nm measured by WLI was too thin for cell patterning. Cell media can puncture the thin PDMS film which causes the neuronal pattern to be lost.

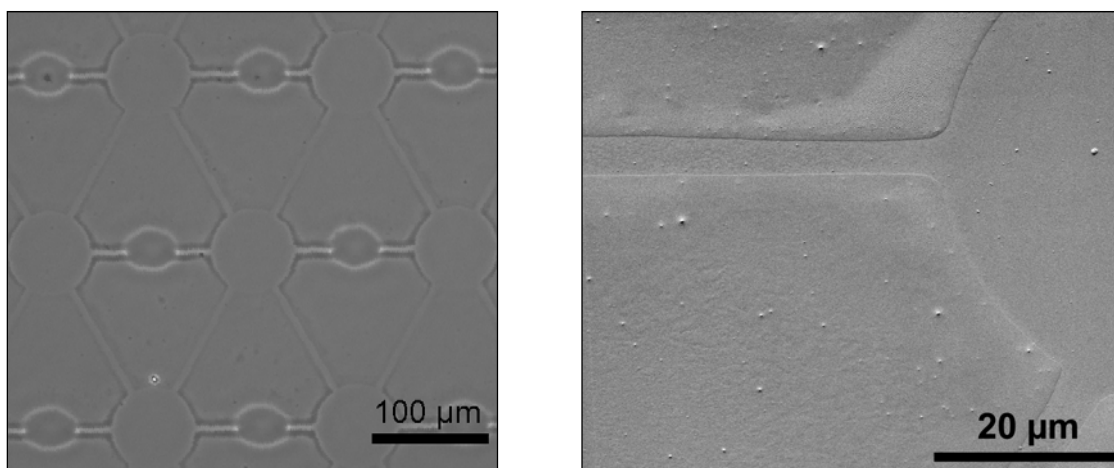*Figure 4.3.1: A third print with partly blocked tracks (left). A fourth print with open tracks showing a PDMS channel width of 3.73 ± 0.35 μm from a 5 μm template.*

Network formation with primary cells was possible (Figure 4.3.2), but with low reproducibility. Based on this PDMS μCP on PLL is not the method which can be used to pattern primary cells. Either the required tracks are blocked with extra PDMS or the print is too thin to resist cell adhesion over ordinary experimental time-scales (days). An alternative patterning method was therefore required to undertake the NFA using primary mouse neurons. The method must provide (i) adhesive coatings of polyamines with or without ECM proteins, (ii) material contrasts that resist neuron and neurite

adhesion and (iii) micron-scale tracks permissive for neurite outgrowth but not sufficiently wide to enable neuron adherence.
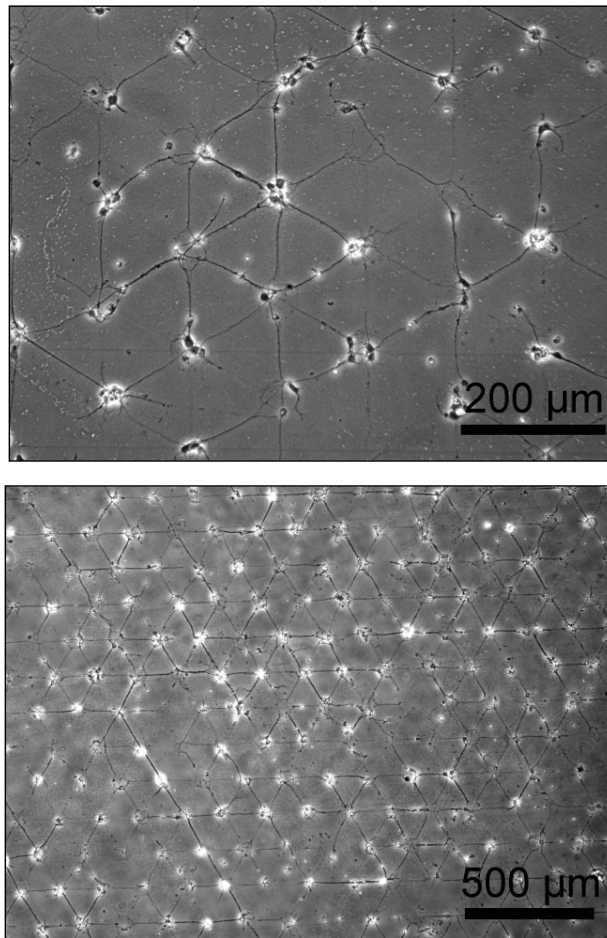

Figure 4.3.2: Primary network on a PDMS print with interconnecting tracks after a week of culture (cpn 1.92; occupancy 91%)

In this chapter we show the development of a patterning technique with micron-scale tracks that combines the protein rejecting qualities of PEG layers with the elastomeric features of soft lithography for rapid pattern replication outside the clean room. Oxygen plasma treatment of a PEG adlayer through a bilayer membrane with multiple through-hole interfaced with interconnecting tracks for protein adhesion were used to pattern neuron cells. The patterning technique was precise and reproducible to determine the optimal dimensions for the formation of high fidelity neuronal networks. We measured the degenerative effect of acrylamide on neurite

outgrowth on the networks as well as the buffering effects of calpeptin and brain-derived neurotrophic factor (BDNF) during co-treatment with acrylamide.

4.3.2 Surface chemistry of PLL-*g*-PEG

PLL-*g*-PEG assembles electrostatically onto the glass substrate (Kenausis et al., 2000) and creates an adlayer, which is protein repellent and thus cell repellent. The highly solvated state of the ether (C-O-C) repeats within the brush-like polymer (Roach et al., 2010) of PLL(20)–*g*[3.5]-PEG(2) causes minimal protein adsorption (< 2 ng/cm²) (Pasche et al., 2003). The PLL-*g*-PEG adlayer was determined with zeta-potential measurements. Surface coating on activated glass was rapid, with the zeta potential rising from approximately -120 mV to -40 mV within minutes. XPS analysis also showed that the presence of the PEG adlayer screens the silicon, causing a >10% reduction in the Si2p signal (see Table 2, Appendix). Protein rejection was confirmed by the stepwise addition of albumin concentration. The zeta potential stayed stable (~ -40 mV) up to a concentration of 18 µM (1.20 mg/mL, Figure 4.3.3), which shows the protein-resistant nature of the PLL-*g*-PEG adlayer. Higher, physiologically irrelevant concentrations were not measured.
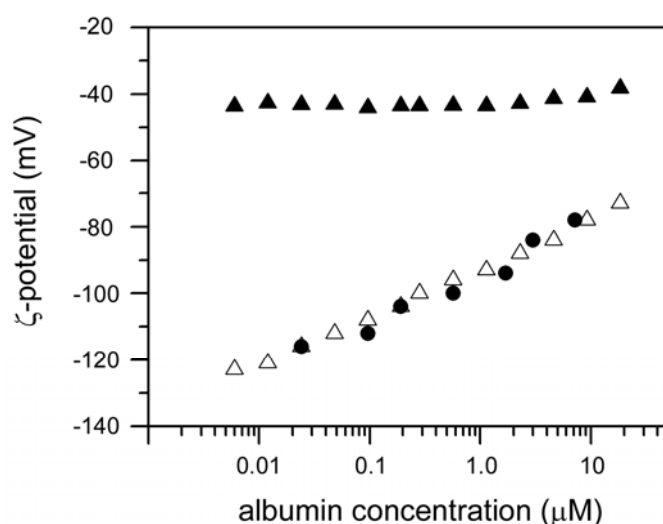

Figure 4.3.3: Zeta potential measurements of glass (black points), PLL-g-PEG (black triangles) and plasma treated PLL-g-PEG (white triangles) recorded during the stepwise addition of 6 nm to 18 µM concentrations of albumin.

XPS was used to identify the effect of plasma treatment on the atomic stoichiometry of the PEGylated surface. The results are documented in Table 2 in the Appendix. The main C1s (*e.g.* C-O-C) and N1s signals from the PLL-*g*-PEG adlayer were markedly diminished while the COOH signal at ~289 eV increased 7-fold. Together with the restoration of the Si2p signals, the data indicate that the adlayer has been oxidized. Similar effects have been observed by the oxidation of PEG surfaces by UV irradiation (Ahmad et al., 2010; Azioune et al., 2009). Furthermore, the contact angle was reduced from 29.1° (SD ± 2.1°) to <5°, a value consistent with oxygen plasma treated glass substrates. The response of the plasma treated PLL-*g*-PEG layer and the plasma treated glass substrate to albumin were nearly identical (Figure 4.3.3). The zeta potential increased from -125 mV to -73 mV during the addition of albumin to a final concentration of 18 μM. These results indicate that plasma treatment disintegrate the PLL-*g*-PEG adlayer and produces a glassy-like surface which is suitable for protein adsorption.

4.3.3 Bilayer membrane for neuronal network patterning

PDMS membranes with through holes have previously been used for surface (Jackman et al., 1999) and cell patterning (Folch et al., 2000; Ostuni et al., 2000; Tourovskaia et al., 2003). A drawback of membranes is the limitation in the pattern design like the inclusion of continuous and interconnected pattern. Furthermore, the membrane stability is limited by the aspect ratio (typically 1) of the mould and the fragility of thin (<10 μm) PDMS membranes, which prevents the inclusion of micron-sized features. To overcome this problem we have developed a bilayer membrane masking approach. The complete membrane has through-hole features which are connected by microchannels (Figure 4.3.4).
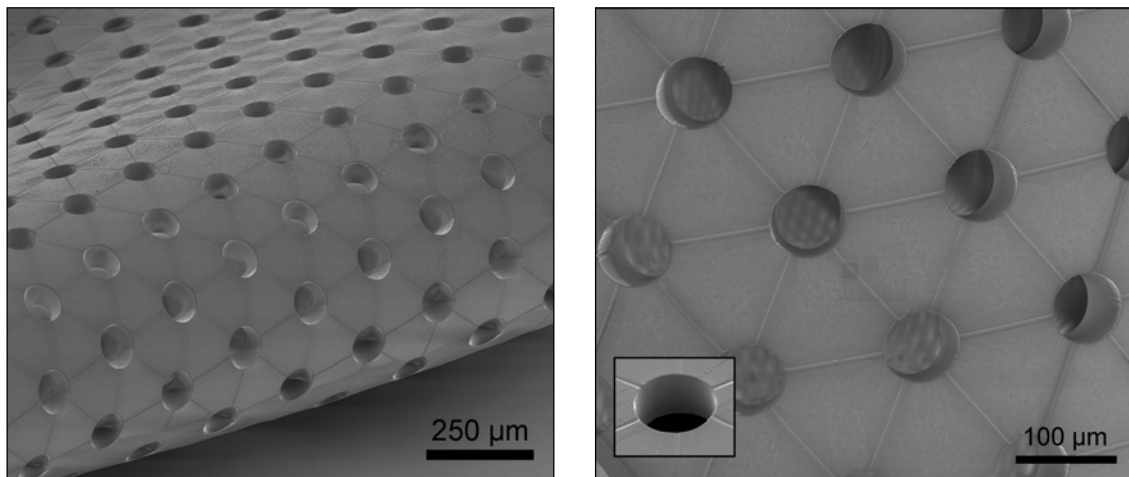
Figure 4.3.4: SEM images of a 50-µm-thick PDMS stencil. The thin stencils are elastomeric, which is necessary for conformal contact. The through-holes have a diameter of 70 µm and are interconnected by 100-µm-long microchannels with a height of 1.0 µm and a width of 3.0 µm.

The microchannels are recessed in the membrane with a depth of ~ 1.0 µm for the production of micron-scale interconnecting patterns by oxygen plasma treatment.

To produce the pattern the bilayer PDMS membrane was simply contacted and gently pressed onto the PLL-*g*-PEG surface. Plasma masking was done for 12 s to produce oxidation patterns in the PEG adlayer with even the smallest channel features of 1 µm width over the entire masked area. The oxygen plasma was able to penetrate through 100-µm-long channels with a cross sectional area of 1 µm² within seconds.
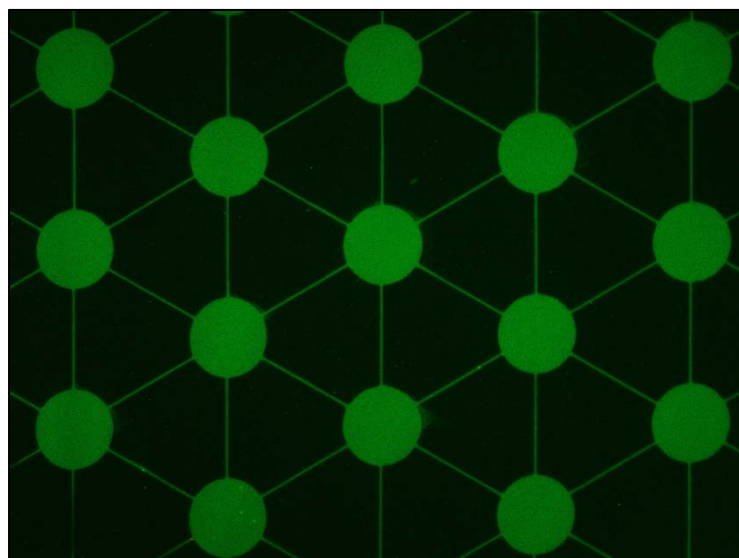

Figure 4.3.5: High fidelity pattern imaged using a FITC-conjugated avidin protein treatment shows the precision plasma-oxidation patterning of PLL-g-PEG.

The oxidized patterns were stained with FITC-conjugated proteins (Fig. 4.3.5). The high resolution (SD ± 220 nm) micron-scale oxidation pattern was perfectly transferred to the PEGylated surface as shown in figure 4.3.6.
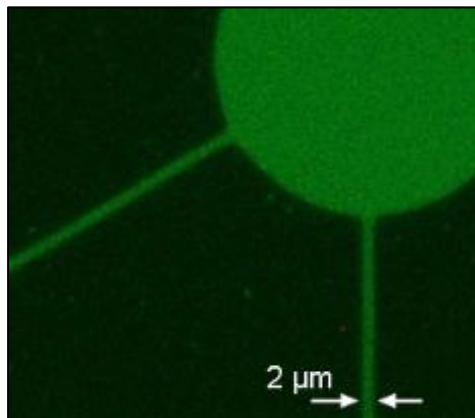

Figure 4.3.6: High magnification image of a FITC-conjugated protein pattern. A membrane with 2-μm-wide tracks was used for plasma stencilling. The FITC-protein-stained tracks had a width of 2 ± 0.22 μm.

The bilayer membranes can be reused around forty times, after this the membranes dry out and get fragile. The conformal contact to the underlying substrate is not guaranteed anymore. The plasma chamber has the capacity for multiple substrates at one time, making plasma masking a rapid and high throughput pattern replication method. These characteristics make this technique highly convenient for meeting the replication demands of typical neurobiology experiments. The oxidized areas were first tested for their suitability to pattern human SH-SY5Y neurons and to guide neurite outgrowth to neighboring nodes. There was no need to pattern adhesion proteins as the culture media include intact proteins which selectively assemble on the oxidized regions to direct the formation of a network. The masked PEGylated surface was not activated by plasma and retained the ability to resist cell adhesion, resulting in high pattern compliance. The occupancy of an array with 367 nodes filled with cells was 97% and a patterning efficiency of >99% was achieved (see Figure 4.3.7). Compared to the former developed NFA based on PDMS μCP the occupancy of this system was dramatically increased by 10-20%. The hydrophobicity of PDMS (Contact angle 107.4 ± 1.5°) makes it more difficult for cells to attach and adhere on surfaces.

PLL-*g*-PEG instead is much less hydrophobic (29.1° ± 2.1°) and facilitates the access to the glass surface.
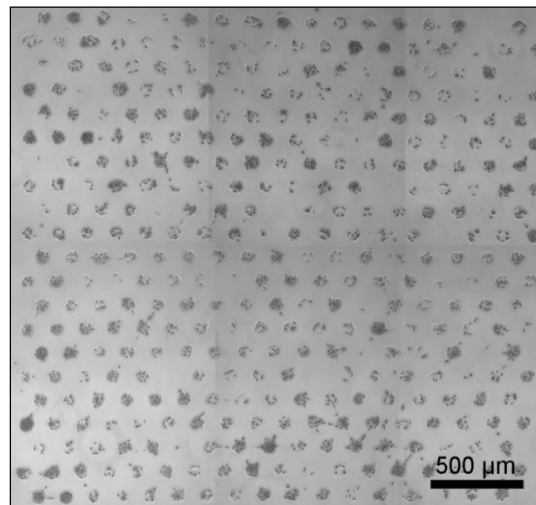

Figure 4.3.7: A complete neuron array of differentiated SH-SY5Y cells 24 h after seeding. 97% of all adhesion nodes are occupied by neurons.

The track features are essential for the formation of the network. Without the tracks the connections per node (cpn) value was limited to 0.012 on day 4, demonstrating that unlike thin film PDMS pattern (0.88 cpn) (Frimat et al., 2009), the PEGylated surface strongly resist the locomotion of the growth cones and the extension of neurite outgrowths. In a preliminary screen the optimal dimensions of the array was determined. Arrays containing 70-μm-diameter nodes and a track length of 100 μm were optimal for good occupancy levels (<90%), high patterning efficiency (<99%) and for the development of high neurite interconnection levels. A neuronal network developed during a 3 day culture period is shown in Fig. 4.3.8, with a larger area (~2 mm²) of the network documented in Fig. 4.3.9.
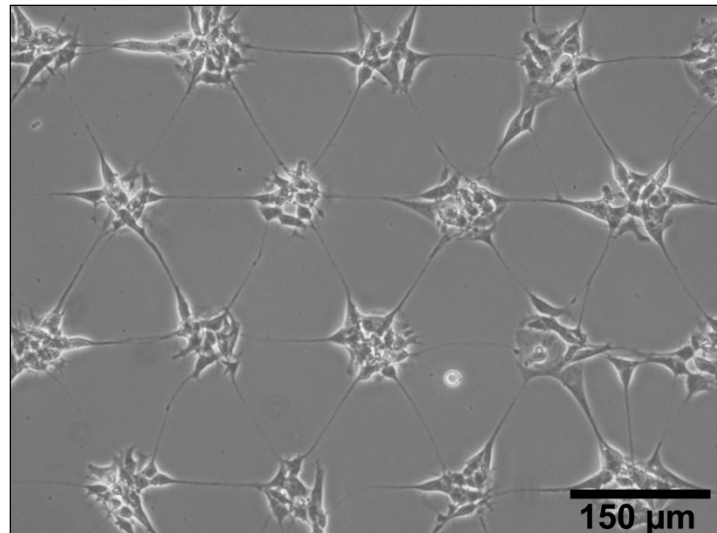
Figure 4.3.8: Differentiated SH-SY5Y neurons perfectly adhere to the array nodes forming a consisting neuronal network after 4 days on chip.
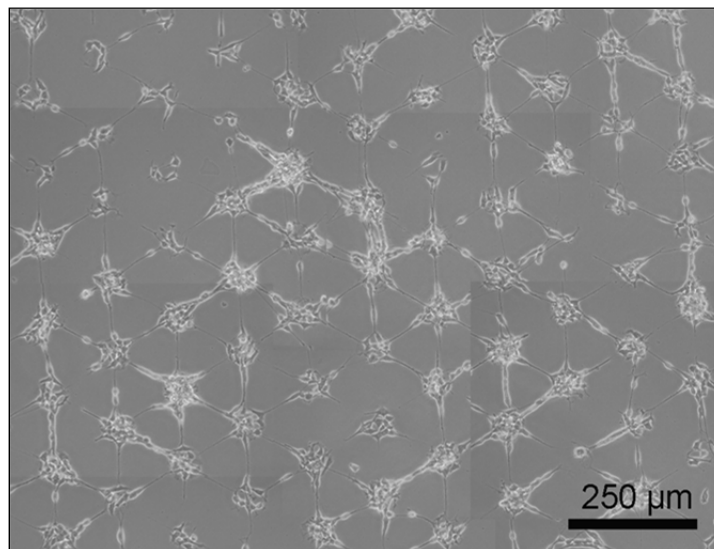
Figure 4.3.9: Image compilation of a neuronal network containing 82 nodes with 111 connections (1.35 cpn) on Day 4.

The neuronal network figures 4.3.8 and 4.3.9 could implicate the thought that the developed network is fixed. The visualization of a neuronal network within an array format by time lapse video microscopy showed the highly dynamic state of the network development. This observation was possible because of no need to fix and stain the arrays which enables network dynamics to be periodically or continuously recorded. The development of a neuronal network on a 0.55 mm² region of an array

with 4-µm-wide tracks was recorded with time lapse video microscopy and can be seen here:

http://www.ifado.de/en/research_applications/research_groups/nbtox/network-dynamics/index.html

Within the 5 day development period the network was highly dynamic. Cells sediment in an equally distributed fashion onto the pattern area subsequently migrated to adherent sites and remained motile, transporting along the 4-µm-wide tracks between nodes. Connections were formed, retracted and re-established, before finally leading to a connection per node value of 1.0. The occurring plasticity within the dynamics of the network formation process is shown in Fig.4.3.10.
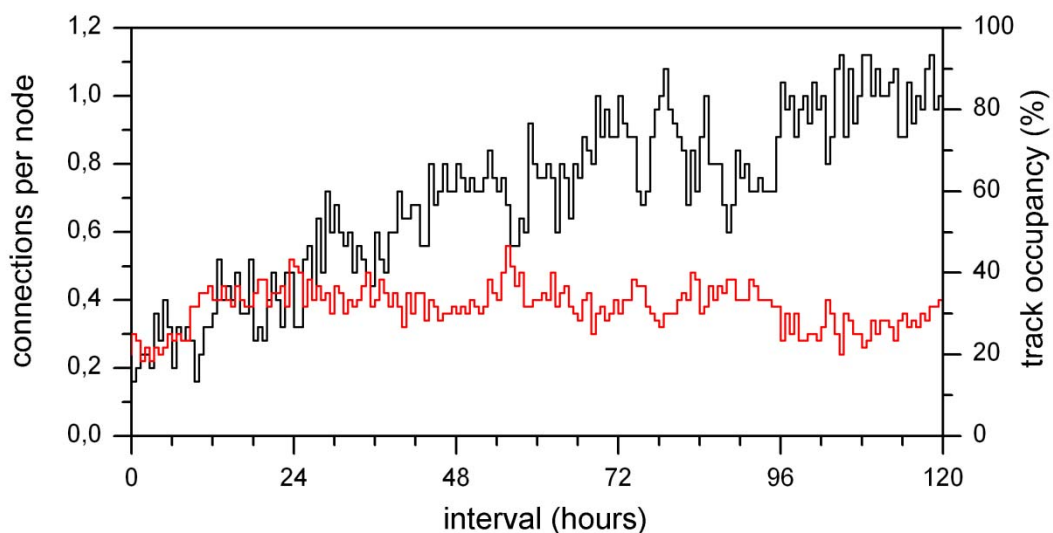
Figure 4.3.10: Network formation and migration dynamics. Track occupancy labeled in red and dynamics of neuronal network formation known as connection per node value in black.

The video documents a high level of cells migration between neighboring nodes using the 4-µm-wide tracks. Empty nodes get occupied by this even after the seeding process. However, such levels of migration limit the ability to score neurite interconnections with a defined length of 100 µm because these cells block the connection tracks resulting in distances either side that do not satisfy the neurite length classification criteria (*i.e.* equal to or greater than a cell length).

4.3.4 Optimum track width for neurite outgrowth

The bilayer membrane plasma masking technique allows the production of precise network patterns. This technique was used for a systematic study of the optimum track width required for the development of highly connected neuronal networks, which has not been reported before. Figure 4.3.10 and 4.3.11 and the above mentioned video clearly illustrate that a track width of 4 µm is excessive, permitting high levels of neuron migration and therefore occupancy.
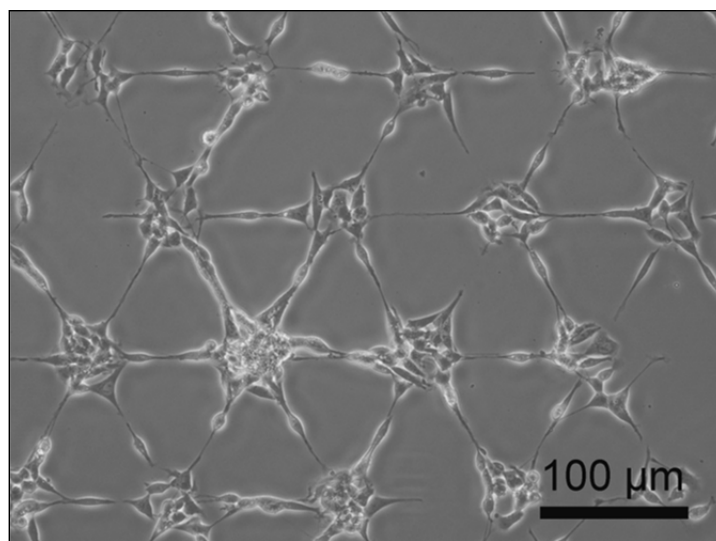
Figure 4.3.11: Array with 4-µm-wide tracks. The wide 4-µm tracks lead to increased migration of the neuron cells with many occupied tracks.

The standardized outgrowth length is a pre-requisite for neurite counting (Frimat et al., 2009; Radio and Mundy, 2008). The adhesion of neurons in tracks is especially unwanted for the network formation assay as this eliminates the advantage of the standardized connection length. To determine the best fitting track width a ranging from 1.0 µm to 3.0 µm were evaluated. Developing network formation levels relative to track width are documented in Figure 4.3.12 (A). Network formation and the neurite outgrowth were sensitive to a track width differences as small as 500 nm. The wider the tracks were the higher was the rate of networking. Track widths of 1-µm produced a 0.58 cpn (SD ± 0.16) during a 4 day development period. A 2.0-µm-wide track array produced a 1.52 cpn (SD ± 0.07) level during the same period. Nevertheless,

the largest tested track width of 3.0-µm developed a neuronal network plateau level by the second day, with a maximum value of only 1.38 cpn (SD ± 0.22) on the third day. These tracks were significantly occupied (~25%) by neurons throughout the assay, prohibiting the scoring of complete neurite outgrowth connections. The track width also correlated with neuron occupancy. The occupy levels was relatively stable throughout the duration of culture for a track width <1 µm (Fig. 3.3.16 (B)).
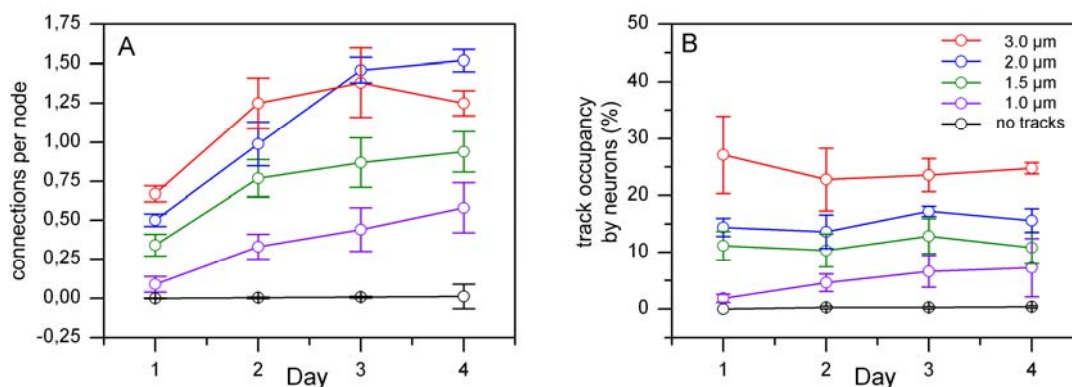
Figure 4.3.12: The amount of connection formation was sensitive to the track width (A). Neuron cells occupying the track features increase with the tracks width (B).

Taking together, the 2-µm-wide tracks were optimal for the formation of high network levels and low track occupancy (~15%). In the following discussion of further experiments arrays containing 70-µm-diameter nodes separated by 100-µm-long tracks with a 2.0 µm width were used.

4.3.5 Network patterning reproducible

Spatially standardized cell assays have to be reproducible in cell patterning purposes to be a valuable tool for biological experiments. The reproducibility of neuron pattern and network formation prepared by plasma masking with a bilayer membrane was measured on the second day of culture. The experiment involved 3 batches, each containing 3 microchips involving 9 arrays with each having 202 nodes. The across chip, chip-to-chip and batch-to-batch reproducibility was excellent. The occupancy levels of the arrays were consistent at 95.0% (SD ± 0.6%). In combination

with the cell repellent quality of the PEG adlayer this led to a patterning efficiencies >99.5%. Network formation levels were 0.91 cpn (SD ± 0.10) on second day in culture presented as a box and whiskers plot in Fig. 4.3.13. Within each batch the chip-to-chip variation (CV) was 7.25%, with batch-to-batch CV of 5.95%. The reason for this variance could be caused in the different passage numbers (9-12), the cell dynamics of the neurons within the network formation process (see Fig 4.3.12) and the natural difference of the behaviour of each cell population.
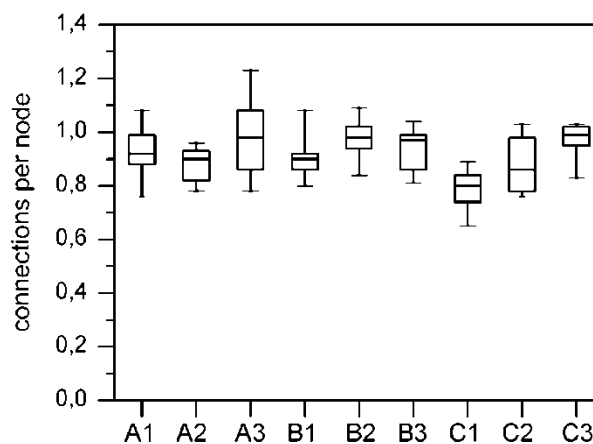
Figure 4.3.13: Network formation reproducibility presented in a box and whiskers plot. The mean, the lower 25th and upper 75th percentiles are shown along with the data extremes. Each batch (A-C) contained three chips, with an across chip network formation level measurement involving 9 arrays.

These data reflect that the bilayer membrane for plasma masking is a reliable and highly reproducibility technique to pattern human SH-SY5Y neuron cells. It directs network formations at consistent levels which makes this technology a valuable tool for neurotoxicity screening. In addition, the assay could also be used for screening for neuroregenerative substances (e.g. Alzheimer-, and Parkinson´s disease), neuronal injury, neuropathological disorders and determine aspects of developmental neurobiology.

4.3.6 Connection definition

The bilayer membrane plasma masking technique produces precise and reproducible network formation assays (Frimat et al., 2009; J. West, DE 10 2009 021 876.9 and PCT/EP2010/002811). The NFA measures neurite outgrowth, a hallmark neurodevelopmental indicator, by quantifying intermodal connection levels. The special hexagonal design of the array with its standardized neurite outgrowth length eliminates the length measurements which are otherwise required to satisfy the morphological neurite classification criteria (Frimat et al., 2009; Radio and Mundy, 2008). The 202 nodes per array were separated by 100 µm, a distance which is also sufficient for the differentiation of neurites into axons with functional synapses (Dotti et al., 1988; Stenger et al., 1998). Often more than one connection is formed between the nodes; the first formed neurite connection often became suspended (Fig. 4.3.14 (A)), thereby vacating the track for outgrowth by another neurite (Fig. 4.3.14 (B)).
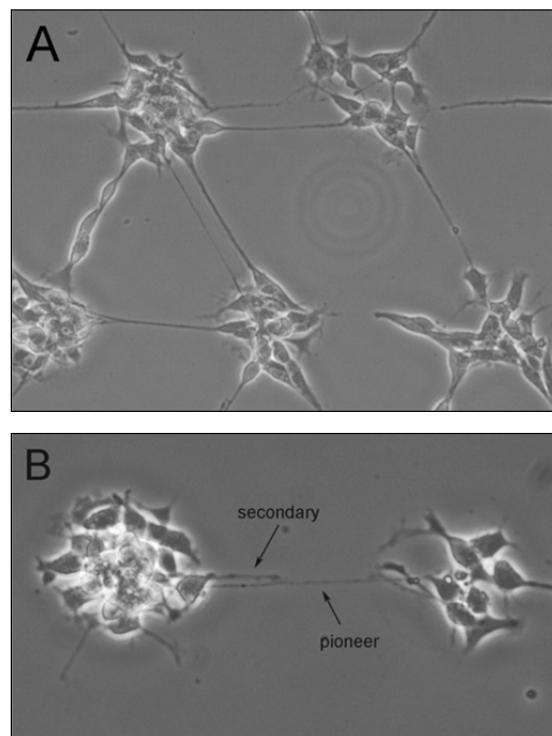

Figure 4.3.14: Neighboring nodes forming multiple connections (A). After the formation of a 'pioneer' connection, a secondary connection can be formed (B).

Outgrowths can also form one thick string between nodes consisting of multiple connections. To avoid difficulties involved in visualizing and counting the number of connections shared between a pair of nodes we chose to score multiple connections as a single connection.

4.3.7 Network degeneration and protection effects

The NFA has previously been used to quantify the dose-dependent inhibition of neurite outgrowth by the neurotoxin acrylamide (Frimat et al., 2009). The characteristics of acrylamide neurotoxicity in humans are central-peripheral distal axonopathy with clinical manifestations like numbness of the hands and feet or altered nerve conduction velocity (Calleman et al., 1994). Acrylamide can also cause degeneration of pre-existing neurite outgrowth *in vitro* (Nordin-Andersson et al., 2003). The modes of action of acrylamide neurotoxicity are various. An elevation of intercellular Ca^{2+} levels mechanistic response, (Nordin-Andersson et al., 2003) driving the Ca^{2+}-dependent up-regulation of calpains. Calpains are a class of cysteine proteases which degrade neurofilament proteins, spectrin, tubulin and microtubule-associated proteins (Axelsson et al., 2006; Goll et al., 2003; Song et al., 1994). At physiological levels calpains control, among other processes, the mobilization of vesicles to depleted release sites and therefore play a critical in synaptic facilitation and post-tetanic potentiation (Khoutorsky and Spira, 2009). However, with a high Ca^{2+} influx calpain is excessively up-regulated, and causes progressive structural damage to the neuronal cytoskeleton and neuronal networks (Axelsson et al., 2006; Song et al., 1994). In contrast, diminished calpain activity is associated with higher neurite outgrowth rates, (Axelsson et al., 2006; Oshima et al., 1989) such that the general calpain inhibitor calpeptin can be used to buffer the degenerative effects of acrylamide (Nordin-Andersson et al., 2003) or evaluated Ca^{2+} levels in general (Das et al., 2006).

The interconnected pattern produced by plasma masking with the bilayer membrane enables the development of high network formation levels which aid the investigation of neurodegenerative processes. In this study we used the NFA with tracks to measure the neurogenerative effects of 0.5 mM and 1.0 mM concentrations

of acrylamide and, by co-treatment, the protective effects of calpeptin (1 µM daily) and brain-derived neurotrophic factor (BDNF, 100 ng/mL). BDNF is a protein with wide ranging functions including promoting the differentiation and survival of central nervous system neurons (Cunha et al., 2009). SH-SY5Y cells were cultured on the arrays for 2 days to establish mature highly connected (~1.3 cpn) networks. Networks were treated with acrylamide for 3 days to effect degeneration. The time course of the degeneration and the buffering effects of co-treatment with calpeptin and BDNF are highlighted in Fig.4.3.15 as cpn values normalized to the controls. The raw data are plotted in the Appendix 3.
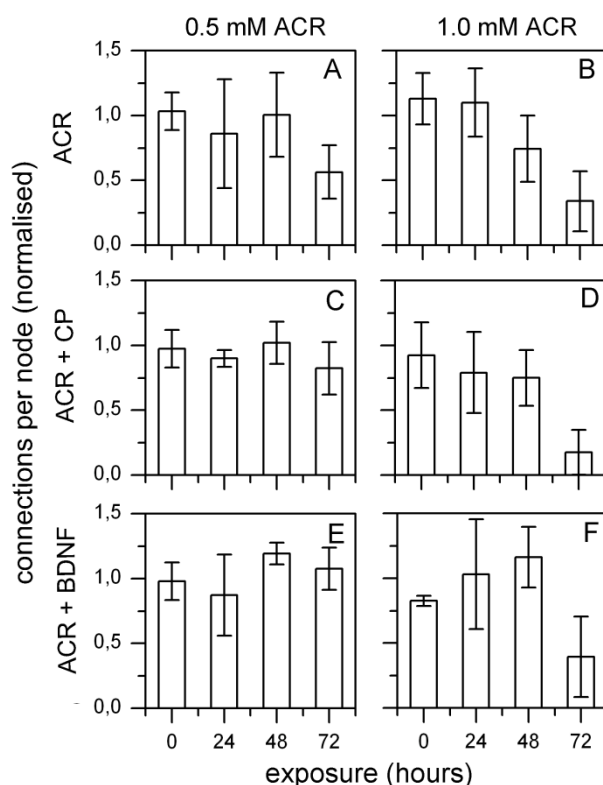
Figure 4.3.15: Network degeneration assay by the exposure to 0.5 mM (A) and 1 mM (B) acrylamide. The buffering effects of 1 µm calpeptin (C,D) and 100 ng/mL BDNF (E,F) in combination with the exposure to 0.5 mM and 1 mM acrylamide. Network levels were normalized to the control samples. All samples were done in triplicate.

ANOVA analysis revealed a significant time-treatment interaction ($F_{(18.42)}$ = 2.19; p = 0.024) indicating dose-dependent network degeneration. With 1 mM acrylamide treatments, degeneration was not evident during the first 48 h, but by 72 h

network levels were significantly reduced. Co-treatment with calpeptin or BDNF was insufficient to prevent the network degeneration.

The neurotoxicity test showed that 72 h of treatment with 0.5 mM acrylamide was also required to see a reduction in the connections per node number (mean difference: -0.46 cpn), but with lower significance ($p = 0.095$). Calpeptin co-treatment was able to buffer the action of acrylamide, with only an 18% mean reduction in network levels compared to 44% without calpeptin. The NFA is a spatial refinement of the neurite outgrowth assay. It has been used previously to measure a 52% reduction in outgrowth levels for neurons treated with 0.5 mM acrylamide for 3 days, with calpeptin co-treatment buffering the reduction to 17% (Nordin-Andersson et al., 2003). The close similarity between the results generated by the different methods underscores the reliability of the NFA, with the benefit of its analytical throughput (Frimat et al., 2009). The data similarity also indicates that patterned culture does not perturb neurite outgrowth.

BDNF protects the network providing a strong buffering capacity, completing maintaining network integrity. It binds to the tyrosine kinase B (TrkB) receptor and impacts various signaling pathways, including activation of the transcription factor CREB. This factor mediates the expression of genes involved in the molecular processes underlying aspects of memory function (Kandal, 2009). SH-SY5Y cells were differentiated with retinoic acid which leads to the expression of TrkB receptors for further differentiation with BDNF of produce cells which exhibit many of the features of mature neurons (Agholme et al., 2010). Beside the general neuroprotective effect, co-treatment with BDNF will therefore stimulate pathways required for fuller maturation of the neuronal networks (Chen et al., 2011). The NFA could be used in combination with other analytical tools to draw associations between toxic molecular and possible neurobehavioural outcomes.

4.3.8 Protein patterning

The successfully establishment of the bilayer PDMS membrane technology for the production of highly developed neuronal networks offered the opportunity to

pattern different sort of cell lines. Next to the standard cell lines like the SH-SY5Y cells, human mesencephalic cells (LUHMES, Lund human mesencephalic) as neuronal model system and dorsal root ganglion cells isolated from mouse were tested on the NFA. Dorsal root ganglion cells were patterned like the SH-SY5Y cells without adhesion molecules (Figure 4.3.16). The pattern was stable for 5 days.
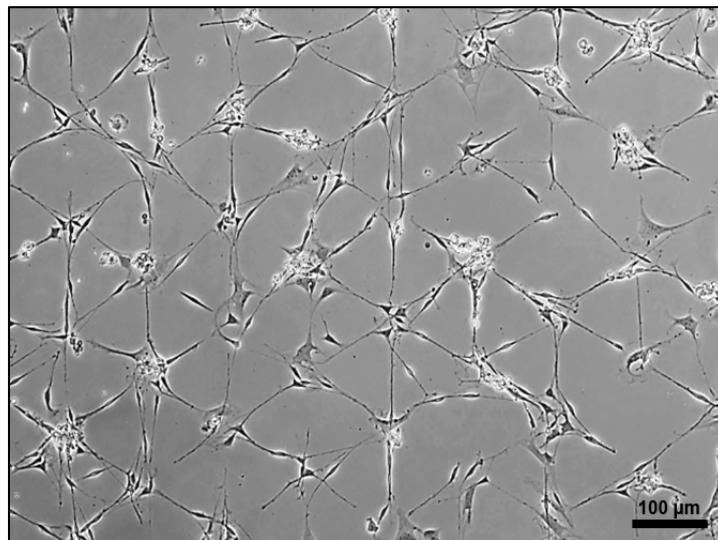
Fig. 4.3.16: Dorsal root ganglion on plasma-stencillined PLL-g-PEG without adhesion molecules. The picture was produced in cooperation with Nicole Schöbel, IfaDo.

LUHMES instead need adhesion proteins to bind properly on surfaces. Two days predifferentiated LUHMES were cultured on plasma stencilling pattern incubated with laminin. The PEGylated regions rejected the adhesion of laminin so that the LUHMES were able to form a spatially defined network. The number of occupied nodes 24 h after seeding was 94.05% (SD ± 8.4%) and the cpn 0.62 ± 0.11. Unfortunately the occupancy decreased in the following 48 hours to just 71.95 ± 5.12%, whereas the cpn increased to 0.84 ± 0.06% on day 3 (Waide, 2011). The reduction in occupancy indicates that lamination as adhesion promoter for neurons alone is not stable enough to attach cells to the underlying glass surface. As the number of cells on chip increase the tension of the cell clusters are too strong and the cells detach. The poor adhesion of laminin is caused by the missing coating of PLL or PLO. To anchor cells for long term culture sufficiently strong on a surface protein pattern are not adhesive enough. A

combination of a poly-amine acting as a kind of glue with laminin (or fibronectin) is needed.
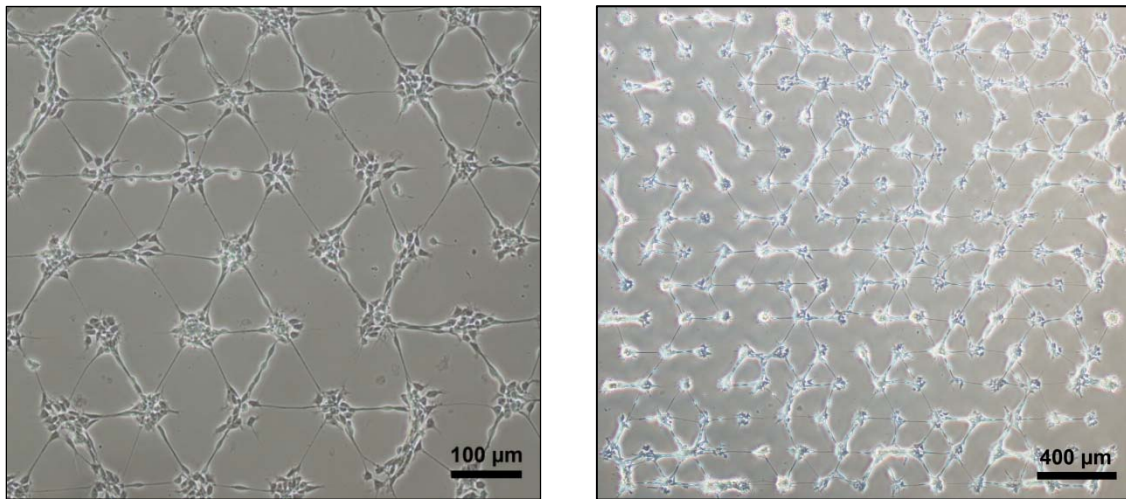
Fig. 4.3.17: LUHMES cells on a laminin pattern passivated by (poly)ethylenglycol. Images were taken 24 h after seeding. The left picture shows a 10x magnification of the LUHMES pattern, while the right picture shows a complete array with 202 adhesion nodes. The pictures were kindly provided by Sarah Waide.

4.4 Outlook and Conclusion

The network formation assay offers several advantages towards the commonly used neurite outgrowth assay:

- NFA measures interconnectivity which is the basis of memory and learning and a higher functional indicator instead of neurite outgrowth.
- Dynamic processes like degeneration and regeneration experiments can be monitored; no fixation or staining is needed.
- Time consuming length measurements of neurite outgrowth is avoided by standardized length of node interconnection tracks, which makes the analysis more rapid and easier.
- Spatial coordinates of the nodes simplify the rediscover of individual neurons and their connections.
- The standardized dimension of the NFA produces more statistically relevant data for cellular response.

In this chapter the successful modification of the NFA by the development of the bilayer membrane technique including track features has been discussed. The track features facilitates the development of a neuronal network. Compared to the standard NFA without tracks the new assay has an increased connectivity up to 65% more neuron connections per day. Its reproducibility and the low number of cells blocking tracks make the new technique to an even stronger spatially standardized analytical display for high throughput neurotoxicity screenings. The toxicity of acrylamide and the protective effects of BDNF and calpeptin have successfully been tested on neuronal networks developed with the bilayer plasma membrane technique. The characterization of the new method has been done with SH-SY5Y cells to compared it with the original PDMS μCP NFA.

The bilayer plasma membrane technique has been developed for the demands of primary neuron cells. The first criteria for the successful pattern of these cells have been fulfilled by including track features. Primary neuron cells are the *in vitro* gold standard for neurotoxicology screening technologies. Their biochemical, electrophysiological characteristics and their *in vivo* like morphology is similar to the SH-SY5Y ones. The widespread adoption of the NFA will be validated by the standards defined by the neurotoxicologists and their guidelines. The field of application is widely spread. Its dynamic networking is useful in developmental neurobiology to investigate network plasticity which is involved in memory formation and learning. The NFA can be used to determine test substances for inhibition, regeneration and degeneration effects of neurite outgrowth. Conclusion of these experiments can help finding therapies for damaged brain tissues, injuries and the prevention of brain triggering conditions like Parkinson and Alzheimer disease. The NFA is also helpful in the clinical trial period developing new drug compounds. Possible drug candidates can be assessed and proven on any effects concerning the nervous system.

In all these disciplinary primary neuron cells or stem cells are used. The consequence out of this is the development of a NFA suiting the demands of these cell types. It is described in the following chapter.

Chapter 5: The Network Formation Assay for Neurons and Neuronal Precursor Cells
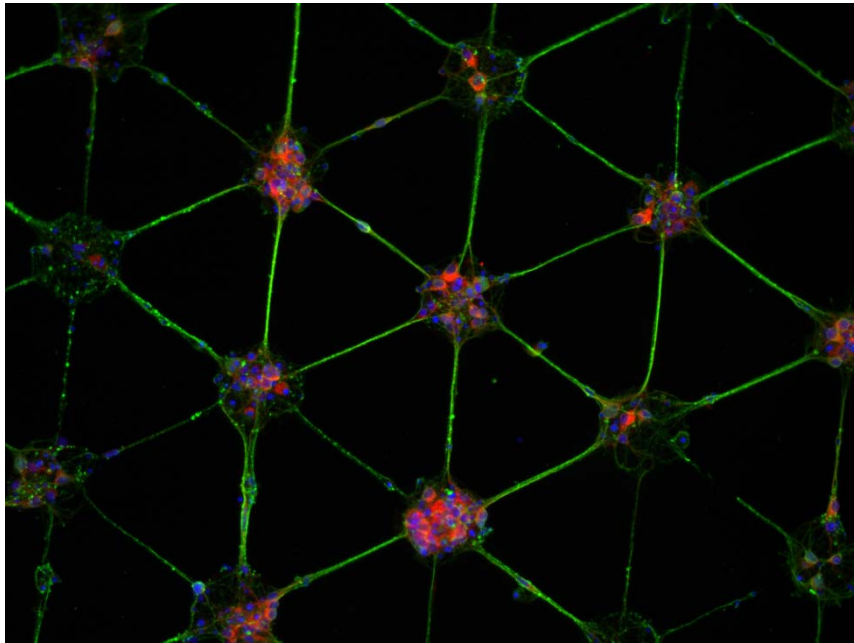
5.1 Introduction

The second generation of the NFA already included the necessary track features to enable network formation by primary and stem cells. We already have shown before that the NFA with tracks had better connections per nodes values culturing the same cell line SH-SY5Y (cpn on day 3: 0.88 for NFA without tracks and cpn of 1.46 ± 0.08 with track features). The transfer of the bilayer membrane plasma masking technique to the demands of primary and stem cells requires adhesion molecules like poly-D-Lysine (PDL), poly-L-ornithine (PLO) and laminin. The extracellular matrix molecule laminin is not able to pattern cells for a long term culture on a substrate. Over time delamination occurs and so cell detachment, which was caused by the forces of the developing network. It is more effective to pattern laminin in combination with a poly-amine. Poly-L-lysine for example binds 10x stronger neuronal

cells on polystyrene than laminin (laminin adhesion force 105 nN, 37°C) (Calof and Lander, 1991; Sagvolden et al., 1999).

The cell repellent PEG adlayer was disintegrated by plasma treatment through the exposed regions in the bilayer membrane. For the patterning of primary cells poly-lysine, which binds well to the activated glass areas, was incubated on the activated chips. Unfortunately unlike proteins and polypeptides, PL has also a high affinity for the PLL-*g*-PEG resulting in a reduced pattern quality (Figure 5.1.1).
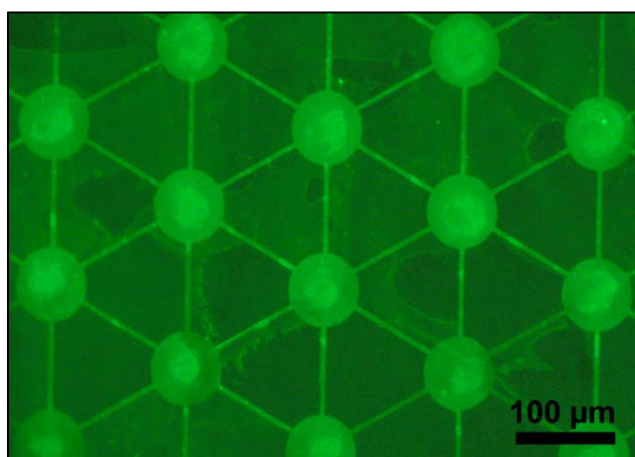
Figure 5.1.1: PLL-FITC staining of a plasma pattern on PLL-g-PEG. PLL-FITC adheres on the activated glass surface and the PLL-g-PEG layer.

The variation of several parameters; PL concentration, incubation time, washing steps and pH change did not lead to pattern improvement. This drawback with the PLL-*g*-PEG chips in combination with PL as adhesion molecules provoked us to explore alternative micropatterning routes. The investigation of alternative methods is documented in this chapter along with a method suitable for the patterning of mouse primary neurons and neuronal precursor cells. In the last part of this thesis the long term stability of NFA chips and the best storage conditions are discussed. In addition to micropattern optimisation and characterization, the degenerative effects of acyrlamide on a primary neuronal network were also measured.

5.2 Material & Methods

5.2.1 Primary cortical neuron cell culture

C57BL/6N mice were purchased from Charles Rivers Laboratories, Germany. Pregnant mouse were put to death 16 days after conception by cervical dislocation. The cortices of the isolated embryos were extracted and transferred into Hanks balanced salt solution (HBSS$^{-/-}$) containing 0.0125% trypsin (PANBiotech). The dissociation process was stopped after 10 min by adding 0.05 mg/mL soy bean trysin inhibitor; free DNA was destroyed using 0.01% (w/v) DNAse. The cells were further dissociated using fire-polished glass pipettes, centrifuged at 200 g for 5 min followed by the suspension in fresh neurobasal media containing 1% (v/v) (PANBiotech), B27 growth supplement (Gibco), 10 µg/mL gentamicine and 0.5 mM stable L-glutamine (PANBiotech). The cells were cultured at 37 °C in a humidified 5% CO_2 atmosphere. Cells were seeded in a concentration of 2.5 x 10^5 cells/mL media exchange took place every 3-4 days by replacing 50% of the old media.

5.2.2 Culture of CGR8 neuronal precursor cells (NPCs)

Neuronal precursor cells (NPCs) were kindly provided by Marcel Leist, University of Konstanz. The cell line was established from the inner cell mass of a 3.5 day male pre-implanation mouse embryo (129/Ola). The differentiation media contained 98.2 mL DMEM/F12, 98.2 mL neurobasal media (PANBiotech), 1 mL N2 (Gibco), 2 mL B27 (Gibco), 0.75 mL stable glutamin (2 mM) (PANBiotech), 150 µL insulin (Sigma-Aldrich), 10 mg BSA fraction V (Roth) and 400 µL β-mercaptoethanol (Gibco). Media was filtered through a 0.22 µm filter. Cells were grown on surfaces covered with 10 µg/mL PLO and 10 µg/mL laminin (Sigma-Aldrich). Media exchange took place every other day with pre-warmed N2/B27. Differentiation is finished after 13 days. The cells were stained by fixing with 4% paraformaldehyde for 10 min and 15 min with 0.5% Triton-X 100. After this the cells were blocked with 5% normal donkey serum (Millipore) for at least 1 h. The first antibody was incubated for 2 h in darkness (NeuN from mouse (1:200), β-3-Tubulin from rabbit in 1% normal donkey serum;

1:2000). The secondary antibody anti rabbit dylight 488 (1:500) or antibody donkey anti mouse dylight 649 (1:500) (Millipore) was incubated for 30 min at room temperature in darkness. DAPI was incubated 1:10000 for 30 min and mount with fluorosave reagent (Invitrogen). A Leica DMI6000 B microscope was used to analyze the cells with a CCD camera DFC 360 FX and the LAS AF Software.

5.2.3 Zeta-Potential Measurements

The zeta potential response of the modified glass surfaces with polyamines and silanes were made in a 1 x PBS (pH 7.0) buffer solution using a SurPASS instrument (Anton Paar, Austria). Measured parameters were stability over time and reaction to poly-L-lysine.

5.2.4 Silanization of glass chips

Glass slides were cleaned with 96% (v/v) ethanol and water washing; afterwards the slides were dried in a nitrogen stream. The slides were activated in 0.2 mbar oxygen plasma (70W, 40 kHz (Femto, Diener Electronic)) for 60 s. The slides were placed in a toluene bath containing 0.1 mM dichlorodimethylsilane (DCDMS; Sigma-Aldrich, Germany), poly(ethylene glycol) methyl ether methacrylate (mPEG; ABCR, Germany) or 2-[methoxy(polyethyleneoxy)-propyl]trichlorosilane (TCS-PEG; ABCR, Germany) for 2-3 h. The slides were exposed for 5 min to nitrogen and rinsed with water free hexane to remove unbound silane groups. Alternatively the activated glass slides can be placed in a sealed slide bath containing 100 µL of the silane. To cover the slide with silanes in gas phase the container has to be heated to at least 100°C. No washing and nitrogen streaming is necessary after this procedure.

5.2.5 Amine glass chip modification

The modification of clean and activated glass slides was similar to the modification with silane groups. The amine transfer took place either in the liquid

phase in toluene or in the gas phase. The concentration of the amine was 0.1 mM in solution and to cover the glass slides in the gas phase 100 µl of the amine solution was taken. Used amine solutions were: diethylentriamine (DETA) bis(trimethoxysilylpropyl)amine (BTMSPA), 3-aminopropyldiisopropylethoxysilane (APDIPES), (3-aminopropyl)triethoxysilane (APTES) ordered from ABCR, Germany.

5.2.6 Microcontact printing of proteins and poly-amines

PDMS stamps with protruding features were plasma activated for 1 min in an oxygen stream and afterwards incubated for 10 min of a 50 µg/mL poly-L-ornithine (PLO) or 0.1 mg/mL PDL solution (Sigma-Aldrich, Germany). The stamps were washed twice with ddH$_2$O and dried in a nitrogen stream. The stamps were dried and protected from dust for another 15 min at room temperature. In order to µCP the arrays the stamps were placed in conformal contact with the slide surface. By gently pushing the stamp onto the slide, the amines get transferred to the PEGylated surface. After a transfer time of at least 30 min the stamps can be peeled off and reused.

5.3 Results & Discussion

5.3.1 Silanes as an alternative to PLL-*g*-PEG?

The bilayer plasma stencilling method worked perfectly with cells that do not need polyamines to mediate cell adhesion on a PLL-*g*-PEG background. The main reason for the development of the NFA was the design of an easier read-out system for chemical tests on neurite outgrowth. The neuron cells commonly used in test assays by the community are primary cells. To evaluate the NFA as a better test assay than the gold standard neurite outgrowth assay it must first be validated with primary cells, in a commonly accepted culture format; i.e. using poly-D-lysine as cell adhesion mediator. With this condition an assay using PLL-*g*-PEG as cell repellent material in combination with the bilayer plasma stencilling method was unsuccessful (Fig 5.1.1.).

Zeta-potential measurements confirm what has already been shown in figure 5.1.1. The electrical potential of the PEG adlayer incubated with a 0.1 mg/mL PLL solution was measured (Figure 5.3.1).
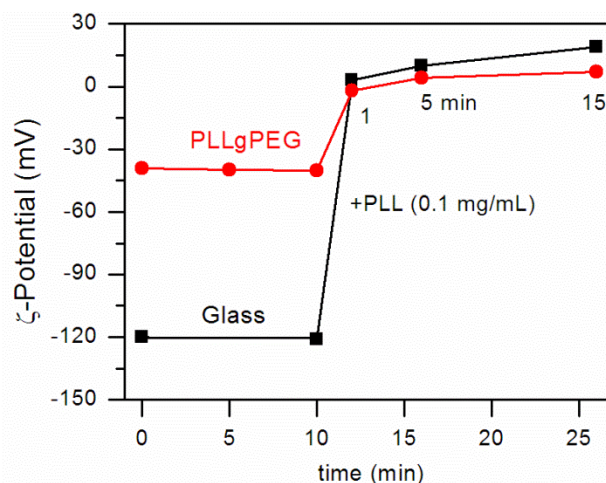

Figure 5.3.1: Zeta potential: a PEGylated and an activated glass slide were incubated for 1, 5 and 15 min with a 0.1 mg/mL PLL solution. Incubation time of 1 min is sufficient to increase the zeta-potential to a neutral/positively-charged state.

The ions in the liquid phase bind tightly to the surface groups and form the fixed layer. The loosely bound liquid phase ions of opposite charge form the mobile layer. The zeta-potential measures the change in potential across the double layer. By adding PLL to a PEGylated surface the zeta-potential rapidly increased from -40 mV up to 7 mV. An incubation time of only 1 min is enough to neutralize the negatively charged PEG surface. PLL reacts equally well with PEG as with activated glass. An additional incubation with PLL for 5 and 15 min did not show a significant change on surface charge compared to the first minute. Instead of using PLL-*g*-PEG as the cell repellent material there is an alternative route, replacing PEG by another cell rejecting material such as hydrophobic silanes. Alkyltrichlorosilane has been used before as a cell non-adhesive material in combination with another silane coupled with an amine for cell attachment (Kleinfeld et al., 1988). The hydrophobic silane dichlorodimethylsilane (DCDMS) resists cell adhesion and has been used next to protein adhesive glass surfaces (Frimat et al., 2009) to pattern cells. Another important aspect is the long term stability of silanized glass slides at RT and in air. Once produced the chips could be stored under normal conditions for around a year. This is an

important issue for the wider use of the microchips in different laboratories around the World.
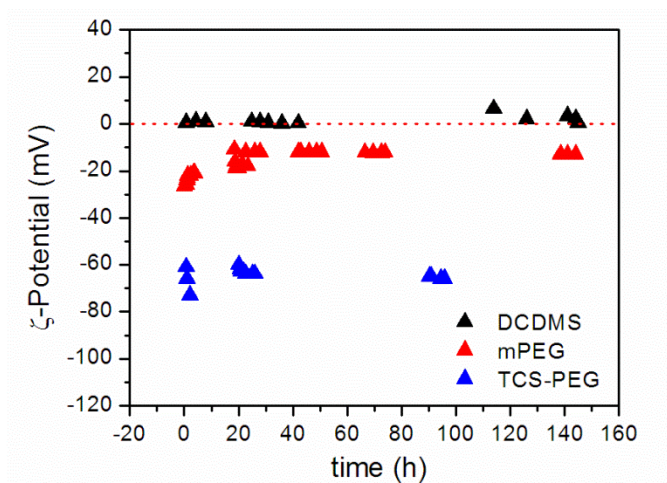
Figure 5.3.2: DCDMS, mPEG and TCS-PEG slides were stored for 1 week at RT in lab air. Zeta-potential measurements showed the constant stability of the silanized slides.

The following silanes were tested as alternatives to the cell repellent PEG: dichlorodimethylsilane (DCDMS), poly(ethylene glycol) methyl ether methacrylate (mPEG) and 2-[methoxy(polyethyleneoxy)propyl]trichlorosilane (TCS-PEG). All three silanes have good long term stability in air as is shown in figure 5.3.2. The affinity of the PLL for the silanes is shown in the following figure 5.3.3.
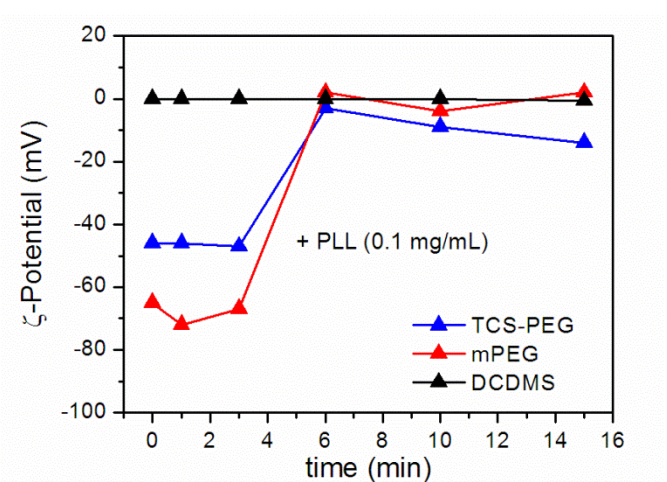
Figure 5.3.3: Zeta-potential measurements of TCS-PEG, mPEG and DCDMS before and after the incubation of 0.1 mg/mL PLL for 1 min.

TCS-PEG and mPEG have a negatively charged surface which interacts with PLL. After the addition of lysine the zeta-potential increased; the surface charge of mPEG was neutralized from - 67 mV to 0 mV. The zeta-potential of TCS-PEG first increased after PLL incubation from - 46 mV to - 3 mV. The most promising candidate is DCDMS providing a neutral surface and does not show a change in surface charge after PLL incubation.

The bilayer membrane was used to plasma the pattern into the silanized glass slides. Lysine coupled with the fluorescent molecule FITC was incubated for 1 min on the pattern. The high affinity of poly-lysine already shown in the zeta-potential measurements was confirmed by the staining procedure. PLL-FITC did not only bind to the activated glass pattern but also to the protected methylated PEG (Figure 5.3.4 left).
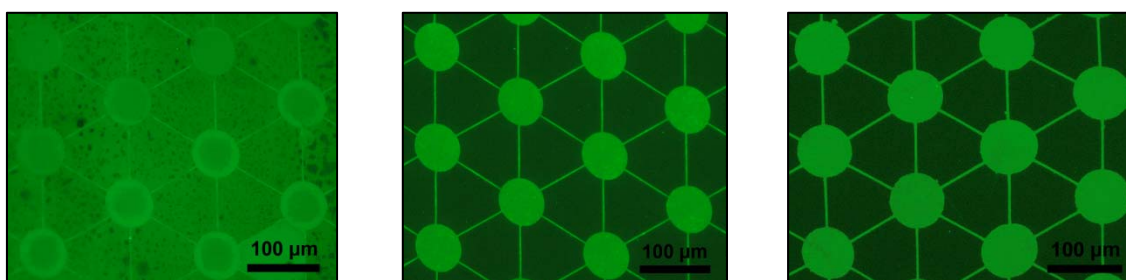
Figure 5.3.4: PLL-FITC staining of pattern produced by the bilayer membrane technique. Pattern produced on mPEG (left), TCS-PEG (mid) and DCDMS (right).

Several different types of washing steps were evaluated to remove the excessive lysine. These included water, PBS, acetone, hexane and ethanol. The specific binding potential of lysine to glass was modified by pH-, temperature- and concentration change. In spite of these numerous efforts, PLL still bound to mPEG. With the lysine binding across the entire chip cells could adhere in all locations. As such, the use of mPEG as cell-repellent material for primary chips was deemed unsuitable.

PLL-FITC did not bind on DCDMS (Fig. 5.3.4 right) and in contrary to the zeta-potential data it did not bind to TCS-PEG (Fig. 5.3.4 mid). Primary mouse cells were isolated and used on plasma patterned and lysine coated DCDMS and TCS-PEG NFA microchips.
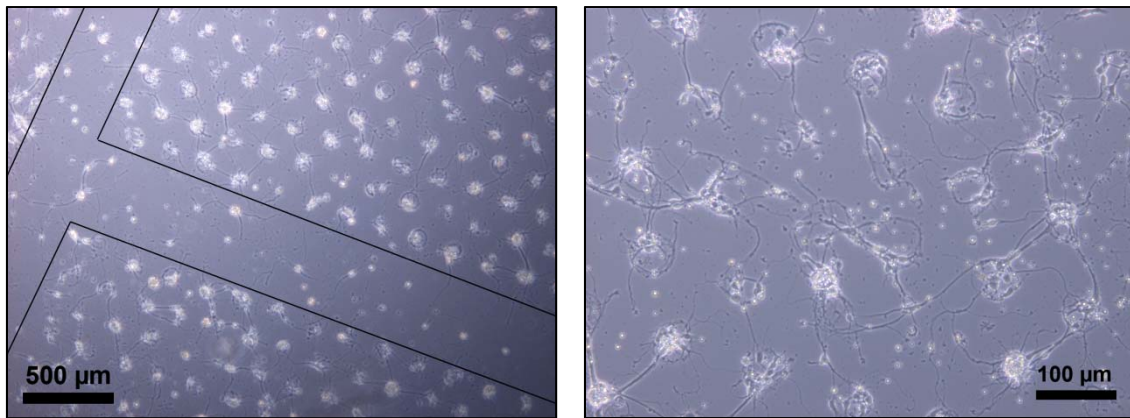
Figure 5.3.5: Primary cortical neurons patterned on lysine on a TCS-PEG background. Cells initially were selectively registered on the pattern, but following 48 hours of culture the cellular pattern became highly disorganised (right).

Pattern of primary cortical neurons (pCNs) were visible for 48 h before the cells grew 'chaotically' with the loss of the structure. Figure 5.3.5 shows in the left part the clear division between two arrays. The cells respect the adhesive pattern, but on closer inspection (right figure) the neurite outgrowth was unstructured. The quality of the patterns produced on TCS-PEG was therefore unsuitable for the NFA with primary neurons.

DCDMS had no affinity for lysine as judged by the zeta-potential measurements and after the staining procedure. The silane has already been used before as backfill material to pattern SH-SY5Y cells with the bilayer plasma membrane (figure 5.3.6). Finally PLL-g-PEG has been used as a standard cell resistant material due to the easier handling and the higher reproducibility.
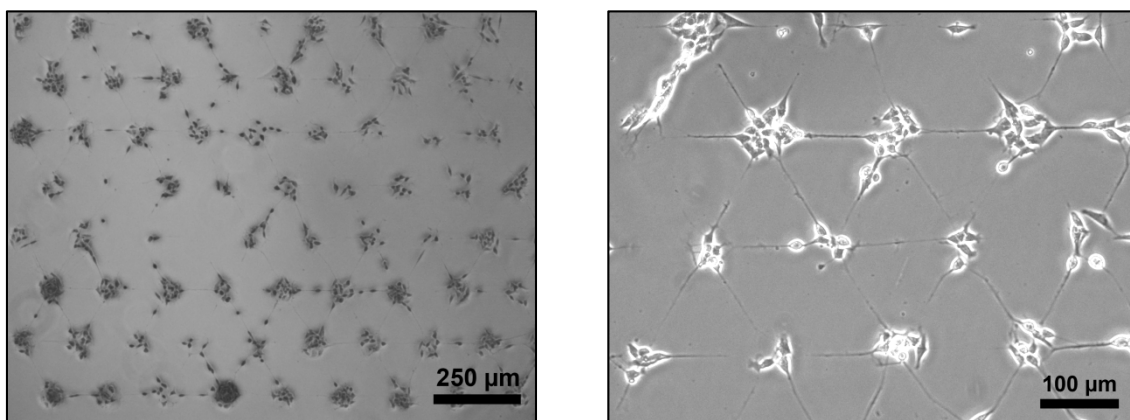
Figure 5.3.6: Network formation after 48 h with SH-SY5Y cells on plasma stenciled silanized (DCDMS) glass slides.

The patterning of pCNs on DCDMS slides was unsuccessful (Fig. 5.3.7). The cells died within 48 hours. DCDMS is a highly hydrophobic material with a contact angle of ~ 106° causing media to be rejected by the surface (*i.e.* the media forms droplets which roll off. Alternatively the microchip floats). Cells in media were not distributed evenly over the slide and instead formed a round droplet caused by the high surface tension. The tension influenced the cell binding and network formation of the sensitive primary cells and might cause their death after 48 h on chip.
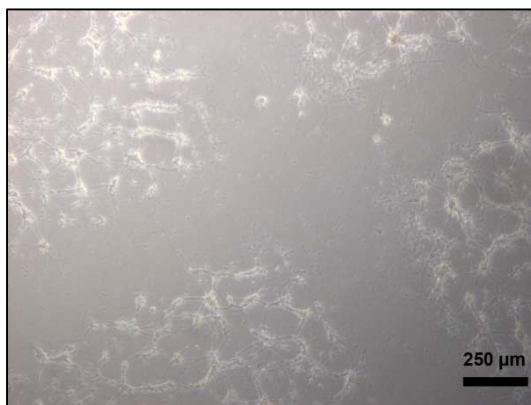
Figure 5.3.7: The bilayer plasma membrane was used to pattern pCNs onto the DCDMS surface. Cells did not effectively organize on the pattern. 48 h after seeding the primary cells died.

The evaluation of several silane-based surface modifications did not identify an adequate replacement for PLL-g-PEG. Next to the mentioned examples of TCS-PEG, mPEG and DCDMS, Octadecyltrichlorosilane (OTS), 3-Glycidopropyltrimethoxysilan (GOPTS) and 3-aminopropyldiisopropylethoxysilane (APDIPES) were also unsuccessful. The NFA microchips consist of two compounds; the cell repellent material PLL-g-PEG and an amine in this case PLL/PDL. The replacement of PLL-g-PEG by silanes was not effective. The alternative that was subsequently tested was to replace the poly-lysine (polyamine) with an amino silane.

5.3.2 Aminosilanes as an alternative to Lysine?

The polymeric amino acids poly-L/D-lysine and poly-L-ornithine bind with PLL-g-PEG modified glass surfaces. It was hypothesized that polylysine and its polycationic analogous ornithine intercalate with the PEG moiety (Fig. 5.3.8).
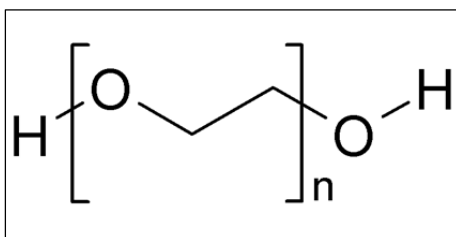
Figure 5.3.8: Chemical structure of poly(ethylene glycol)

In culture media or dissolved in buffer the amine groups of poly-L-lysine (Fig. 5.3.9 left) and poly-L-ornithine (Fig. 5.3.9 right) are protonated and may interact with the free electron groups of the oxygen in PEG. The polycationic property of these molecules allows the interaction with anionic sites on cells to mediate adhesion. Lysine/ornithine bound to a culture plate possesses a uniform positive charge which is preferred by several cell types especially primary neurons (PLL/PDL) or neuronal precursor cells (PLO).
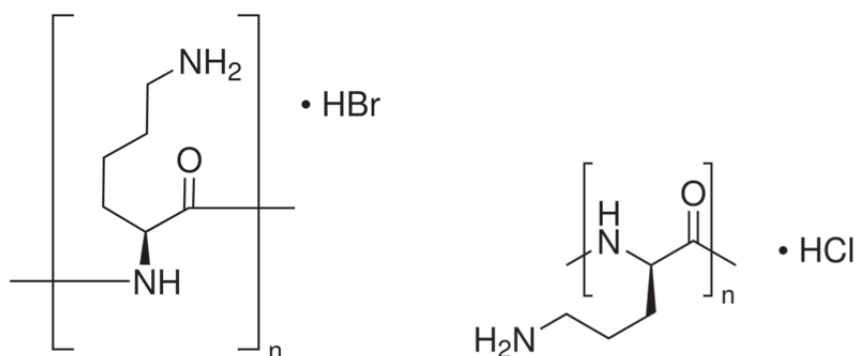
Figure 5.3.9: Structure of the amine analogous poly-l-lysine (left) and poly-l-ornithine (right). Lysine amino acid chain consists of one more methyl-group than ornithine.

The question is whether the amino acids can be replaced by a different sort of molecules such as aminosilanes? The silanes could be bound covalently to the plasma cleaned and activated glass surface next to PLL-*g*-PEG. The following aminosilanes were tested: Diethylenetriamine (DETA), bis(trimethoxysilylpropyl)amine (BTMSPA), 3-aminopropyldiisopropylethoxysilane (APDIPES), (3-aminopropyl) triethoxysilane (APTES). DETA has been used before with OTS (Octadecyltrichlorosilane) to pattern glial cells (St John et al., 1997) and APTES with neuroblastoma cells (Ranieri et al.,

1993). Primary cells were cultured in culture dishes coated with the aminosilanes. pCNs grew and developed neurite outgrowth on all aminosilane surfaces. Silanized glass slides coupled with BTMSPA and APDIPES are stable at room temperature and in lab air for at least a period of one week (fig 5.3.10). This stability is a desirable quality for the NFA microchip.
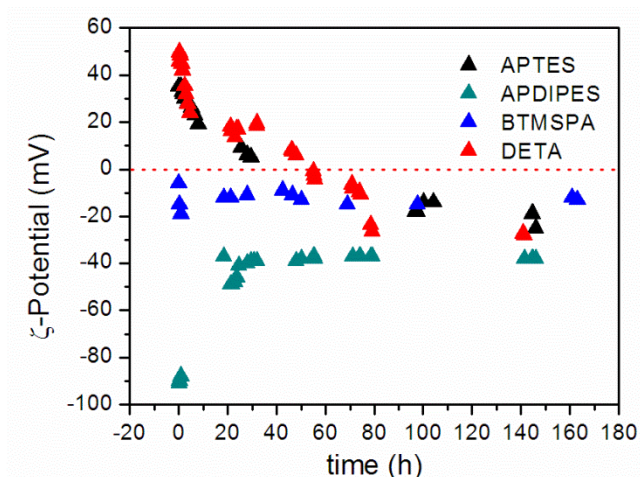
Figure 5.3.10: Zeta-potential measurement of aminosilanes. Slides were stored at room temperature in lab air for one week. BTMSPA is the most stable candidate.

DETA and APTES provide the highest amount of amine groups on the surface, but hydrolyze under media conditions, are lost from the surface and cause cell death (data not shown). APDIPES did not have sufficient stability which might be caused by steric hindrance (Zhang et al., 2010). BTMSPA is stable in culture conditions, but has a lower coverage of amine groups. The amines were tested in combination with PLL-*g*-PEG and DCDMS as cell repellent materials. Glass slides were PEGylated for 1 h or methylated for 2-3 h at 100°C in gas phase. In conclusion, no combination has worked effectively. In most cases no pattern was visible. The combination of the aminosilanes with PEG was also ineffective, with cell growth equally distributed across the entire chip surface. This could be a result of the aminosilanes either displacing the PEG or intercalating within the gaps between molecules. The only pattern observed was with a combination of DETA and DCDMS (Fig.5.3.11). However, patterns were lost following 4 days in culture and results were not sufficiently reproducible. Together these features indicate a loss of stability.
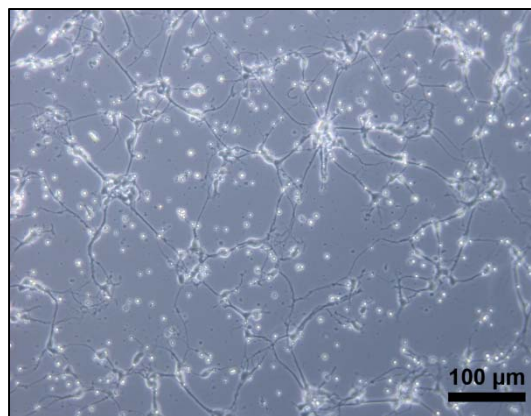
Figure 5.3.11: Pattern produced with DETA/DCDMS using pCNs. The quality of the pattern was poor and not reproducible. The cells were able to bind to the tracks as well as the adhesion nodes.

Finding and replacing lysine and ornithine with a suitable aminosilane was not successful. Indeed, all tested amines were suitable for cell adhesion and neurite outgrowth, but not as a cellular pattern. In summary, the only silane of value was DCDMS which introduced problems of media and cell addition whereas the combination of PLL-*g*-PEG with aminosilanes did not produce a pattern. PLL-*g*-PEG is still the best choice cell repellent material as it is hydrophilic (CA 29.12 ± 2.8°) and facilitates the contact of cells to the adhesion spots. To successfully develop the NFA for primary and stem cells the polyamine-PEG binding effect was choosen to exploit. PDL and PLO bind perfectly on PLL-*g*-PEG, excess PDL and PLO distributes over the chip and prevents the patterning of cells. To overcome this problem I chose to print a monolayer of lysine or ornithine on a PEGylated glass slide to prepare a pattern.

5.3.3 NFA for Primaries

Microcontact printing is an established method to print molecules or proteins on surfaces. Commonly after molecular printing the free areas are passivated with a cell repellent backfill material such as PEG or the printing is undertaken on non-adhesive polystyrene. In our study PDL or PLO was printed on glass slides covered with PLL-*g*-PEG.
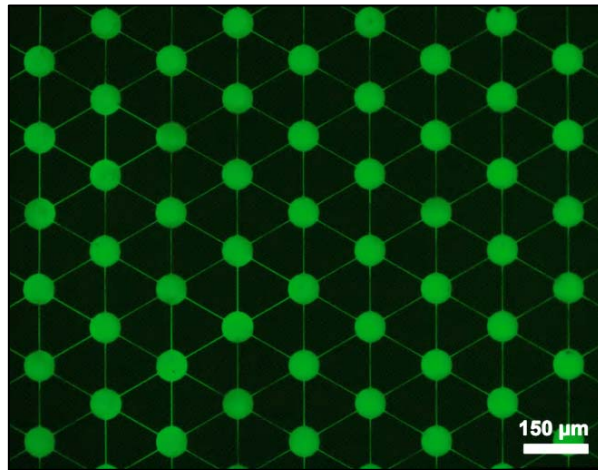
Figure 5.3.12: Microcontact print of the NFA structure with PLL-FITC on PLL-g-PEG. The print quality was of high quality and the process was highly reproducible.

Printing PL on PLL-*g*-PEG produced high quality patterns and was highly reproducible. The print was stable in media during a period of one week: The fluorescent intensity did not decay and did not spread. The remaining question was, *if the monolayer of PDL/PLO is sufficient to mediate cell adhesion and for how long?* Primary cells were seeded on a chip with a PDL print. Network development is shown in Fig. 5.3.13.
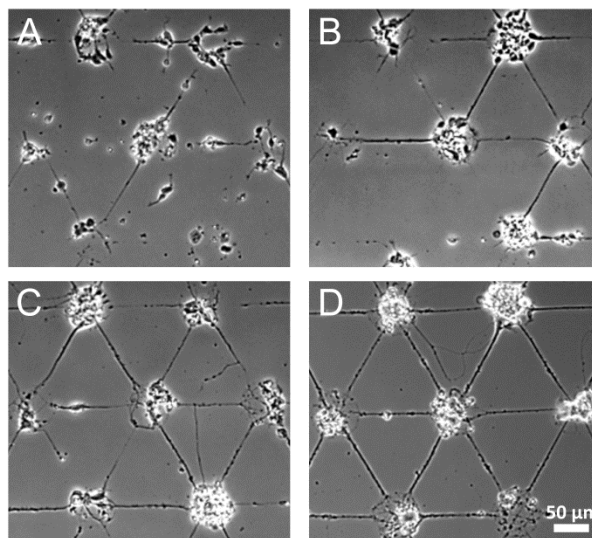
Figure 5.3.13: Network development of pCNs on the PL printed on PLL-g-PEG. Within the first 24 h the cells began to become registered on the NFA pattern (A). Three days after seeding the beginning of a network has been formed (B) and is nearly completed after 6 days (C). The cpn value and the diameter of the neurite connections increased until it reached the maximum ((D); 19 days in culture). The experiment has been done in co-operation with Julia Sisnaiske, IfaDo.

Within the first 24 h the cells began to form a network with 0.12 ± 0.03 connections per node cpn and an occupancy of 95.3 ± 1.08% (Fig. 5.3.14). In the first 24-48 h time was required for the cells to organize themselves on the array. The widely distributed character is reflected in the cells in track (cit) number of 23 ± 2.25% on day 1 which is reduced to 8.9 ± 1.43% on day 8. Within a week the network was fully developed with a cpn value of 2.52 ± 0.09, that is close to the maximum possible value of 2.73 cpn.
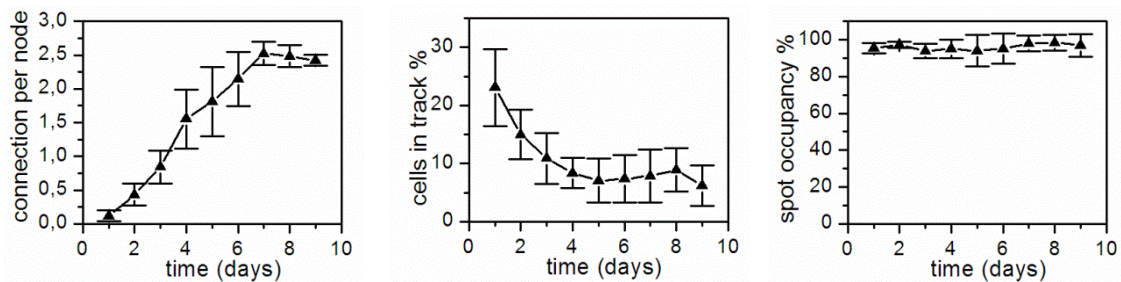
Figure 5.3.14: The development of pCNs on the NFA as measured using connection per nodes, cells in track (%) and node occupancy (%) during 9 days of culture. The experiment was done in triplicate and in cooperation with Julia Sisnaiske, IfaDo.

It was possible to culture the pCNs longer than one month on chip. In the end the network attained the maximum amount of cpn, although the occupancy decreased to 82.7%. pCNs prefer the state of cell clusters, which could explain the low occupancy number.
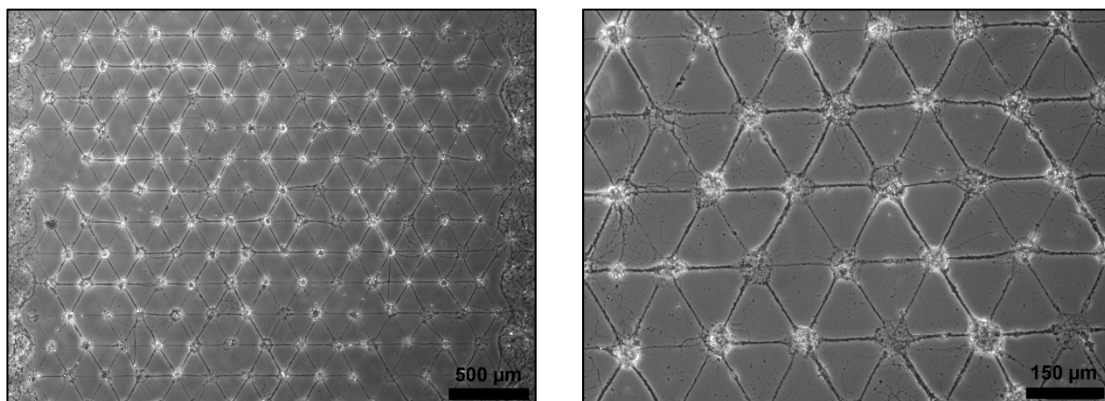
Figure 5.3.15: Primary neuronal network on a PLL-g-PEG coated surface following one month in culture. A fully complete network showing one array on chip with all spots occupied (left) and the maximum amount of connections per node (right).

Single cells patterned in a spot used the developed connections as "railways" to cluster together with other patterned cells in neighbouring nodes. An impression of a perfect developed primary network one month on chip is shown in figure 5.3.15.

After the successful establishment of the NFA for pCNs an inhibition and degeneration assay with the neurotoxin acyrlamide was undertaken. In the inhibition assay the primary cells were treated 24 h after seeding with acrylamide in the concentration range of 6 μM to 2 mM. In the degeneration assay the network was established over a period of four days (cpn: ~1.5) before treated with acrylamide in the range of 16 μM up to 5 mM (Figure 5.3.16).
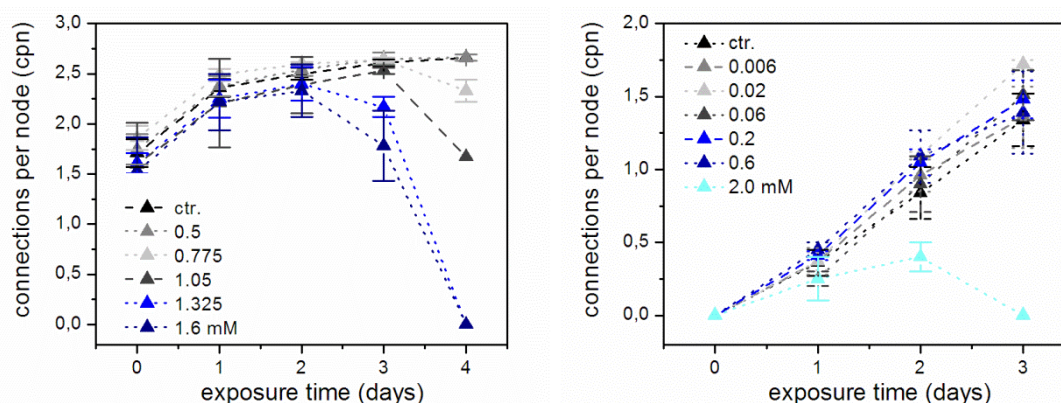
Figure 5.3.16: Degeneration assay; Dose response experiment with acrylamide. Shown here is the concentration range of 0.5 mM up to 1.6 mM on primary cells (left). Inhibition assay: concentration range of 0.006 mM up to 2 mM. Only the highest concentration of 2 mM inhibits the neurite outgrowth (right). All experiments were done in triplicate and in cooperation with Julia Sisnaiske, IfaDo.

As shown before with the SH-SY5Y cell line the NFA could be used to distinguish between cytotxity and neurotoxicity in inhibition assays. The calculated EC_{50}- and EC_{20}-values for pCNs in concern of cytotxocity were in the same concentration range than the one measured by CellTiter-Blue® assay (Inhibition assay NFA: EC_{50} / EC_{20}: 1.51 (0.79-2.47) mM / 1.47 (0.84-2.43) mM after 72 h incubation; CellTiter-Blue® EC_{50} / EC_{20}: 1.51 (1.21-1.81) mM / 0.39 (0.29-0.53) mM after 24 h of incubation). The measured EC_{50}- (0.70 (1.79-2.30) mM) and EC_{20}-values (0.67 (0.20-1.18) mM for neurite degeneration 72 h after incubation with acrylamide was much lower than the ones for cytotoxicity. The degeneration assay was not as sensitive as the inhibition assay. It was

not possible to distinguish between cyto- and neurotoxicity (Effective Concentration for neurotoxicity EC_{50} / EC_{20}: 0.93 (0.65-1.36) mM / 0.77 (0.56-1.29) mM; Effective concentration for cytotoxicity: 0.62 (0.56-0.70) mM / 0.59 (0.54-0.69) mM). Problematic were the multi-interconnections formed by the pCNs as strong bundles which did not get disintegrated by acrylamide and thus lower the sensitivity of the network formation assay.

In future the design layout will be modified with a spot diameter of 40-50 μm and a track width of 1.5 μm (instead of 70 μm spot diameter and 2 μm tracks) to avoid bundle formations and cell clustering. For further information on the topic of neurotoxicity on primary and stem cells please view the doctor thesis of Julia Sisnaiske (Sisnaiske, 2013).

5.3.4 Long term stability NFA

An important criterion for the widespread use of the NFA method is the possibility to ship and store the chips for long periods of time. The surface chemistry combines cell repellent material PLL-*g*-PEG in combination with a μCP of PDL. PLL-*g*-PEG has been shown to be sensitive to air (in the laboratory) at room temperature (Figure 5.3.17).
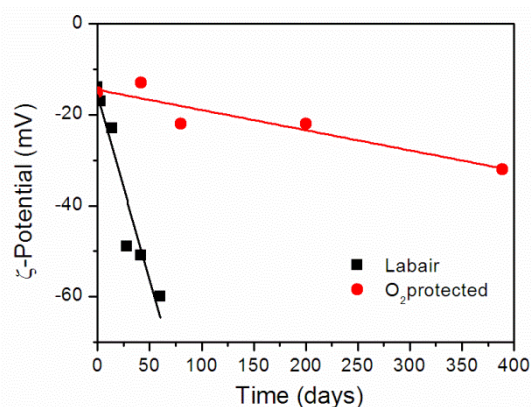
Figure 5.3.17: Zeta-potential measurements on PEGylated glass chips stored in lab air and at RT, as well as O$_2$ protected in a N$_2$-atmosphere at +8°C over a period of 400 days.

The zeta-potential of chips stored under lab conditions decrease from -14 mV to -60 mV within the first 60 days. Tests with cells have shown that chips stored for

only one day in the lab have a dramatically increased number (10 ± 5 unspecific binding cells on an area of 1.45 mm² on the control (-80°C in Ar) compared to 73 ± 51 unspecific binding cells on chips stored in the lab) of non-specifically bound cells, rendering them unsuitable for NFA experiments.

Chips stored under N_2-atmosphere at +8°C were much more stable, with the zeta-potential reduced by only -18 mV to -32 mV during an entire year. The stability can be increased by storing the chips in N_2 at -80°C. PEGylated chips stored under these conditions remained cell repellent for at least a month. Experiments are ongoing to further increase the stability of PLL-*g*-PEG slides for long term storage. Chips with a µCP of PDL could be stored for two weeks, nevertheless freshly prepared prints produce the highest quality patterns. This is made possible by the soft lithography approach which is straightforward for the biologists to prepare themselves. The establishment of a business selling the reagents and stamps for the biologist to do everything themselves is one future opportunity to find the NFA. An increase in the long term stability was also possible by storing the chips in an argon atmosphere at -80°C. After 4 month the material retained it's ability to prevent cell adhesion (Figure 5.3.18). In comparison, samples stored in argon at room temperature lost their ability to effectively prevent cell adhesion within 5 days.

PLL-*g*-PEG can adsorb spontaneously from aqueous solution onto negatively charged surfaces such as plasma activated glass (SiO_2) by electrostatic interaction. The positively charged PLL backbone interacts with the negative charged oxide surface. A monolayer is formed with the PEG chains orientated to the aqueous solution. The degradation of the PLL-g-PEG chains can take place by the auto-oxidation of the ethylene glycol groups, a process which is faster at RT than at -80°C (Luk et al., 2000; Ostuni et al., 2001). Most probably, however, the PLL-g-PEG was hydrolyzed. PEG was coupled by ester-chemistry to the PLL. Esters are prone to be hydrolyzed in acid as well as in basic conditions. The PLL-g-PEG stability under physiological pH in media was consistently good, with no degradation observed in long term cell culture experiments.
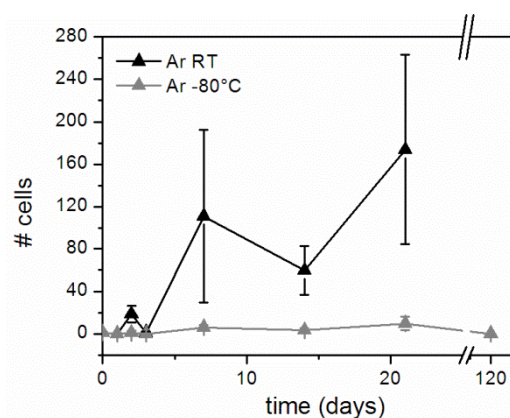
Figure 5.3.18: The number of cells binding on a PEGylated glass chip stored in argon at room temperature and in argon at -80°C. 2.0 x 10^5 cells were seeded in 2 mL media. After 24 h of adhesion the slides were washed thoroughly with PBS and stored in 1.5 mL PBS. An area of 1.45 mm² was screened for cells. The experiment was done in triplicate by Melanie Krüger.

In conclusion, prepared PEGylated glass slides can easily be stored in argon or nitrogen atmosphere by -80°C for months with intact cell repellent qualities. The chips could be shipped in argon/nitrogen and on carbon dioxide ice.

5.4 Outlook and Conclusion

In this chapter we describe the adaption of the NFA for primary cells. Primary and neuronal precursors are self-renewing and fully differentiated cells are the gold standard for data validation. Our bilayer plasma membrane patterning technique on PEGylated glass was unsuitable for backfilling with PL and PO, adhesion molecules needed by the cells to adhere to a surface. Replacing PL and PO by aminated silanes was also unsuitable. It was possible to replace PLL-*g*-PEG by DCDMS or TCS-PEG cell repellent materials. The pattern stability, cell viability on chip and reproducibility were not sufficient to provide an acceptable alternative to PLL-*g*-PEG. Instead the high affinity of PL and PO was used to μCP the poly-amine on the PLL-*g*-PEG surface. The resulting patterns were of high homogeneity, reproducibility and the primary network was stable in culture for over a month. PEGylated glass slides can be stored in argon atmosphere for at least four months without losing its cell repellent characteristic, stabilizing the PEG for long term experiments. In the future another hydrophilic

polymer poly-*L*-lysine-g-poly(2-methyl-2-oxazoline) (PLL-*g*-PMOXA) will be investigate, which is more stable in oxidative environments than PLL-*g*-PEG. The zeta-potential stayed constant for a glass slide covered with PMOXA stored under lab conditions for one week (Appendix 4). PMOXA is also equally effective in preventing protein adhesion and also prevents cell adhesion (Konradi et al., 2012). NFA produced with PMOXA as cell repellent material could be more easily stored and shipped without anti-oxidation measures.

The network formation assay has been successfully established for primary cells. The read-out of connectivity is a more precise and sensitive analytical end-point than cell viability. In the future, neuronal precursor (stem) cells will be patterned on the NFA microchips. Already it is possible to pattern these mouse cells with a µCP of PLO followed by an overnight coating of laminin (Figure 5.4.1).
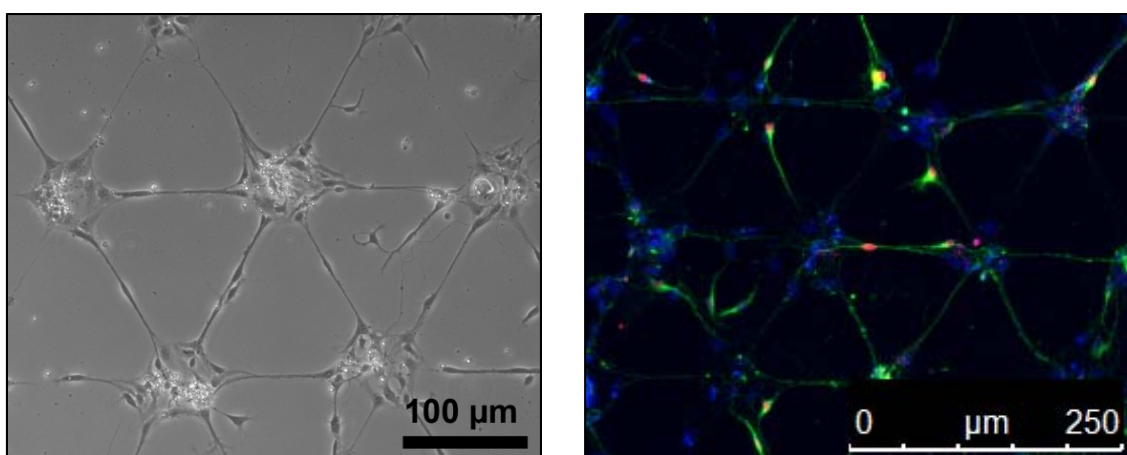
Figure 5.4.1: Neuronal precursor cells (NPCs) on a µCP of PLO and Laminin following 5 days in culture (left). Immunostaining: Nucleus of the differentiated NPCs was stained with DAPI (Blue) and mature neurons were identified with β-3-tubulin (green) and NeuN (neuron-specific nuclear protein; red) (right). Pictures were kindly provided by Vanessa Hausherr, IfaDo.

Using the neuronal precursor cell line (CGR 8 cell line) instead of the primary cell is of great promise to the 3Rs intiative. The pluripotent stem cells, once they are differentiated, are identical in morphology and functionality to primary neurons (Sisnaiske, 2013). Stem cells are self-renewing, so that primary cells obtained from animals are no longer required. This could further reduce the amount of animals needed to test chemicals for their neurotoxicity and neurodevelopmental effects.

Chapter 6: Conclusion
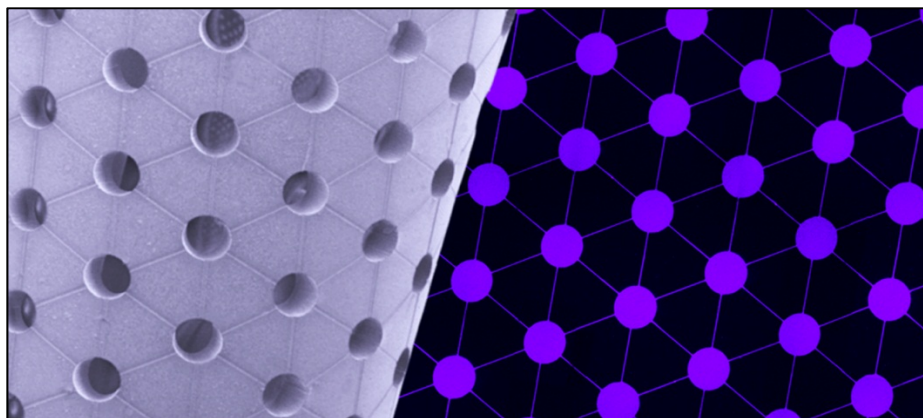
The research documented in this thesis describes the development of two novel *in vitro* microarray technologies, one suitable for the culture of tumour spheroids and the other for neurotoxicity testing.

The spatially standardized tumour spheroid culture platform was developed using PDMS microcontact printing. These microarrays automatically produce scalable tumour spheroids with diameters of 200 μm to 550 μm. Cells growing on the platform do not just aggregate together, but grow from a monolayer, producing mass transfer gradients within the spheroids which appropriately mimic avascularised tumours *in vivo*. The array dimensions dictate the spheroid model type and the development of metabolic and pathophysiological gradients. The microarray technology allows the mass production of highly uniform tumour spheroids with different scales and different gradient magnitudes for the *in situ* or *ex situ* analysis of potential anticancer treatments. Also the influence of cell proliferation rate, impact of scale and metabolic status on drugs can be determined. All together these benefits show the large potential of the array format for the widespread adoption of the tumour spheroid model in anti-cancer treatment investigation, especially with the focus in on obtaining high throughput data from metabolically-relevant tumour models. The arrayed HT29 tumour spheroids were physically and biologically characterized before final chemosensitivity testing. Transferring this microarray technique into industrial standard microtiter plates will allow high-throughput-screenings that greatly enhance

the potential of the spheroid array format for spheroid research in both fundamental research and commercial applications.

Bilayer plasma membrane technique is a cell patterning approach that was successfully developed to pattern neuron cells in another spatially standardized microarray format, the network formation assay (NFA). The NFA is a rapid, sensitive and reproducible analytical platform based on the neurite outgrowth assay with further microarray modifications (Frimat et al., 2009). It is a new *in vitro* method with predictive value for high throughput hazard classification of 100.000 untested or inadequately tested chemicals. The hexagonal geometry with equal distance to neighbouring nodes standardizes the neurite outgrowth length and eliminates the time intensive task of length measurements. The standardized coordinates of nodes and outgrowth tracks makes the NFA a reliable format for high-throughput screenings. In addition, the NFA measures interconnectivity which is the basis of memory and learning and a higher functional indicator than neurite outgrowth alone. The bilayer plasma membrane technique was successfully used to advance the NFA with the inclusion of features. Compared to the standard NFA without tracks the new assay has an increased connectivity; up to 65% more neuron connections per day. Dynamic processes like degeneration and regeneration experiments have been and can be monitored without fixation or staining. Its reproducibility and the low number of unspecific bound cells make the new technique a greatly improved spatial standardized analytical display for high throughput neurotoxicity screenings.

Furthermore, the network formation assay has been modified to meet the demands of gold standard *ex vivo* murine neurons and neuronal precursor cells. An established cell patterning technique, the microcontact printing, was used to pattern poly-amines on a PLL-*g*-PEG non-cell adhering background. Primary cells accepted the arrays containing track features. The reproducibility and pattern quality as well as the long term stability of cell pattern were excellent, making the NFA for primary cells a reliable tool for neuroscientists. The PEGylated glass slides can be stored in argon atmosphere at -80°C at least four month without losing its cell repellent characteristic, stabilizing the PEG for long term experiments. Currently, another hydrophilic polymer poly-*L*-lysine-g-poly(2-methyl-2-oxazoline) (PLL-*g*-PMOXA) is being tested, which is

more stable in oxidative environments than PLL-*g*-PEG. PMOXA is equally effective in preventing protein adhesion and should so likewise deny cell binding (Konradi et al., 2012). NFA produced with PMOXA as the cell repellent material can be stored and shipped without any oxidation preventative measures. The network formation assay has been successfully established for primary cells. In future neuronal precursor cells will be arrayed on the NFA chips. Already these mouse cells have been patterned with a µCP of PLO and a laminin coating overnight, but it needs further investigation with regard to cell number and assay design. In summary, these demonstrations and developments will promote the widespread adoption of the NFA by scientists to aid the neurotoxicity testing effort.

The simple cell patterning techniques and microarray tools for biological applications enable the biologists to readily adopt and handle spatial organized cell cultures. The *in vitro* microarray systems enhance and complement the gold standard techniques, which allow scientists to gain additional analytical information from cell biology experiments. In the future, microtechnologies will be increasingly available and more frequently used by biologists to spatially control cells for more reproducible, accurate and quantitative data analysis. These microarray techniques can be transferred into microtiter plates allowing high-throughput screenings coupled with automated image analysis capabilities. The spatial control of cellular cultures allows the spatial organization of *in vivo* tissues to be better mimicked and enables the development of assays that address unmet challenges in cell biology. Next to the spatial benefits microarray technologies equally reduce the amount of resources, making these systems an inexpensive alternative. Especially the use of test animals can be dramatically reduced using new microarray approaches. In summary, this thesis demonstrates that it is possible to design powerful tools based on microtechnology innovations to aid cell biology research in both academic and industrial settings.

Appendix

Table 1 *Summary of the conditions and results from the irinotecan dose response experiment. Diameter and volumetric growth values are from the control spheroids. The experiment was undertaken in triplicate with each replicate involving the measurement of 8 individual spheroids. Standard deviation values are prefixed with ±.*

culture condition	exposure (day)	spheroid start (µm)	spheroid end (µm)	mean volumetric growth µm³	IC_{50} (µm)
monolayer	4-7	-	-	-	32 (95% CI 22-49)
400-µm-pitch	4-7	165 ± 4	175 ± 7	4.4×10^5	102 (95% CI 49-239)
400-µm-pitch	11-14 (hypoxic)	191 ± 8	192 ± 9	5.6×10^4	307 (95% CI 144-634)
1500-µm pitch	4-7	168 ± 8	240 ± 12	4.6×10^6	62 (95% CI 23-96)
1500-µm pitch	10-13 (hypoxic)	307 ± 32	363 ± 20	9.8×10^6	224 (95% CI 123-408)

Table 2 *XPS atomic percentage data from the PLL-g-PEG adlayer with and without 60s oxygen plasma treatment*

electron level:	O1s (at. %)	C1s 1 (at. %)	C1s 2 (at. %)	C1s 3 (at. %)	C1s 4 (at. %)	N1s (at. %)	Si2p 1 (at. %)	Si2p 2 (at. %)
probable species:(Beamson, 1992)	all	C–C, C–H	C–O–C, C–<u>OH</u>, C–N, C–NH_3^+, C=N, C$\equiv$N	C=O, O–C–O, N–C–O, N–C$\equiv$O	O–COOH, N–(C=O)O	N–C, N$\equiv$C, N–C=O, N–(C=O)O, NH_3^+, $N(CH_3)_3^+$	Si^0	SiO_2
sample								
native <u>Si</u>	35.56	2.04	0.45	0.89	0.82	0.53	47.65	12.06
PEGylated <u>Si</u>	33.52	2.77	12.72	1.64	0.26	1.45	39.23	8.88
Plasma treated PEGylated <u>Si</u>	34.80	0.92	0.18	0.21	1.78	0.53	48.25	13.33
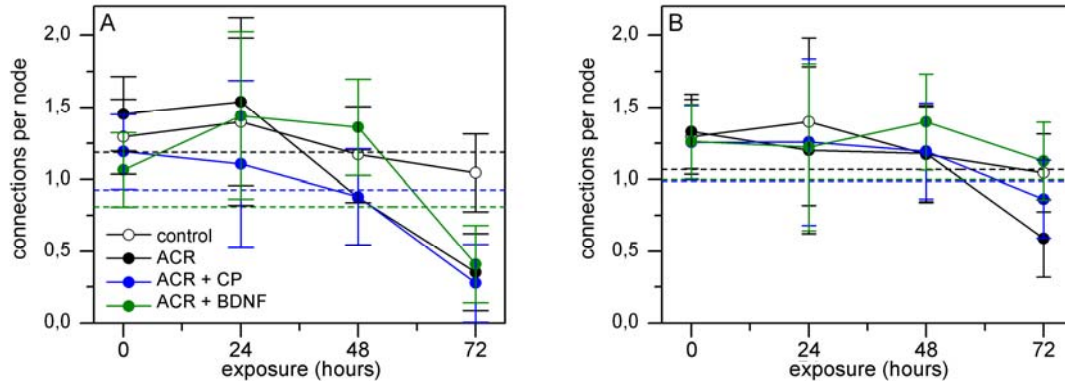
Appendix 3: Degeneration and protection effects on SH-SY5Y cells. Dynamics of acrylamide (ACR) included network degeneration and protective effects of 1 µM calpeptin (CP) and 100 ng/mL BDNF. The network was treated with 0.5 mM ACR (A) and 1.0 mM (B). Confidence intervals beneath the appropriately colored dotted lines indicate a significant (p<0.05) reduction compared to the initial value (self-control comparison).

Appendix 4: Zeta-potential measurements of PMOXA
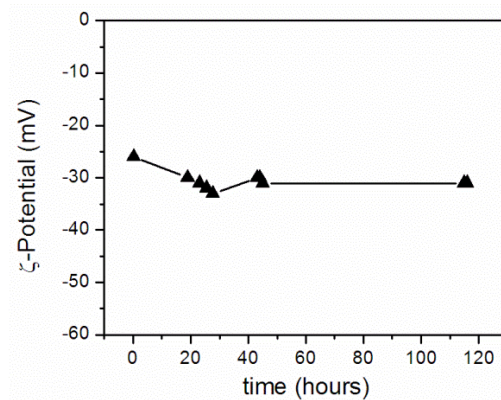
Appendix 4: Zeta-potential measurements: PMOXA stayed stable under lab condition for five days, no oxidation processes detectable.

References

Abbott, A. (2003). Cell culture: biology's new dimension. *Nature* 424, 870-2.

Adem, A., Mattsson, M. E., Nordberg, A. and Pahlman, S. (1987). Muscarinic receptors in human SH-SY5Y neuroblastoma cell line: regulation by phorbol ester and retinoic acid-induced differentiation. *Brain Res* 430, 235-42.

Adlerz, L., Beckman, M., Holback, S., Tehranian, R., Cortes Toro, V. and Iverfeldt, K. (2003). Accumulation of the amyloid precursor-like protein APLP2 and reduction of APLP1 in retinoic acid-differentiated human neuroblastoma cells upon curcumin-induced neurite retraction. *Brain Res Mol Brain Res* 119, 62-72.

Agholme, L., Lindstrom, T., Kagedal, K., Marcusson, J. and Hallbeck, M. (2010). An In Vitro Model for Neuroscience: Differentiation of SH-SY5Y Cells into Cells with Morphological and Biochemical Characteristics of Mature Neurons. *Journal of Alzheimers Disease* 20, 1069-1082.

Ahmad, S. A., Hucknall, A., Chilkoti, A. and Leggett, G. J. (2010). Protein Patterning by UV-Induced Photodegradation of Poly(oligo(ethylene glycol) methacrylate) Brushes. *Langmuir* 26, 9937-9942.

Akinari Iwasaki, T. M., Go Tazaki, Hitoshi Tsuruta, Hiroshi Egusa, Hiroyuki Miyajima, Taiji Sohmura. (2009). Mass Fabrication of Small Cell Spheroids by Using Micro-patterned Tissue Culture Plate. *Advanced Engineering Materials* 11, 801-804.

Alang Ahmad, S., Hucknall, A., Chilkoti, A. and Leggett, G. J. Protein patterning by UV-induced photodegradation of poly(oligo(ethylene glycol) methacrylate) brushes. *Langmuir* 26, 9937-42.

Alvarez, M., Long, H., Onyia, J., Hock, J., Xu, W. and Bidwell, J. (1997). Rat osteoblast and osteosarcoma nuclear matrix proteins bind with sequence specificity to the rat type I collagen promoter. *Endocrinology* 138, 482-9.

André Bernard, E. D., Heinz Schmid, Bruno Michel, Hans Rudolf Bosshard and Hans Biebuyck. (1998). Printing Patterns of Proteins. *Langmuir* 14, 2225-2229.

Axelsson, V., Holback, S., Sjogren, M., Gustafsson, H. and Forsby, A. (2006). Gliotoxin induces caspase-dependent neurite degeneration and calpain-mediated general cytotoxicity in differentiated human neuroblastoma SH-SY5Y cells. *Biochem Biophys Res Commun* 345, 1068-74.

Azioune, A., Storch, M., Bornens, M., Thery, M. and Piel, M. (2009). Simple and rapid process for single cell micro-patterning. *Lab Chip* 9, 1640-2.

References

Beamson, B. (1992). In High resolution XPS of organic polymers: The Scienta ESCA 300 Database. *Wiley, Chichester*.

Bernard, A., Delamarche, E., Schmid, H., Michel, B., Bosshard, H. R. and Biebuyck, H. (1998). Printing patterns of proteins. *Langmuir* 14, 2225-2229.

Bernard, A., Renault, J. P., Michel, B., Bosshard, H. R. and Delamarche, E. (2000). Microcontact printing of proteins. *Advanced Materials* 12, 1067-1070.

Birgersdotter, A., Sandberg, R. and Ernberg, I. (2005). Gene expression perturbation in vitro - A growing case for three-dimensional (3D) culture systems. *Seminars in Cancer Biology* 15, 405-412.

Brunton, G. F. and Wheldon, T. E. (1980). The Gompertz equation and the construction of tumour growth curves. *Cell Tissue Kinet* 13, 455-60.

Butor, C. and Davoust, J. (1992). Apical to basolateral surface area ratio and polarity of MDCK cells grown on different supports. *Exp Cell Res* 203, 115-27.

Calleman, C. J., Wu, Y., He, F., Tian, G., Bergmark, E., Zhang, S., Deng, H., Wang, Y., Crofton, K. M., Fennell, T. et al. (1994). Relationships between biomarkers of exposure and neurological effects in a group of workers exposed to acrylamide. *Toxicol Appl Pharmacol* 126, 361-71.

Calof, A. L. and Lander, A. D. (1991). Relationship between Neuronal Migration and Cell-Substratum Adhesion - Laminin and Merosin Promote Olfactory Neuronal Migration but Are Antiadhesive. *Journal of Cell Biology* 115, 779-794.

Castel, D., Pitaval, A., Debily, M. A. and Gidrol, X. (2006). Cell microarrays in drug discovery. *Drug Discov Today* 11, 616-22.

Chaudhury, M. K. and Whitesides, G. M. (1992). Correlation between surface free energy and surface constitution. *Science* 255, 1230-2.

Chen, C. S., Mrksich, M., Huang, S., Whitesides, G. M. and Ingber, D. E. (1997). Geometric control of cell life and death. *Science* 276, 1425-8.

Chen, C. S., Mrksich, M., Huang, S., Whitesides, G. M. and Ingber, D. E. (1998). Micropatterned surfaces for control of cell shape, position, and function. *Biotechnol Prog* 14, 356-63.

Chen, T. J., Cheng, H. M., Wang, D. C. and Hung, H. S. (2011). Nonlethal aluminum maltolate can reduce brain-derived neurotrophic factor-induced Arc expression through interrupting the ERK signaling in SH-SY5Y neuroblastoma cells. *Toxicology Letters* 200, 67-76.

References

Chignola, R., Schenetti, A., Andrighetto, G., Chiesa, E., Foroni, R., Sartoris, S., Tridente, G. and Liberati, D. (2000). Forecasting the growth of multicell tumour spheroids: implications for the dynamic growth of solid tumours. *Cell Prolif* 33, 219-29.

Clarke, M. F., Dick, J. E., Dirks, P. B., Eaves, C. J., Jamieson, C. H., Jones, D. L., Visvader, J., Weissman, I. L. and Wahl, G. M. (2006). Cancer stem cells--perspectives on current status and future directions: AACR Workshop on cancer stem cells. *Cancer Res* 66, 9339-44.

Coecke, S., Goldberg, A. M., Allen, S., Buzanska, L., Calamandrei, G., Crofton, K., Hareng, L., Hartung, T., Knaut, H., Honegger, P. et al. (2007). Workgroup report: incorporating in vitro alternative methods for developmental neurotoxicity into international hazard and risk assessment strategies. *Environ Health Perspect* 115, 924-31.

Corey, J. M., Wheeler, B. C. and Brewer, G. J. (1996). Micrometer resolution silane-based patterning of hippocampal neurons: critical variables in photoresist and laser ablation processes for substrate fabrication. *IEEE Trans Biomed Eng* 43, 944-55.

Cornish, T., Branch, D. W., Wheeler, B. C. and Campanelli, J. T. (2002). Microcontact printing: A versatile technique for the study of synaptogenic molecules. *Molecular and Cellular Neuroscience* 20, 140-153.

Csucs, G., Kunzler, T., Feldman, K., Robin, F. and Spencer, N. D. (2003a). Microcontact printing of macromolecules with submicrometer resolution by means of polyolefin stamps. *Langmuir* 19, 6104-6109.

Csucs, G., Michel, R., Lussi, J. W., Textor, M. and Danuser, G. (2003b). Microcontact printing of novel co-polymers in combination with proteins for cell-biological applications. *Biomaterials* 24, 1713-20.

Cukierman, E., Pankov, R., Stevens, D. R. and Yamada, K. M. (2001). Taking cell-matrix adhesions to the third dimension. *Science* 294, 1708-1712.

Cunha, C., Angelucci, A., D'Antoni, A., Dobrossy, M. D., Dunnett, S. B., Berardi, N. and Brambilla, R. (2009). Brain-derived neurotrophic factor (BDNF) overexpression in the forebrain results in learning and memory impairments. *Neurobiology of Disease* 33, 358-368.

Dardousis, K., Voolstra, C., Roengvoraphoj, M., Sekandarzad, A., Mesghenna, S., Winkler, J., Ko, Y., Hescheler, J. and Sachinidis, A. (2007). Identification of differentially expressed genes involved in the formation of multicellular tumor spheroids by HT-29 colon carcinoma cells. *Mol Ther* 15, 94-102.

Das, A., Garner, D. P., Del Re, A. M., Woodward, J. J., Kumar, D. M., Agarwal, N., Banik, N. L. and Ray, S. K. (2006). Calpeptin provides functional neuroprotection to rat retinal ganglion cells following Ca2+ influx. *Brain Res Mol Brain Res* 1084, 146-157.

References

De Silva, M. N., Desai, R. and Odde, D. J. (2004). Micro-patterning of animal cells on PDMS substrates in the presence of serum without use of adhesion inhibitors. *Biomed Microdevices* 6, 219-22.

De Silva, M. N., Paulsen, J., Renn, M. J. and Odde, D. J. (2006). Two-step cell patterning on planar and complex curved surfaces by precision spraying of polymers. *Biotechnol Bioeng* 93, 919-27.

Desoize, B., Gimonet, D. and Jardiller, J. C. (1998). Cell culture as spheroids: an approach to multicellular resistance. *Anticancer Res* 18, 4147-58.

Desoize, B. and Jardillier, J. (2000). Multicellular resistance: a paradigm for clinical resistance? *Crit Rev Oncol Hematol* 36, 193-207.

Detrait, E., Lhoest, J. B., Knoops, B., Bertrand, P. and van den Bosch de Aguilar, P. (1998). Orientation of cell adhesion and growth on patterned heterogeneous polystyrene surface. *J Neurosci Methods* 84, 193-204.

Dietrich, C. F. Ultraschall-Kurs. *Book*.

Dinh, N. D., Chiang, Y. Y., Hardelauf, H., Baumann, J., Jackson, E., Waide, S., Sisnaiske, J., Frimat, J. P., van Thriel, C., Janasek, D. et al. (2013). Microfluidic construction of minimalistic neuronal co-cultures. *Lab Chip* 13, 1402-12.

Dotti, C. G., Sullivan, C. A. and Banker, G. A. (1988). The Establishment of Polarity by Hippocampal-Neurons in Culture. *Journal of Neuroscience* 8, 1454-1468.

Douvas, A., Argitis, P., Misiakos, K., Dimotikali, D., Petrou, P. S. and Kakabakos, S. E. (2002). Biocompatible photolithographic process for the patterning of biomolecules. *Biosens Bioelectron* 17, 269-78.

Dubessy, C., Merlin, J. M., Marchal, C. and Guillemin, F. (2000). Spheroids in radiobiology and photodynamic therapy. *Crit Rev Oncol Hematol* 36, 179-92.

Falconnet, D., Csucs, G., Grandin, H. M. and Textor, M. (2006). Surface engineering approaches to micropattern surfaces for cell-based assays. *Biomaterials* 27, 3044-3063.

Falconnet, D., Koenig, A., Assi, T. and Textor, M. (2004). A combined photolithographic and molecular-assembly approach to produce functional micropatterns for applications in the biosciences. *Advanced Functional Materials* 14, 749-756.

Fink, J., Thery, M., Azioune, A., Dupont, R., Chatelain, F., Bornens, M. and Piel, M. (2007). Comparative study and improvement of current cell micro-patterning techniques. *Lab Chip* 7, 672-80.

Folch, A., Jo, B. H., Hurtado, O., Beebe, D. J. and Toner, M. (2000). Microfabricated elastomeric stencils for micropatterning cell cultures. *Journal of Biomedical Materials Research* 52, 346-353.

Folch, A. and Toner, M. (2000). Microengineering of cellular interactions. *Annu Rev Biomed Eng* 2, 227-56.

Forsby, A. and Blaauboer, B. (2007). Integration of in vitro neurotoxicity data with biokinetic modelling for the estimation of in vivo neurotoxicity. *Hum Exp Toxicol* 26, 333-8.

Francisco, H., Yellen, B. B., Halverson, D. S., Friedman, G. and Gallo, G. (2007). Regulation of axon guidance and extension by three-dimensional constraints. *Biomaterials* 28, 3398-407.

Frankel, A., Man, S., Elliott, P., Adams, J. and Kerbel, R. S. (2000). Lack of multicellular drug resistance observed in human ovarian and prostate carcinoma treated with the proteasome inhibitor PS-341. *Clin Cancer Res* 6, 3719-28.

Friedrich, J., Ebner, R. and Kunz-Schughart, L. A. (2007a). Experimental anti-tumor therapy in 3-D: spheroids--old hat or new challenge? *Int J Radiat Biol* 83, 849-71.

Friedrich, J., Eder, W., Castaneda, J., Doss, M., Huber, E., Ebner, R. and Kunz-Schughart, L. A. (2007b). A reliable tool to determine cell viability in complex 3-d culture: the acid phosphatase assay. *J Biomol Screen* 12, 925-37.

Friedrich, J., Seidel, C., Ebner, R. and Kunz-Schughart, L. A. (2009). Spheroid-based drug screen: considerations and practical approach. *Nat Protoc* 4, 309-24.

Frimat, J. P., Menne, H., Michels, A., Kittel, S., Kettler, R., Borgmann, S., Franzke, J. and West, J. (2009). Plasma stencilling methods for cell patterning. *Anal Bioanal Chem* 395, 601-9.

Frimat, J. P., Sisnaiske, J., Subbiah, S., Menne, H., Godoy, P., Lampen, P., Leist, M., Franzke, J., Hengstler, J. G., van Thriel, C. et al. (2009). The network formation assay: a spatially standardized neurite outgrowth analytical display for neurotoxicity screening. *Lab Chip* 10, 701-9.

Fukuda, J., Sakai, Y. and Nakazawa, K. (2006). Novel hepatocyte culture system developed using microfabrication and collagen/polyethylene glycol microcontact printing. *Biomaterials* 27, 1061-70.

Gallego-Perez, D., Higuita-Castro, N., Sharma, S., Reen, R. K., Palmer, A. F., Gooch, K. J., Lee, L. J., Lannutti, J. J. and Hansford, D. J. High throughput assembly of spatially controlled 3D cell clusters on a micro/nanoplatform. *Lab Chip* 10, 775-82.

References

Ghosh, S., Joshi, M. B., Ivanov, D., Feder-Mengus, C., Spagnoli, G. C., Martin, I., Erne, P. and Resink, T. J. (2007). Use of multicellular tumor spheroids to dissect endothelial cell-tumor cell interactions: a role for T-cadherin in tumor angiogenesis. *FEBS Lett* 581, 4523-8.

Glicklis, R., Merchuk, J. C. and Cohen, S. (2004). Modeling mass transfer in hepatocyte spheroids via cell viability, spheroid size, and hepatocellular functions. *Biotechnol Bioeng* 86, 672-80.

Goll, D. E., Thompson, V. F., Li, H., Wei, W. and Cong, J. (2003). The calpain system. *Physiol Rev* 83, 731-801.

Goubko, C. A. and Cao, X. D. (2009). Patterning multiple cell types in co-cultures: A review. *Materials Science & Engineering C-Materials for Biological Applications* 29, 1855-1868.

Graber, D. J., Zieziulewicz, T. J., Lawrence, D. A., Shain, W. and Turner, J. N. (2003). Antigen binding specificity of antibodies patterned by microcontact printing. *Langmuir* 19, 5431-5434.

Gregoire, F. M., Smas, C. M. and Sul, H. S. (1998). Understanding adipocyte differentiation. *Physiol Rev* 78, 783-809.

Griffith, L. G. and Swartz, M. A. (2006). Capturing complex 3D tissue physiology in vitro. *Nature Reviews Molecular Cell Biology* 7, 211-224.

Hardelauf, H., Frimat, J. P., Stewart, J. D., Schormann, W., Chiang, Y. Y., Lampen, P., Franzke, J., Hengstler, J. G., Cadenas, C., Kunz-Schughart, L. A. et al. Microarrays for the scalable production of metabolically relevant tumour spheroids: a tool for modulating chemosensitivity traits. *Lab Chip* 11, 419-28.

Hartung, T. and Rovida, C. (2009). Chemical regulators have overreached. *Nature* 460, 1080-1.

Healy, K. E., Lom, B. and Hockberger, P. E. (1994). Spatial distribution of mammalian cells dictated by material surface chemistry. *Biotechnol Bioeng* 43, 792-800.

Healy, K. E., Thomas, C. H., Rezania, A., Kim, J. E., McKeown, P. J., Lom, B. and Hockberger, P. E. (1996). Kinetics of bone cell organization and mineralization on materials with patterned surface chemistry. *Biomaterials* 17, 195-208.

Hirschhaeuser, F., Menne, H., Dittfeld, C., West, J., Mueller-Klieser, W. and Kunz-Schughart, L. A. Multicellular tumor spheroids: an underestimated tool is catching up again. *J Biotechnol* 148, 3-15.

Horch, R. E., Kopp, J., Kneser, U., Beier, J. and Bach, A. D. (2005). Tissue engineering of cultured skin substitutes. *J Cell Mol Med* 9, 592-608.

References

Howes, A. L., Chiang, G. G., Lang, E. S., Ho, C. B., Powis, G., Vuori, K. and Abraham, R. T. (2007). The phosphatidylinositol 3-kinase inhibitor, PX-866, is a potent inhibitor of cancer cell motility and growth in three-dimensional cultures. *Mol Cancer Ther* 6, 2505-14.

Hsiang, Y. H., Lihou, M. G. and Liu, L. F. (1989). Arrest of replication forks by drug-stabilized topoisomerase I-DNA cleavable complexes as a mechanism of cell killing by camptothecin. *Cancer Res* 49, 5077-82.

Hsiao, A. Y., Torisawa, Y. S., Tung, Y. C., Sud, S., Taichman, R. S., Pienta, K. J. and Takayama, S. (2009). Microfluidic system for formation of PC-3 prostate cancer co-culture spheroids. *Biomaterials* 30, 3020-7.

http://www.nc3rs.org.uk.

Hyun, J., Zhu, Y. J., Liebmann-Vinson, A., Beebe, T. P. and Chilkoti, A. (2001). Microstamping on an activated polymer surface: Patterning biotin and streptavidin onto common polymeric biomaterials. *Langmuir* 17, 6358-6367.

Inaba, R., Khademhosseini, A., Suzuki, H. and Fukuda, J. (2009). Electrochemical desorption of self-assembled monolayers for engineering cellular tissues. *Biomaterials* 30, 3573-9.

Ingram, M., Techy, G. B., Saroufeem, R., Yazan, O., Narayan, K. S., Goodwin, T. J. and Spaulding, G. F. (1997). Three-dimensional growth patterns of various human tumor cell lines in simulated microgravity of a NASA bioreactor. *In Vitro Cell Dev Biol Anim* 33, 459-66.

Ivascu, A. and Kubbies, M. (2006). Rapid generation of single-tumor spheroids for high-throughput cell function and toxicity analysis. *J Biomol Screen* 11, 922-32.

J. West, J.-P. F., J. Sisnaiske, C. van Thriel and J. G. Hengstler. (DE 10 2009 021 876.9 and PCT/EP2010/002811).

Jackman, R. J., Duffy, D. C., Cherniavskaya, O. and Whitesides, G. M. (1999). Using elastomeric membranes as dry resists and for dry lift-off. *Langmuir* 15, 2973-2984.

James, C. D., Davis, R. C., Kam, L., Craighead, H. G., Isaacson, M., Turner, J. N. and Shain, W. (1998). Patterned protein layers on solid substrates by thin stamp microcontact printing. *Langmuir* 14, 741-744.

Jaxel, C., Kohn, K. W., Wani, M. C., Wall, M. E. and Pommier, Y. (1989). Structure-activity study of the actions of camptothecin derivatives on mammalian topoisomerase I: evidence for a specific receptor site and a relation to antitumor activity. *Cancer Res* 49, 1465-9.

References

Jiang, Y., Pjesivac-Grbovic, J., Cantrell, C. and Freyer, J. P. (2005). A multiscale model for avascular tumor growth. *Biophys J* 89, 3884-94.

Kale, S., Biermann, S., Edwards, C., Tarnowski, C., Morris, M. and Long, M. W. (2000). Three-dimensional cellular development is essential for ex vivo formation of human bone. *Nat Biotechnol* 18, 954-8.

Kam, L., Shain, W., Turner, J. N. and Bizios, R. (1999). Correlation of astroglial cell function on micro-patterned surfaces with specific geometric parameters. *Biomaterials* 20, 2343-50.

Kamei, K., Guo, S., Yu, Z. T., Takahashi, H., Gschweng, E., Suh, C., Wang, X., Tang, J., McLaughlin, J., Witte, O. N. et al. (2009). An integrated microfluidic culture device for quantitative analysis of human embryonic stem cells. *Lab Chip* 9, 555-63.

Kandal, E. R. (2009). *J. Neurosci.* 29(41), 12748-12756.

Kane, R. S., Takayama, S., Ostuni, E., Ingber, D. E. and Whitesides, G. M. (1999). Patterning proteins and cells using soft lithography. *Biomaterials* 20, 2363-76.

Karacali, B., Vamvakidou, A. P. and Tozeren, A. (2007). Automated recognition of cell phenotypes in histology images based on membrane- and nuclei-targeting biomarkers. *BMC Med Imaging* 7, 7.

Karp, J. M., Yeh, J., Eng, G., Fukuda, J., Blumling, J., Suh, K. Y., Cheng, J., Mahdavi, A., Borenstein, J., Langer, R. et al. (2007). Controlling size, shape and homogeneity of embryoid bodies using poly(ethylene glycol) microwells. *Lab Chip* 7, 786-94.

Kelm, J. M. and Fussenegger, M. (2004). Microscale tissue engineering using gravity-enforced cell assembly. *Trends Biotechnol* 22, 195-202.

Kelm, J. M., Timmins, N. E., Brown, C. J., Fussenegger, M. and Nielsen, L. K. (2003). Method for generation of homogeneous multicellular tumor spheroids applicable to a wide variety of cell types. *Biotechnol Bioeng* 83, 173-80.

Kenausis, G. L., Voros, J., Elbert, D. L., Huang, N. P., Hofer, R., Ruiz-Taylor, L., Textor, M., Hubbell, J. A. and Spencer, N. D. (2000). Poly(L-lysine)-g-poly(ethylene glycol) layers on metal oxide surfaces: Attachment mechanism and effects of polymer architecture on resistance to protein adsorption. *Journal of Physical Chemistry B* 104, 3298-3309.

Kern, J., Steurer, M., Gastl, G., Gunsilius, E. and Untergasser, G. (2009). Vasohibin inhibits angiogenic sprouting in vitro and supports vascular maturation processes in vivo. *BMC Cancer* 9, 284.

References

Khatau, S. B., Hale, C. M., Stewart-Hutchinson, P. J., Patel, M. S., Stewart, C. L., Searson, P. C., Hodzic, D. and Wirtz, D. (2009). A perinuclear actin cap regulates nuclear shape. *Proc Natl Acad Sci U S A* 106, 19017-22.

Khetani, S. R. and Bhatia, S. N. (2008). Microscale culture of human liver cells for drug development. *Nat Biotechnol* 26, 120-6.

Khoutorsky, A. and Spira, M. E. (2009). Activity-dependent calpain activation plays a critical role in synaptic facilitation and post-tetanic potentiation. *Learning & Memory* 16, 129-141.

Klein, C. L., Scholl, M. and Maelicke, A. (1999). Neuronal networks in vitro: formation and organization on biofunctionalized surfaces. *J Mater Sci Mater Med* 10, 721-7.

Kleinfeld, D., Kahler, K. H. and Hockberger, P. E. (1988). Controlled outgrowth of dissociated neurons on patterned substrates. *J Neurosci* 8, 4098-120.

Kojima, R., Yoshimoto, K., Takahashi, E., Ichino, M., Miyoshi, H. and Nagasaki, Y. (2009). Spheroid array of fetal mouse liver cells constructed on a PEG-gel micropatterned surface: upregulation of hepatic functions by co-culture with nonparenchymal liver cells. *Lab Chip* 9, 1991-3.

Konradi, R., Acikgoz, C. and Textor, M. (2012). Polyoxazolines for nonfouling surface coatings--a direct comparison to the gold standard PEG. *Macromol Rapid Commun* 33, 1663-76.

Krueger, S., Kalinski, T., Wolf, H., Kellner, U. and Roessner, A. (2005). Interactions between human colon carcinoma cells, fibroblasts and monocytic cells in coculture--regulation of cathepsin B expression and invasiveness. *Cancer Lett* 223, 313-22.

Kumar, A. and Whitesides, G. M. (1993). Features of Gold Having Micrometer to Centimeter Dimensions Can Be Formed through a Combination of Stamping with an Elastomeric Stamp and an Alkanethiol Ink Followed by Chemical Etching. *Applied Physics Letters* 63, 2002-2004.

Kunz-Schughart, L. A., Freyer, J. P., Hofstaedter, F. and Ebner, R. (2004). The use of 3-D cultures for high-throughput screening: the multicellular spheroid model. *J Biomol Screen* 9, 273-85.

Kunz-Schughart, L. A., Groebe, K. and Mueller-Klieser, W. (1996). Three-dimensional cell culture induces novel proliferative and metabolic alterations associated with oncogenic transformation. *Int J Cancer* 66, 578-86.

Kunz-Schughart, L. A., Schroeder, J. A., Wondrak, M., van Rey, F., Lehle, K., Hofstaedter, F. and Wheatley, D. N. (2006). Potential of fibroblasts to regulate the formation of three-dimensional vessel-like structures from endothelial cells in vitro. *Am J Physiol Cell Physiol* 290, C1385-98.

References

Lahann, J., Balcells, M., Rodon, T., Lee, J., Choi, I. S., Jensen, K. F. and Langer, R. (2002). Reactive polymer coatings: A platform for patterning proteins and mammalian cells onto a broad range of materials. *Langmuir* 18, 3632-3638.

Lauer, L., Klein, C. and Offenhausser, A. (2001). Spot compliant neuronal networks by structure optimized micro-contact printing. *Biomaterials* 22, 1925-32.

Lee, J., Cuddihy, M. J., Cater, G. M. and Kotov, N. A. (2009). Engineering liver tissue spheroids with inverted colloidal crystal scaffolds. *Biomaterials* 30, 4687-94.

Lehnert, D., Wehrle-Haller, B., David, C., Weiland, U., Ballestrem, C., Imhof, B. A. and Bastmeyer, M. (2004). Cell behaviour on micropatterned substrata: limits of extracellular matrix geometry for spreading and adhesion. *J Cell Sci* 117, 41-52.

Lein, P., Silbergeld, E., Locke, P. and Goldberg, A. M. (2005). In vitro and other alternative approaches to developmental neurotoxicity testing (DNT). *Environ Toxicol Pharmacol* 19, 735-44.

Leist, M., Kadereit, S. and Schildknecht, S. (2008). Food for thought... on the real success of 3R approaches. *Altex* 25, 17-32.

Liu, D., McIlvain, H. B., Fennell, M., Dunlop, J., Wood, A., Zaleska, M. M., Graziani, E. I. and Pong, K. (2007). Screening of immunophilin ligands by quantitative analysis of neurofilament expression and neurite outgrowth in cultured neurons and cells. *J Neurosci Methods* 163, 310-20.

Livak, K. J. and Schmittgen, T. D. (2001). Analysis of relative gene expression data using real-time quantitative PCR and the 2(-Delta Delta C(T)) Method. *Methods* 25, 402-8.

Luk, Y. Y., Kato, M. and Mrksich, M. (2000). Self-assembled monolayers of alkanethiolates presenting mannitol groups are inert to protein adsorption and cell attachment. *Langmuir* 16, 9604-9608.

Malmsten, M., Emoto, K. and Van Alstine, J. M. (1998). Effect of chain density on inhibition of protein adsorption by poly(ethylene glycol) based coatings. *Journal of Colloid and Interface Science* 202, 507-517.

Maniotis, A. J., Chen, C. S. and Ingber, D. E. (1997). Demonstration of mechanical connections between integrins, cytoskeletal filaments, and nucleoplasm that stabilize nuclear structure. *Proc Natl Acad Sci U S A* 94, 849-54.

Marusic, M., Bajzer, Z., Vuk-Pavlovic, S. and Freyer, J. P. (1994). Tumor growth in vivo and as multicellular spheroids compared by mathematical models. *Bull Math Biol* 56, 617-31.

References

McBeath, R., Pirone, D. M., Nelson, C. M., Bhadriraju, K. and Chen, C. S. (2004). Cell shape, cytoskeletal tension, and RhoA regulate stem cell lineage commitment. *Dev Cell* 6, 483-95.

Michel, B., Bernard, A., Bietsch, A., Delamarche, E., Geissler, M., Juncker, D., Kind, H., Renault, J. P., Rothuizen, H., Schmid, H. et al. (2001). Printing meets lithography: Soft approaches to high-resolution printing. *Ibm Journal of Research and Development* 45, 697-719.

Millet, L. J., Stewart, M. E., Sweedler, J. V., Nuzzo, R. G. and Gillette, M. U. (2007). Microfluidic devices for culturing primary mammalian neurons at low densities. *Lab Chip* 7, 987-94.

Mori, R., Sakai, Y. and Nakazawa, K. (2008). Micropatterned organoid culture of rat hepatocytes and HepG2 cells. *J Biosci Bioeng* 106, 237-42.

Morooka, T. and Nishida, E. (1998). Requirement of p38 mitogen-activated protein kinase for neuronal differentiation in PC12 cells. *J Biol Chem* 273, 24285-8.

Mourzina, Y., Kaliaguine, D., Schulte, P. and Offenhausser, A. (2006). Patterning chemical stimulation of reconstructed neuronal networks. *Anal Chim Acta* 575, 281-9.

Mrksich, M., Dike, L. E., Tien, J., Ingber, D. E. and Whitesides, G. M. (1997). Using microcontact printing to pattern the attachment of mammalian cells to self-assembled monolayers of alkanethiolates on transparent films of gold and silver. *Exp Cell Res* 235, 305-13.

Mueller-Klieser, W. (1987). Multicellular spheroids. A review on cellular aggregates in cancer research. *J Cancer Res Clin Oncol* 113, 101-22.

Mueller-Klieser, W. (1997). Three-dimensional cell cultures: from molecular mechanisms to clinical applications. *Am J Physiol* 273, C1109-23.

Mueller-Klieser, W. (2000). Tumor biology and experimental therapeutics. *Crit Rev Oncol Hematol* 36, 123-39.

N.C. Rivron, E. J. V., R. Truckenmüller, J. Rouwkema, S. Le Gac, A. van den Berg and C.A. van Blitterswijk. (2012) Tissue deformation spatially modulates VEGF signaling and angiogenesis. *PNAS* 109, 6886-6891

Nakazawa, K., Izumi, Y., Fukuda, J. and Yasuda, T. (2006). Hepatocyte spheroid culture on a polydimethylsiloxane chip having microcavities. *J Biomater Sci Polym Ed* 17, 859-73.

Nam, Y., Branch, D. W. and Wheeler, B. C. (2006). Epoxy-silane linking of biomolecules is simple and effective for patterning neuronal cultures. *Biosens Bioelectron* 22, 589-97.

References

Nelson, C. M. and Bissell, M. J. (2006). Of extracellular matrix, scaffolds, and signaling: Tissue architecture regulates development, homeostasis, and cancer. *Annual Review of Cell and Developmental Biology* 22, 287-309.

Nelson, C. M., Raghavan, S., Tan, J. L. and Chen, C. S. (2003). Degradation of micropatterned surfaces by cell-dependent and -independent processes. *Langmuir* 19, 1493-1499.

Nelson, C. M. and Tien, J. (2006). Microstructured extracellular matrices in tissue engineering and development. *Curr Opin Biotechnol* 17, 518-23.

Nordin-Andersson, M., Forsby, A., Heldring, N., Dejongh, J., Kjellstrand, P. and Walum, E. (1998). Neurite degeneration in differentiated human neuroblastoma cells. *Toxicol In Vitro* 12, 557-60.

Nordin-Andersson, M., Walum, E., Kjellstrand, P. and Forsby, A. (2003). Acrylamide-induced effects on general and neurospecific cellular functions during exposure and recovery. *Cell Biol Toxicol* 19, 43-51.

Olive, P. L. and Durand, R. E. (1994). Drug and radiation resistance in spheroids: cell contact and kinetics. *Cancer Metastasis Rev* 13, 121-38.

Ong, S. M., Zhang, C., Toh, Y. C., Kim, S. H., Foo, H. L., Tan, C. H., van Noort, D., Park, S. and Yu, H. (2008). A gel-free 3D microfluidic cell culture system. *Biomaterials* 29, 3237-44.

Oshima, M., Koizumi, S., Fujita, K. and Guroff, G. (1989). Nerve Growth Factor-Induced Decrease in the Calpain Activity of Pc12 Cells. *Journal of Biological Chemistry* 264, 20811-20816.

Ostuni, E., Chapman, R. G., Liang, M. N., Meluleni, G., Pier, G., Ingber, D. E. and Whitesides, G. M. (2001). Self-assembled monolayers that resist the adsorption of proteins and the adhesion of bacterial and mammalian cells. *Langmuir* 17, 6336-6343.

Ostuni, E., Kane, R., Chen, C. S., Ingber, D. E. and Whitesides, G. M. (2000). Patterning mammalian cells using elastomeric membranes. *Langmuir* 16, 7811-7819.

Otsuka, H., Hirano, A., Nagasaki, Y., Okano, T., Horiike, Y. and Kataoka, K. (2004). Two-dimensional multiarray formation of hepatocyte spheroids on a microfabricated PEG-brush surface. *Chembiochem* 5, 850-5.

Pahlman, S., Mamaeva, S., Meyerson, G., Mattsson, M. E., Bjelfman, C., Ortoft, E. and Hammerling, U. (1990). Human neuroblastoma cells in culture: a model for neuronal cell differentiation and function. *Acta Physiol Scand Suppl* 592, 25-37.

References

Pahlman, S., Ruusala, A. I., Abrahamsson, L., Mattsson, M. E. and Esscher, T. (1984). Retinoic acid-induced differentiation of cultured human neuroblastoma cells: a comparison with phorbolester-induced differentiation. *Cell Differ* 14, 135-44.

Palmer, D. W. and Decker, S. K. (1973). Microscopic Circuit Fabrication on Refractory Superconducting Films. *Review of Scientific Instruments* 44, 1621-1624.

Pampaloni, F., Reynaud, E. G. and Stelzer, E. H. K. (2007). The third dimension bridges the gap between cell culture and live tissue. *Nature Reviews Molecular Cell Biology* 8, 839-845.

Park, J., Cho, C. H., Parashurama, N., Li, Y., Berthiaume, F., Toner, M., Tilles, A. W. and Yarmush, M. L. (2007). Microfabrication-based modulation of embryonic stem cell differentiation. *Lab Chip* 7, 1018-28.

Pasche, S., De Paul, S. M., Voros, J., Spencer, N. D. and Textor, M. (2003). Poly(L-lysine)-graft-poly(ethylene glycol) assembled monolayers on niobium oxide surfaces: A quantitative study of the influence of polymer interfacial architecture on resistance to protein adsorption by ToF-SIMS and in situ OWLS. *Langmuir* 19, 9216-9225.

Patrito, N., McCague, C., Norton, P. R. and Petersen, N. O. (2007). Spatially controlled cell adhesion via micropatterned surface modification of poly(dimethylsiloxane). *Langmuir* 23, 715-9.

Poland, J., Sinha, P., Siegert, A., Schnolzer, M., Korf, U. and Hauptmann, S. (2002). Comparison of protein expression profiles between monolayer and spheroid cell culture of HT-29 cells revealed fragmentation of CK18 in three-dimensional cell culture. *Electrophoresis* 23, 1174-84.

Powers, M. J., Domansky, K., Kaazempur-Mofrad, M. R., Kalezi, A., Capitano, A., Upadhyaya, A., Kurzawski, P., Wack, K. E., Stolz, D. B., Kamm, R. et al. (2002). A microfabricated array bioreactor for perfused 3D liver culture. *Biotechnol Bioeng* 78, 257-69.

Qin, D., Xia, Y. and Whitesides, G. M. Soft lithography for micro- and nanoscale patterning. *Nat Protoc* 5, 491-502.

Radio, N. M., Breier, J. M., Shafer, T. J. and Mundy, W. R. (2008). Assessment of chemical effects on neurite outgrowth in PC12 cells using high content screening. *Toxicol Sci* 105, 106-18.

Radio, N. M. and Mundy, W. R. (2008). Developmental neurotoxicity testing in vitro: models for assessing chemical effects on neurite outgrowth. *Neurotoxicology* 29, 361-76.

Ramm, P., Alexandrov, Y., Cholewinski, A., Cybuch, Y., Nadon, R. and Soltys, B. J. (2003). Automated screening of neurite outgrowth. *J Biomol Screen* 8, 7-18.

References

Rangarajan, A., Hong, S. J., Gifford, A. and Weinberg, R. A. (2004). Species- and cell type-specific requirements for cellular transformation. *Cancer Cell* 6, 171-183.

Ranieri, J. P., Bellamkonda, R., Jacob, J., Vargo, T. G., Gardella, J. A. and Aebischer, P. (1993). Selective neuronal cell attachment to a covalently patterned monoamine on fluorinated ethylene propylene films. *J Biomed Mater Res* 27, 917-25.

Ravenscroft, M. S., Bateman, K. E., Shaffer, K. M., Schessler, H. M., Jung, D. R., Schneider, T. W., Montgomery, C. B., Custer, T. L., Schaffner, A. E., Liu, Q. Y. et al. (1998). Developmental neurobiology implications from fabrication and analysis of hippocampal neuronal networks on patterned silane-modified surfaces. *Journal of the American Chemical Society* 120, 12169-12177.

Reyes, D. R., Perruccio, E. M., Becerra, S. P., Locascio, L. E. and Gaitan, M. (2004). Micropatterning neuronal cells on polyelectrolyte multilayers. *Langmuir* 20, 8805-11.

Rhee, S. W., Taylor, A. M., Tu, C. H., Cribbs, D. H., Cotman, C. W. and Jeon, N. L. (2005). Patterned cell culture inside microfluidic devices. *Lab Chip* 5, 102-7.

Ricci-Vitiani, L., Lombardi, D. G., Pilozzi, E., Biffoni, M., Todaro, M., Peschle, C. and De Maria, R. (2007). Identification and expansion of human colon-cancer-initiating cells. *Nature* 445, 111-5.

Roach, P., Parker, T., Gadegaard, N. and Alexander, M. R. (2010). Surface strategies for control of neuronal cell adhesion: A review. *Surface Science Reports* 65, 145-173.

Roca-Cusachs, P., Alcaraz, J., Sunyer, R., Samitier, J., Farre, R. and Navajas, D. (2008). Micropatterning of single endothelial cell shape reveals a tight coupling between nuclear volume in G1 and proliferation. *Biophysical Journal* 94, 4984-95.

Rodriguez-Enriquez, S., Gallardo-Perez, J. C., Aviles-Salas, A., Marin-Hernandez, A., Carreno-Fuentes, L., Maldonado-Lagunas, V. and Moreno-Sanchez, R. (2008). Energy metabolism transition in multi-cellular human tumor spheroids. *J Cell Physiol* 216, 189-97.

Romanova, E. V., Fosser, K. A., Rubakhin, S. S., Nuzzo, R. G. and Sweedler, J. V. (2004). Engineering the morphology and electrophysiological parameters of cultured neurons by microfluidic surface patterning. *Faseb Journal* 18, 1267-9.

Ruiz, A., Buzanska, L., Gilliland, D., Rauscher, H., Sirghi, L., Sobanski, T., Zychowicz, M., Ceriotti, L., Bretagnol, F., Coecke, S. et al. (2008). Micro-stamped surfaces for the patterned growth of neural stem cells. *Biomaterials* 29, 4766-74.

Ruiz, S. A. and Chen, C. S. (2007). Microcontact printing: A tool to pattern. *Soft Matter* 3, 168-177.

Russell, W. M. (1995). The development of the three Rs concept. *Altern Lab Anim* 23, 298-304.

Sagvolden, G., Giaever, I., Pettersen, E. O. and Feder, J. (1999). Cell adhesion force microscopy. *Proc Natl Acad Sci U S A* 96, 471-476.

Sakai, S., Ito, S., Ogushi, Y., Hashimoto, I., Hosoda, N., Sawae, Y. and Kawakami, K. (2009). Enzymatically fabricated and degradable microcapsules for production of multicellular spheroids with well-defined diameters of less than 150 microm. *Biomaterials* 30, 5937-42.

Sakai, Y. and Nakazawa, K. (2007). Technique for the control of spheroid diameter using microfabricated chips. *Acta Biomater* 3, 1033-40.

Santini, M. T., Rainaldi, G. and Indovina, P. L. (1999). Multicellular tumour spheroids in radiation biology. *Int J Radiat Biol* 75, 787-99.

Schaffner, P. and Dard, M. M. (2003). Structure and function of RGD peptides involved in bone biology. *Cell Mol Life Sci* 60, 119-32.

Schauer, K., Duong, T., Bleakley, K., Bardin, S., Bornens, M. and Goud, B. Probabilistic density maps to study global endomembrane organization. *Nat Methods* 7, 560-6.

Scholl, M., Sprossler, C., Denyer, M., Krause, M., Nakajima, K., Maelicke, A., Knoll, W. and Offenhausser, A. (2000). Ordered networks of rat hippocampal neurons attached to silicon oxide surfaces. *J Neurosci Methods* 104, 65-75.

Seok, J., Warren, H. S., Cuenca, A. G., Mindrinos, M. N., Baker, H. V., Xu, W., Richards, D. R., McDonald-Smith, G. P., Gao, H., Hennessy, L. et al. (2013). Genomic responses in mouse models poorly mimic human inflammatory diseases. *Proc Natl Acad Sci U S A* 110, 3507-12.

Shah, S. S., Howland, M. C., Chen, L. J., Silangcruz, J., Verkhoturov, S. V., Schweikert, E. A., Parikh, A. N. and Revzin, A. (2009). Micropatterning of proteins and mammalian cells on indium tin oxide. *ACS Appl Mater Interfaces* 1, 2592-601.

Shanks, N., Greek, R. and Greek, J. (2009). Are animal models predictive for humans? *Philos Ethics Humanit Med* 4, 2.

Shi, P., Shen, K. and Kam, L. C. (2007). Local presentation of L1 and N-cadherin in multicomponent, microscale patterns differentially direct neuron function in vitro. *Dev Neurobiol* 67, 1765-76.

Siegel, A. C., Shevkoplyas, S. S., Weibel, D. B., Bruzewicz, D. A., Martinez, A. W. and Whitesides, G. M. (2006). Cofabrication of electromagnets and microfluidic systems in poly(dimethylsiloxane). *Angew Chem Int Ed Engl* 45, 6877-82.

References

Sikavitsas, V. I., Temenoff, J. S. and Mikos, A. G. (2001). Biomaterials and bone mechanotransduction. *Biomaterials* 22, 2581-93.

Singh, S. K., Hawkins, C., Clarke, I. D., Squire, J. A., Bayani, J., Hide, T., Henkelman, R. M., Cusimano, M. D. and Dirks, P. B. (2004). Identification of human brain tumour initiating cells. *Nature* 432, 396-401.

Singhvi, R., Kumar, A., Lopez, G. P., Stephanopoulos, G. N., Wang, D. I., Whitesides, G. M. and Ingber, D. E. (1994). Engineering cell shape and function. *Science* 264, 696-8.

Sisnaiske, J. (2013). Neurotoxische Effekte von Acyrlamid in humanen und murinen *in vitro* Modellen - Untersuchungen der Zellfunktion und -struktur.

Song, D. K., Malmstrom, T., Kater, S. B. and Mykles, D. L. (1994). Calpain inhibitors block Ca(2+)-induced suppression of neurite outgrowth in isolated hippocampal pyramidal neurons. *J Neurosci Res* 39, 474-81.

Sorribas, H., Padeste, C. and Tiefenauer, L. (2002). Photolithographic generation of protein micropatterns for neuron culture applications. *Biomaterials* 23, 893-900.

St John, P. M., Kam, L., Turner, S. W., Craighead, H. G., Issacson, M., Turner, J. N. and Shain, W. (1997). Preferential glial cell attachment to microcontact printed surfaces. *J Neurosci Methods* 75, 171-7.

Stein, A. M., Demuth, T., Mobley, D., Berens, M. and Sander, L. M. (2007). A mathematical model of glioblastoma tumor spheroid invasion in a three-dimensional in vitro experiment. *Biophys J* 92, 356-65.

Stenger, D. A., Hickman, J. J., Bateman, K. E., Ravenscroft, M. S., Ma, W., Pancrazio, J. J., Shaffer, K., Schaffner, A. E., Cribbs, D. H. and Cotman, C. W. (1998). Microlithographic determination of axonal/dendritic polarity in cultured hippocampal neurons. *J Neurosci Methods* 82, 167-73.

Suh, K. Y., Kim, Y. S. and Lee, H. H. (2001). Capillary force lithography. *Advanced Materials* 13, 1386-1389.

Sutherland, R. M. (1988). Cell and environment interactions in tumor microregions: the multicell spheroid model. *Science* 240, 177-84.

Sutherland, R. M., McCredie, J. A. and Inch, W. R. (1971). Growth of multicell spheroids in tissue culture as a model of nodular carcinomas. *J Natl Cancer Inst* 46, 113-20.

Tamura, T., Sakai, Y. and Nakazawa, K. (2008). Two-dimensional microarray of HepG2 spheroids using collagen/polyethylene glycol micropatterned chip. *J Mater Sci Mater Med* 19, 2071-7.

References

Taylor, A. M., Blurton-Jones, M., Rhee, S. W., Cribbs, D. H., Cotman, C. W. and Jeon, N. L. (2005). A microfluidic culture platform for CNS axonal injury, regeneration and transport. *Nat Methods* 2, 599-605.

Taylor, A. M., Rhee, S. W., Tu, C. H., Cribbs, D. H., Cotman, C. W. and Jeon, N. L. (2003). Microfluidic Multicompartment Device for Neuroscience Research. *Langmuir* 19, 1551-1556.

Thakar, R. G., Cheng, Q., Patel, S., Chu, J., Nasir, M., Liepmann, D., Komvopoulos, K. and Li, S. (2009). Cell-shape regulation of smooth muscle cell proliferation. *Biophysical Journal* 96, 3423-32.

Théry, M., Pepin, A., Dressaire, E., Chen, Y. and Bornens, M. (2006a). Cell distribution of stress fibres in response to the geometry of the adhesive environment. *Cell Motil Cytoskeleton* 63, 341-55.

Théry, M., Racine, V., Pepin, A., Piel, M., Chen, Y., Sibarita, J. B. and Bornens, M. (2005). The extracellular matrix guides the orientation of the cell division axis. *Nature Cell Biology* 7, 947-53.

Théry, M., Racine, V., Piel, M., Pepin, A., Dimitrov, A., Chen, Y., Sibarita, J. B. and Bornens, M. (2006b). Anisotropy of cell adhesive microenvironment governs cell internal organization and orientation of polarity. *Proc Natl Acad Sci U S A* 103, 19771-6.

Thomas, C. H., Lhoest, J. B., Castner, D. G., McFarland, C. D. and Healy, K. E. (1999). Surfaces designed to control the projected area and shape of individual cells. *J Biomech Eng* 121, 40-8.

Timmins, N. E., Harding, F. J., Smart, C., Brown, M. A. and Nielsen, L. K. (2005). Method for the generation and cultivation of functional three-dimensional mammary constructs without exogenous extracellular matrix. *Cell Tissue Res* 320, 207-10.

Timmins, N. E. and Nielsen, L. K. (2007). Generation of multicellular tumor spheroids by the hanging-drop method. *Methods Mol Med* 140, 141-51.

Toh, Y. C., Zhang, C., Zhang, J., Khong, Y. M., Chang, S., Samper, V. D., van Noort, D., Hutmacher, D. W. and Yu, H. (2007). A novel 3D mammalian cell perfusion-culture system in microfluidic channels. *Lab Chip* 7, 302-9.

Torisawa, Y. S., Chueh, B. H., Huh, D., Ramamurthy, P., Roth, T. M., Barald, K. F. and Takayama, S. (2007). Efficient formation of uniform-sized embryoid bodies using a compartmentalized microchannel device. *Lab Chip* 7, 770-6.

Torisawa, Y. S., Mosadegh, B., Luker, G. D., Morell, M., O'Shea, K. S. and Takayama, S. (2009). Microfluidic hydrodynamic cellular patterning for systematic formation of co-culture spheroids. *Integr Biol (Camb)* 1, 649-54.

References

Tourovskaia, A., Barber, T., Wickes, B. T., Hirdes, D., Grin, B., Castner, D. G., Healy, K. E. and Folch, A. (2003). Micropatterns of chemisorbed cell adhesion-repellent films using oxygen plasma etching and elastomeric masks. *Langmuir* 19, 4754-4764.

Ungrin, M. D., Joshi, C., Nica, A., Bauwens, C. and Zandstra, P. W. (2008). Reproducible, ultra high-throughput formation of multicellular organization from single cell suspension-derived human embryonic stem cell aggregates. *PLoS One* 3, e1565.

Vogt, A. K., Wrobel, G., Meyer, W., Knoll, W. and Offenhausser, A. (2005). Synaptic plasticity in micropatterned neuronal networks. *Biomaterials* 26, 2549-57.

von Philipsborn, A. C., Lang, S., Bernard, A., Loeschinger, J., David, C., Lehnert, D., Bastmeyer, M. and Bonhoeffer, F. (2006). Microcontact printing of axon guidance molecules for generation of graded patterns. *Nature Protocols* 1, 1322-8.

Waide, S. (2011). Preparation and analysis of spatially defined neuronal networks. *Bachelor Thesis*.

Wang, W., Itaka, K., Ohba, S., Nishiyama, N., Chung, U. I., Yamasaki, Y. and Kataoka, K. (2009). 3D spheroid culture system on micropatterned substrates for improved differentiation efficiency of multipotent mesenchymal stem cells. *Biomaterials* 30, 2705-15.

Welle, A., Horn, S., Schimmelpfeng, J. and Kalka, D. (2005). Photo-chemically patterned polymer surfaces for controlled PC-12 adhesion and neurite guidance. *J Neurosci Methods* 142, 243-50.

Wenger, A., Kowalewski, N., Stahl, A., Mehlhorn, A. T., Schmal, H., Stark, G. B. and Finkenzeller, G. (2005). Development and characterization of a spheroidal coculture model of endothelial cells and fibroblasts for improving angiogenesis in tissue engineering. *Cells Tissues Organs* 181, 80-8.

Wheeler, B. C., Corey, J. M., Brewer, G. J. and Branch, D. W. (1999). Microcontact printing for precise control of nerve cell growth in culture. *J Biomech Eng* 121, 73-8.

Whitesides, G. M. (2006). The origins and the future of microfluidics. *Nature* 442, 368-373.

Whitesides, G. M., Ostuni, E., Takayama, S., Jiang, X. and Ingber, D. E. (2001). Soft lithography in biology and biochemistry. *Annu Rev Biomed Eng* 3, 335-73.

Wissner-Gross, Z. D., Scott, M. A., Ku, D., Ramaswamy, P. and Fatih Yanik, M. Large-scale analysis of neurite growth dynamics on micropatterned substrates. *Integr Biol (Camb)* 3, 65-74.

Wu, L. Y., Di Carlo, D. and Lee, L. P. (2008). Microfluidic self-assembly of tumor spheroids for anticancer drug discovery. *Biomed Microdevices* 10, 197-202.

Acknowledgement

Xia, Y. N. and Whitesides, G. M. (1998a). Soft lithography. *Angewandte Chemie-International Edition* 37, 551-575.

Xia, Y. N. and Whitesides, G. M. (1998b). Soft lithography. *Annual Review of Materials Science* 28, 153-184.

Yamada, K. M. and Cukierman, E. (2007). Modeling tissue morphogenesis and cancer in 3D. *Cell* 130, 601-610.

Yang, T. T., Sinai, P. and Kain, S. R. (1996). An acid phosphatase assay for quantifying the growth of adherent and nonadherent cells. *Anal Biochem* 241, 103-8.

Yoshimoto, K., Ichino, M. and Nagasaki, Y. (2009). Inverted pattern formation of cell microarrays on poly(ethylene glycol) (PEG) gel patterned surface and construction of hepatocyte spheroids on unmodified PEG gel microdomains. *Lab Chip* 9, 1286-9.

Zegers, M. M., O'Brien, L. E., Yu, W., Datta, A. and Mostov, K. E. (2003). Epithelial polarity and tubulogenesis in vitro. *Trends Cell Biol* 13, 169-76.

Zhang, F., Sautter, K., Larsen, A. M., Findley, D. A., Davis, R. C., Samha, H. and Linford, M. R. (2010). Chemical vapor deposition of three aminosilanes on silicon dioxide: surface characterization, stability, effects of silane concentration, and cyanine dye adsorption. *Langmuir* 26, 14648-54.

Zhang, M., Desai, T. and Ferrari, M. (1998). Proteins and cells on PEG immobilized silicon surfaces. *Biomaterials* 19, 953-60.

Zhang, X., Wang, W., Yu, W., Xie, Y., Zhang, X., Zhang, Y. and Ma, X. (2005). Development of an in vitro multicellular tumor spheroid model using microencapsulation and its application in anticancer drug screening and testing. *Biotechnol Prog* 21, 1289-96.

Acknowledgement

An interesting and exciting time has passed. In the last three and a half years I was in the lucky position to do research with many experienced and qualified people. Especially my supervisor Dr. Jonathan West was a source of knowledge and his way of leading our mini-miniaturization group was fantastic. His enthusiasm and joy at work was catching. He was the best supervisor I can think of, challenging and promoting. Thank You!

I would also like to thank PD Dr. Joachim Franzke for his support and the time he spent to convince me to like giving presentations. A special thanks to Dr. Dirk Janasek who surprisingly and suddenly had to lead me and my project.

Last man or better woman standing: Sarah Waide! The last years would have been extremely lonely without you, especially the last one. The last lab rats of the miniaturization group remaining in ISAS Campus.

Thank you Dr. Peter Jacob for all your input and the fruitful discussion we had not just about scientific topics and your friendship.

My highest respect to the IfaDo-"Mädels" Julia Sisnaiske, Vanessa Hausherr und Dr. Nicole Schöbel, who had the hardest part in our NFA project: They killed the mice! Thank you also Dr. Christoph van Thriel for the relaxed working environment.

The completion of this thesis would have not been possible without the help of Ulrich Marggraf, Norman Ahlmann, Ya-Yu Chiang, Dr. Jean-Philippe Frimat, Susanne Funken, Maria Becker, Silke Kittel and the ISAS team.

A special thank goes to my first examiner Prof. Tiller, who helped me a lot to better understand the mechanism of surface coatings. I really enjoyed the fruitful and relaxed discussions we had.

At least I would like to thank my family for the never ending support. Ever when I needed time for writing, someone of you took care of Erik. I offer my final blessings to my husband Dominik and my wonderful child Erik.

Curriculum vitae

Name	Heike Hardelauf, née Menne
Date of Birth	15.09.1982
Place of Birth	Kreuztal, Germany
Nationality	German
E-Mail	Heike.Hardelauf@gmx.de

Education

09/2009 – present

PhD Research

Leibniz - Institut für Analytische Wissenschaften - ISAS - e.V., Dortmund

Thesis title: "Development and Characterization of *in vitro* Microarray Technologies for Cell Biology"

10/2007 – 08/2009

Master Degree

College of Chemical Biology, Technische Universitat Dortmund

Title of Master thesis: "Micropatterning for the massively parallel production of 3D tumour spheroids."

10/2003 – 09/2007

Bachelor Degree

College of Chemical Biology, Technische Universitat Dortmund

Title of Bachelor thesis: „Construction of a novel self-assembly expression vector by recombinant cloning."

Awards

- Top cited article of 2009-2011 in Journal of Biotechnology: „Multicellular tumor spheroids: An underestimated tool is catching up again. "

- Best Poster Award bio.dortmund 2011: "High fidelity neuronal networks formed using bilayer plasma stencilling. "

- Biocartis Best Poster and Flash Presentation Award at NanoBioTech; 2009

- Best Analytical and Bioanalytical Chemistry Paper Award 2009 from Springer; 2010

- S-BLOC Fellowship 2009-2012